Report
P-21-04
April 2022

Hydrological monitoring in Forsmark – surface waters, ground moisture and ground temperature

October 1, 2019–September 30, 2020

Kent Werner
Aryani Atmosudirdjo

SVENSK KÄRNBRÄNSLEHANTERING AB

SWEDISH NUCLEAR FUEL
AND WASTE MANAGEMENT CO

Box 3091, SE-169 03 Solna
Phone +46 8 459 84 00
skb.se

SVENSK KÄRNBRÄNSLEHANTERING

ISSN 1651-4416
SKB P-21-04
ID 1928585

April 2022

Hydrological monitoring in Forsmark – surface waters, ground moisture and ground temperature

October 1, 2019–September 30, 2020

Kent Werner, WSP Sverige AB

Aryani Atmosudirdjo, Svensk Kärnbränslehantering AB

Keywords: Stream, Pond, Lake, Gauging station, Flume, Water level, Discharge, Electrical conductivity, Temperature, Moisture, AP SFK-17-035.

Data in SKB's database can be changed for different reasons. Minor changes in SKB's database will not necessarily result in a revised report. Data revisions may also be presented as supplements, available at www.skb.se.

This report is published on www.skb.se

© 2022 Svensk Kärnbränslehantering AB

Summary

This document reports the monitoring of water level, which is used to calculate water depth, EC (electrical conductivity), temperature, and water-depth based calculations of discharge at four gauging stations in four streams in Forsmark during the hydrological year 2019/2020 (October 1, 2019–September 30, 2020). SKB's Hydro Monitoring System (HMS) was used to collect and store all data. Quality-controlled, high-resolution data on water level, EC and temperature were transferred from HMS to SKB's primary database Sicada. Moreover, hourly average discharge was calculated based on quality-controlled water-level data and delivered separately to Sicada.

During the 2019/2020 hydrological year the average discharge for the four stations was c 17–30 L/s. The average EC and temperature of stream water were c 24–33 mS/m and 6–8 °C, respectively. It is noted that the statistics for the hydrological year 2019/2020 presented in the report are affected by some data gaps due to technical problems. Flumes and observation wells have been levelled annually during the period 2012–2017, and it is recommended to repeat the annual levelling also in the future. The validity of stage-discharge relationships and associated parameters has been checked by independent discharge measurements in 2004–2006, and recently in 2013–2017. Independent discharge measurements need to be performed also in the future.

The report also presents an overview of and uses some results from meteorological and other hydrology-related monitoring, for which data gathering and quality control are not part of the present work. The objective is to provide illustrative examples on integrated evaluations that may provide insight into near-surface hydrological interactions and long-term trends. Specifically, the overview and the integrated evaluations include data from meteorological monitoring and monitoring/observations of "winter parameters" (ice coverage; there was no snow coverage during the winter 2019/2020), data from surface-water level and temperature monitoring in lakes and ponds, and data from monitoring of ground temperature and water content.

Sammanfattning

Denna rapport beskriver övervakning av vattennivå, som används för beräkning av vattendjup, EC (elektrisk konduktivitet), temperatur samt vattendjupsbaserade beräkningar av vattenföring vid fyra vattenföringsstationer i fyra bäckar i Forsmark under det hydrologiska året 2019/2020 (1 oktober 2019–30 september 2020). SKB:s Hydro Monitoring System (HMS) användes för att samla in och lagra alla data. Kvalitetskontrollerade, högupplösta data på vattennivå, EC och temperatur överfördes från HMS till SKB:s primärdatabas Sicada. Timmedelvärden på vattenföring beräknades utifrån kvalitetskontrollerade vattennivådata och levererades separat till Sicada.

Under det hydrologiska året 2019/2020 var den genomsnittliga vattenföringen vid de fyra stationerna cirka 17–30 l/s). Bäckvattnets genomsnittliga EC och temperatur var cirka 24–33 mS/m respektive 6–8 °C. Det hydrologiska året 2019/2020 innehåller några dataluckor på grund av tekniska problem. Mätrännor och observationsrör har avvägts årligen under perioden 2012–2017, och rekommendationen är årliga avvägningar även i framtiden. Giltigheten för avbördningsekvationer och tillhörande parametrar har kontrollerats genom oberoende vattenföringsmätningar 2004–2006 och 2013–2017. Oberoende vattenföringsmätningar behöver genomföras även i framtiden.

Rapporten innehåller även en översikt över och använder resultat från meteorologisk och annan hydrologirelaterad övervakning, för vilken datainsamling och -granskning inte ingår i detta arbete. Syftet är att illustrera hur integrerade utvärderingar kan ge insikt om hydrologiska processer i ytsystemet samt långsiktiga trender. Översikten och de integrerade utvärderingarna inkluderar meteorologisk övervakning, mätningar/observationer av ”vinterparametrar” (istäckning; det fanns inget snötäcke vintern 2019/2020), övervakning av ytvattennivå och -temperatur i sjöar och gölar, samt övervakning av marktemperatur och markvattenhalt.

Contents

1 Introduction and objectives

This document reports the monitoring of water level, EC (electrical conductivity), temperature, and water-level based calculations of discharge at four gauging stations (Figure 1-1 and Table 1-1) in four streams in Forsmark during the hydrological year October 1, 2019–September 30, 2020. The report also provides an overview of and uses some results from other hydrology-related monitoring in Forsmark. The monitoring provides data and information for various types of conceptual and quantitative modelling, such as water and mass balances, which in turn form the basis for site descriptions, assessments of long-term radiological safety and environmental impact assessments.

A hydrological year is characterised by approximately equal storages of water within surface and subsurface reservoirs in the beginning and in the end of the year, facilitating terrestrial water-balance studies. In Sweden, this period is usually chosen to occur during the months of October to September (September to August in northern Sweden), when there normally are no or very small storages of water in the form of snow and ice (Bergström 1993).

Figure 1-1. *Locations and associated sub-catchment areas of the four stream-gauging stations. The PFM005764 sub-catchment area includes the PFM002667 sub-catchment area, which in turn includes the PFM002668 sub-catchment area.*

Table 1-1. Sub-catchment areas of the four gauging stations (Johansson and Juston 2011b).

Gauging station id	Sub-catchment area id	Size of sub-catchment area (km^2)
PFM005764	AFM001267	5.59
PFM002667	AFM001268	3.01
PFM002668	AFM001269	2.28
PFM002669	AFM001270	2.83

Previous monitoring and discharge calculations are reported in Johansson and Juston (2007, 2009, 2011a, b) for the period April 2004–December 2010, and in Werner (2014a, b, 2016, 2017, 2018a, b, 2019, 2020) for the period January 1, 2011–September 30, 2019. The monitoring was carried out in accordance with relevant parts of activity plan AP SFK-17-035 (Table 1-2), which is an SKB-internal controlling document. Table 1-2 lists reports of regular quality control of water-level data (for further details, see Section 3.4.1). Quality control was performed on four occasions during the data period of this report.

SKB's Hydro Monitoring System (HMS) was used to collect and store all data. From HMS, quality-controlled data were transferred to SKB's primary Site Characterisation database (*Sicada*), where they are traceable by the activity plan number (cf Table 1-1). Only data in Sicada are accepted for further interpretation and modelling. The data presented in this report are regarded as copies of the original data. If data errors are found, data in databases are revised but will not necessarily result in a revision of the report, although the normal procedure is that major data revisions entail a report revision.

If not stated otherwise, coordinates in this report are given in the coordinate systems SWEREF 99 18 00 (horisontal) and RH 2000 (vertical), i.e. vertical (Z) coordinates are expressed in terms of elevation (m) above the RH 2000 datum (0 m elevation). Note that the coordinate systems RT 90 2.5 gon V/0:15 (horisontal) and RHB 70 (vertical) were used up to and including the Werner (2018a) monitoring report. Times are in HMS stored in the time zone GMT+1 (no DST); this time zone is used also in this report.

In connection to Table 1-1 and Figure 1-1, it is noted that the sub-catchment area boundaries (SDEADM.POS_FM_VTN_5441) for PFM002667 and PFM002668 were updated in December 2006, and therefore do not match the boundaries shown in the original stream-gauge installation report (Johansson 2005). Also note that the sub-catchment area of stream-gauging station PFM005764 (AFM001267) includes the upstream sub-catchment area AFM001268, which in turn includes the upstream AFM001269 sub-catchment area. The sub-catchment-area boundaries are determined based on a digital elevation model (DEM) with a horizontal resolution of 10 m (Brunberg et al. 2004). It is recommended to revise sub-catchment area boundaries when a new DEM is available, supported by field checks of road culverts. Culverts conduct water across road embankments, which act as sub-catchment area boundaries along road stretches without culverts.

Table 1-2. Controlling internal documents and quality-control documents for the activity.

Activity plan	SKBdoc id, version
AP SFK 17-035 – Hydrologisk och hydrogeologisk monitering, Platsförvaltning Forsmark 2018–2020	1613611, ver 1.4
Projekt Kärnbränsleförvaret, quality-control reports	
Monitering Forsmark och SFR: Kvalitetskontroll av yt- och grundvattenövervakning Juni–oktober 2019	1883365, ver 1.0
Monitering Forsmark och SFR: Kvalitetskontroll av yt- och grundvattenövervakning November 2019–februari 2020	1898587, ver 1.0
Hydrologisk och hydrogeologisk övervakning Forsmark och SFR: Kvalitetskontroll av yt- och grundvattenövervakning Februari–juni 2020	1909177, ver 1.0
Hydrologisk och hydrogeologisk övervakning Forsmark och SFR: Kvalitetskontroll av yt- och grundvattenövervakning Juni–oktober 2020	1924271, ver 1.0

2 Methods for stream monitoring

This chapter presents methods for monitoring of water level, EC, temperature and calculation of stream discharge. Methods for other hydrology-related monitoring are described in the references of Chapter 4 and references therein.

2.1 Gauging stations and data-collection systems

Long-throated flumes are used for water-level monitoring and associated discharge calculations. Such flumes were selected mainly due to the limitations set by the flat landscape, the need for accurate measurements, and the desire to avoid fish-migration obstacles (Johansson 2005). This type of flume provides accurate measurements over a relatively wide discharge range and it works under a high degree of submergence (Robinson 1966, 1968, Kilpatrick and Schneider 1983, Clemmens et al. 2001).

At three of the gauging stations, two different types of flumes were installed to obtain good accuracy over a wide range of discharge in the intervals < 20 L/s and > 20 L/s (see details below). The flumes are made of stainless steel. Five of the six flumes use standard factory designs (Plasti-Fab Inc.), whereas two are custom made using the design software WinFlume (Wahl et al. 2000). The flume designs are presented in Johansson (2005), whereas further details on technical installations at the gauging stations are shown in Werner (2014a, Appendix 1).

The gauging stations are equipped as follows:

- **PFM005764:** There are two flumes of standard factory designs at this gauging station, one small flume (discharge range < 20 L/s) and one large flume (discharge range > 20 L/s). The flumes were originally installed in November 2003, and measurements were initiated in March 2004. Due to damming problems at high discharge, the station was reconstructed and the flumes were reinstalled in October 2004 (Johansson 2005). The station was refurbished and reconstructed in August 2014, including replacement of the small flume (Werner 2016). On January 9, 2018, monitoring using a water-level bubbler (YSI Waterlog Amazon Bubbler) was initiated in the observation well connected to the large flume. The intention is to measure water level using the bubbler in parallel with pressure-sensor measurements (for further details, see Section 2.4.1).
- **PFM002667:** Previously, there were two flumes at this gauging station, one small and one large. The small flume had a standard factory design, whereas the large flume was designed using the WinFlume software. These flumes were installed in October 2004, and measurements were initiated in December 2004. In August 2018, the station was refurbished and reconstructed and the two flumes were replaced by a single flume (Werner 2019).
- **PFM002668:** There is a single, large flume at this gauging station, designed using the WinFlume software. The flume was installed in October 2004, and measurements were initiated in December 2004.
- **PFM002669:** There are two flumes at this gauging station, one small and one large. The small flume has a standard factory design, whereas the large flume is designed using the WinFlume software. The flumes were installed in October 2004, and measurements were initiated in December 2004. The small flume was stolen in July 2007. It was replaced and both flumes (and also the observation wells) were reinstalled in November 2007. The station was refurbished and reconstructed in August–September 2015 (Werner 2017).

As illustrated in Werner (2014a, Appendix 1), water levels in flumes are measured by vented pressure sensors (see Section 2.2) installed in observation wells located alongside each flume. At the stations PFM002667–68, EC and temperature sensors are mounted on the outside of screened tubes located in the streams (all sensors were installed inside the tubes up to March 2012; see Werner 2014a). As part of the PFM005764, PFM002669 and PFM002667 refurbishments and reconstructions in 2014, 2015 and 2018, respectively, the tubes hosting the EC and temperature sensors were moved to the grating, and the sensors were again installed inside the tubes. In their new positions, the tubes communicate with the stream water not only through the tube screen but also through the open tube bottom. Moreover, in December 2014–January 2015 the EC and temperature sensors at PFM002668 were moved to another location at the station, in order to avoid a rapid that is formed on the downstream side of the flume (Werner 2016).

Table A1-1 in Appendix 1 presents geographical positions of the gauging stations and elevations of upstream edges of flume bottoms and of top of observation wells. Elevations of upstream edges are used for calculation and adjustment of water levels and water depth-based calculation of stream discharges (Johansson and Juston 2011b). As described in more detail in Section 3.4.3, 2012–2017 levelling campaigns indicate that all flumes may have moved vertically since they were installed, including movements during the period 2012–2017. However, the levelling performed at time of the original flume installations had less accuracy compared to the 2012–2017 levelling, which implies that actual vertical movements subsequent to flume installations are uncertain. The influence of vertical flume movements on discharge calculations, and reduction of potential errors by manual water-depth measurements, are described in Section 3.4.3 and also in Werner (2014a, Appendix 2).

Table 2-1 presents flume-specific, recommended discharge intervals and discharge equations, i.e. equations and associated parameters used to convert water depths to stream discharges. The recommended equations, parameters and discharge intervals are derived using the WinFlume software, including flumes of standard factory designs (i.e. equations, parameters and intervals provided by the manufacturer are not used). The applicability of equations and parameters have been investigated by independent discharge measurements (see Section 2.3). As shown in Table 2-1, the upper discharge limit for the small flumes is 20 L/s, which corresponds to a water depth of approximately 0.23 m. According to Johansson (2005), the mathematical errors associated with the truncated stage-discharge relationships are less than ± 2 % for all flumes in Forsmark.

Table 2-1. Stage-discharge relationships (discharge equations) for the flumes and associated recommended discharge ranges. Q = discharge (L/s), h = water depth (m). The PFM005764 large-flume equation up to Oct. 1, 2004 was based on calibration measurements under subcritical flow conditions (Johansson 2005).

Id	Discharge eq.	Recommended range (L/s)
PFM005764		
Nov. 27, 2003–Oct. 1, 2004		
Small flume (QFM1:1)	$Q = 864.9 \cdot h^{2.576}$	0–20
Large flume (QFM1:2)	$Q = 1\,175 \cdot h^{2.15}$	20–70
Oct. 5, 2004–		
Small flume (QFM1:1)	$Q = 864.9 \cdot h^{2.576}$	0–20
Large flume (QFM1:2)	$Q = 2\,298 \cdot (h + 0.03459)^{2.339}$	20–1 400
PFM002667		
Dec. 8, 2004–Aug. 16, 2018		
Small flume (QFM2:1)	$Q = 864.9 \cdot h^{2.576}$	0–20
Large flume (QFM2:2)	$Q = 2\,001.5 \cdot (h + 0.02660)^{2.561}$	20–500
Aug. 30, 2018–		
QFM2	$Q = 978.5744646 \cdot h^{2.577}$	0–150
PFM002668		
QFM3	$Q = 979.1 \cdot h^{2.574}$	0–250
PFM002669		
Small flume (QFM4:1)	$Q = 864.9 \cdot h^{2.576}$	0–20
Large flume (QFM4:2)	$Q = 1\,117.6 \cdot (h + 0.02727)^{2.604}$	20–920

The data collecting system, which is part of HMS, consists of a computer that collects data from a large number of data loggers and associated sensors. The computer is connected to the SKB Ethernet LAN. All data were collected by means of pressure, EC and temperature transducers, which previously were connected to Mitec Sat60 GSM data loggers, connected on-line by means of GSM telephony. At stations equipped with temperature-sensitive Mitec data loggers, the measured water level must be compensated for temperature (e.g. Werner 2016). Therefore, previous monitoring reports used temperature-compensated water levels available in so called HBV channels (previously denoted BH) in HMS. Uncompensated water levels, which are available in HMV channels (previously denoted MH) in HMS, were used in the discharge calculations of Johansson and Juston (2007, 2009, 2011a, b) for the period April 2004–December 2010. Differences in compensated and uncompensated water levels are discussed as part of the evaluation of the PFM005764 refurbishment and reconstruction (Werner 2016). However, no systematic analysis has yet been performed on the difference in calculated discharge using compensated or uncompensated water levels.

As part of the 2014 and 2018 refurbishments and reconstructions, temperature-sensitive Mitec data loggers were switched to a temperature-insensitive dataTaker DT85 data logger at PFM005764 (Werner 2016) and a temperature-insensitive Cube300S data logger at PFM002667 (Werner 2019). Moreover, at PFM002668 and -2669 Mitec loggers were replaced by Cube300S data loggers in 2019 (April 17 and 27, respectively).

Water levels at the upstream edge of flumes were measured using vented Druck PTX 1830 pressure sensors (full scale pressure range 1.5 m w.c., accuracy 0.1 % of full scale). EC (electrical conductivity) was measured by GLI 3442 sensors, range 0–200 mS/m, accuracy 0.1 % of full scale, whereas temperature was measured using Mitec MSTE106 (range 0–120 °C) and Sat60 (range –40 to +120 °C).

In connection to the PFM002667 refurbishment and reconstruction in 2018, the Druck pressure sensor was replaced by a LevelTroll 700 pressure sensor, whereas the EC and temperature sensors were replaced by a single Aqua TROLL 200 sensor (Werner 2019). Furthermore, LevelTroll 700 pressure sensors and Aqua TROLL 200 EC and temperature sensors replaced previous sensors at PFM002668 and -2669 in April 2019 (cf above).

2.2 Practical experiences, field inspections and independent discharge measurements

For summaries of practical experiences, field inspections and independent discharge measurements (discharge measurements independent of ordinary water-level measurements and flow calculations) up to the end of the 2017/2018 hydrological year, the reader is referred to previous data reports (Werner 2014a, b, 2016, 2017, 2018a, b, 2019) and reports from independent discharge measurements (Bergqvist 2014a, b, c, Werner 2015, Ryman and Strömbeck 2016, 2018). With few exceptions, independent discharge measurements have only been performed when the prevailing discharge is above the discharge interval for the small flumes, as it is practically difficult to perform measurements when discharges are small.

Experiences, inspections and other investigations have led to the conclusion that the gauging stations need to be refurbished and reconstructed to improve their performance, accuracy of measurements and to make them more stable and thereby suitable for long-term monitoring. In accordance with this conclusion, refurbishments and reconstructions of the PFM005764 station (Werner 2016) and the PFM002669 station (Werner 2017) were done during August 2014 and August–September 2015, and the PFM002667 station was refurbished and reconstructed in August 2018 (Werner 2019).

2.3 Data handling and post processing

2.3.1 General

Data on water levels, electrical conductivities and temperatures were collected to and stored in HMS, and quality-controlled data were transferred to the Sicada database. Hourly average discharge values were calculated based on the quality-controlled water-level data and flume-bottom levels (cf Table A1-1 in Appendix 1) and also transferred to Sicada.

2.3.2 Water-level calibration

As mentioned in Section 2.1, water levels in the flumes are measured by pressure sensors installed in observation wells located alongside of each flume. The pressure data from the data loggers were converted to water levels by a linear equation. As part of the regular quality control (Section 3.4.1), water depths in the flumes were regularly measured using a folding rule. In order to provide a basis for evaluations of water-depth measurements, manual sounding of observation wells has also been done in parallel with the water-depth measurements since July 2013.

As part of the regular quality control, water levels measured automatically in observation wells were compared to manually measured water levels (flume-bottom level + water depth), and adjusted in case of poor fit (difference of a few millimetres or more) to manual measurements. Specifically, the linear equation for each flume involves a flume-specific calibration constant, which also includes a flume-independent factor for conversion from water pressure to water level. This constant was adjusted in cases of two or more subsequent mismatches between manual and automatic water-level measurements, at a point in time approximately midway between the manual measurements. Hence, calibration constants were not adjusted as a result of solitary mismatches.

Table 2-2 lists those dates at which the flume- and instrument-specific calibration constants have been adjusted, from initiation of water-level measurements up to the end of 2019. It is recommended that future monitoring reports also present directions and magnitudes of calibration-constant adjustments. As can be seen in the table, calibration constants have regularly been adjusted in order to maintain fits between manual and automatic water-level measurements. Flumes were reinstalled and taken into new operation at PFM005764 and PFM002669 in October 2004 and November 2007 (the PFM002669 observation wells were also reinstalled), respectively. Moreover, the PFM005764 small-flume observation well was reinstalled (lowered) in September 2006. As seen in Table A1-1 in Appendix 1, irrespective of the PFM005764 well reinstallation (September 2006), the PFM002669 flume and well reinstallation (November 2007), and also irrespective of results of repeated levelling campaigns, originally measured flume-bottom levels have been kept as reference levels. Deliberate or naturally caused well and flume movements have been handled by calibration-constant adjustments. Moreover, temperature compensations of Mitec loggers (introduced in December 2005) are noted in the HMV channels of HMS, but have not rendered any calibration-constant adjustments.

2.3.3 Controls of EC and temperature

As mentioned in Section 2.1, EC and temperature sensors are mounted on the outside of the PFM002668 screened tube (downstream of the flume), and inside the screened tubes upstream of the flumes at the other stations (after refurbishments). Linear equations were used also to convert data from the EC and temperature sensors. As part of the regular quality control (Chapter 3), EC and temperature were measured outside of tubes using a hand-held instrument. Changes of calibration constants were made in connection to the PFM005764 and PFM002667 refurbishments and reconstructions in August 2014 and 2018 (switches to dataTaker and Cube loggers). Changes were also made in connection to switches from Mitec to Cube loggers at PFM002668 and -2669 in April 2019.

2.3.4 Recording interval

Recording intervals were irregular, generally varying between 1 minute and 30 minutes (10 minutes for water level). The scanning frequency is once per minute. Except the set recording interval (10 minutes), a water-level data value is recorded if the water-level change between scanning events is larger than 1–2 mm. For EC and temperature, except the set recording interval a data value is recorded if the EC change is > 0.1 mS/m and the temperature change is > 0.1 °C, respectively.

Table 2-2. Dates for water-level calibration-constant adjustments at each gauging station, from initiation of water-level measurements up to the end of 2020.

Gauging station and flume	Adjustment dates (YYYY-MM-DD)
PFM005764	
Small flume	2004-03-01, 2004-08-06, 2004-10-07 (reinstallation of flume), 2005-07-01, 2005-08-01, 2005-10-22, 2005-12-13 (temp. comp.), 2006-04-15, 2006-05-01, 2006-09-13 (reinstallation of obs. well), 2006-12-19, 2007-04-15, 2007-06-15, 2007-08-01, 2007-09-01, 2007-11-01, 2009-01-16, 2009-07-01, 2009-09-01, 2010-07-01, 2010-08-01, 2011-12-01, 2012-01-01, 2013-03-01, 2013-07-01, 2014-08-26 (refurbishment, switch from Mitec to dataTaker logger), 2015-06-27, 2015-07-06, 2016-01-01, 2016-07-01, 2017-12-07, 2017-12-11, 2018-05-04, 2019-06-13, 2019-08-13, 2020-05-19, 2020-10-19
Large flume	2004-03-01, 2004-08-06, 2004-10-07 (reinstallation of flume), 2005-01-11, 2005-10-22, 2005-12-13 (temp. comp.), 2007-09-24, 2007-12-01, 2008-01-15, 2008-08-09, 2009-03-10, 2009-05-01, 2009-09-01, 2011-09-01, 2011-10-01, 2014-08-26 (refurbishment, switch from Mitec to dataTaker logger), 2016-04-14, 2017-01-27, 2017-05-24, 2019-05-03, 2019-06-11, 2020-02-07, 2020-10-26 Water-level bubbler: 2018-01-09, 2019-05-03, 2019-06-11, 2020-05-27, 2020-07-01
PFM002667	
Small flume	2004-10-01, 2005-12-15 (temp. comp.), 2006-10-20, 2006-12-15, 2007-09-06, 2008-08-01, 2008-11-01, 2009-03-12, 2010-06-01, 2010-07-01, 2011-11-10, 2012-03-08, 2012-05-10, 2012-09-01, 2012-10-01, 2013-09-01, 2014-02-01, 2014-11-11, 2015-02-11, 2015-03-25, 2015-06-25, 2017-03-15, 2017-04-26
Large flume	2004-10-01, 2005-02-14, 2005-04-01, 2005-05-01, 2005-12-15 (temp. comp.), 2006-12-15, 2007-01-01, 2007-09-06, 2007-11-01, 2008-01-01, 2008-08-09, 2008-09-01, 2008-11-15, 2009-03-12, 2009-07-01, 2009-08-01, 2009-10-26, 2010-05-01, 2010-09-01, 2012-05-16, 2012-07-16, 2013-04-15, 2013-06-01, 2017-03-15, 2017-05-15
PFM002667	2018-10-25 (refurbishment, switch from Mitec to Cube logger)
PFM002668	2004-10-01, 2005-07-22, 2005-12-15 (temp. comp.), 2006-08-20, 2006-10-23, 2008-08-09, 2009-07-01, 2009-11-01, 2010-05-15, 2010-06-15, 2011-12-10, 2012-01-10, 2013-07-01, 2013-12-01, 2014-06-01, 2014-10-01, 2015-10-02, 2017-06-26, 2018-12-26, 2019-04-17 (switch from Mitec to Cube logger), 2019-07-15, 2020-04-07, 2020-05-15
PFM002669	
Small flume	2004-10-01, 2005-08-05, 2005-12-15 (temp. comp.), 2006-02-10, 2006-02-23, 2007-11-12 (reinstallation of flume and obs. well), 2008-07-02, 2008-08-09, 2008-09-01 (no change of cal. const.), 2008-12-01, 2009-03-02, 2009-09-01, 2010-02-01, 2011-11-01, 2011-12-01, 2012-03-01, 2012-04-01, 2015-09-15 (refurbishment), 2017-11-28, 2019-04-26, 2019-04-27 (switch from Mitec to Cube logger), 2019-05-03, 2019-06-15, 2020-01-01, 2020-01-24, 2020-03-01, 2020-06-01
Large flume	2004-10-01, 2005-02-14, 2005-08-05, 2005-12-15 (temp. comp.), 2006-02-10, 2006-10-25, 2007-06-30 (reinstallation of flume and obs. well), 2008-02-12, 2009-03-04, 2009-03-27, 2009-07-01, 2009-08-01, 2012-11-01, 2011-12-01, 2012-07-01, 2012-10-01, 2012-10-08, 2013-01-08, 2013-04-15, 2013-06-01, 2014-06-01, 2014-11-01, 2015-09-15 (refurbishment), 2019-04-27 (switch from Mitec to Cube logger), 2019-06-26, 2019-10-19 (twice), 2019-10-23, 2019-10-25, 2020-01-01, 2020-01-24

2.3.5 Calculation of discharge

Discharge was calculated for each flume using water levels stored in the HBV channels (previously denoted BH) in HMS. The calculation procedure consisted of the following steps:

- Quality control of the October 1, 2019–September 30, 2020 high-resolution water-level dataset (see Section 3.4.2).
- Calculation of hourly average water levels using the high-resolution, screened dataset.
- Calculation of hourly average discharges for each flume using hourly average water levels, the stage-discharge relationships shown in Table 2-1, and the bottom level at the upstream edge of each flume shown in Table A1-1 in Appendix 1.

Table 2-3 presents levelled small-flume bottom elevations and elevations to signify zero discharge. If the hourly average water level is at or below the zero-discharge levels for the small flumes the discharge is set to zero (Johansson 2005). Specifically, these levels represent the levels of the connections between pipes and observation wells, which due to installation issues are above the bottom of the upstream edge of three of the four small flumes. As can be seen in Table 2-3, this issue has been resolved at the refurbished gauging stations; the PFM005764 small-flume observation well was also reinstalled in September 2006. In Table 3-2 it is noted that the single flume at PFM002667 is levelled in the coordinate system RH 2000 (Hermansson 2019). Elevation in the RHB 70 system is calculated as RH 2000 – 0.185 m.

There is a single flume at gauging stations PFM002667 and -2668, whereas there are two flumes at the other two stations (PFM005764 and -2669) with given discharge ranges (cf Table 2-1). For the latter gauging stations, a single discharge time series for each station was obtained according to the station-specific discharge-calculation rules described below. In some cases, these rules lead to short-term, artificial discharge fluctuations. Specifically, such fluctuations occur during periods with transitions between the small and the large flume at PFM005764 and -2669, i.e. when the discharge calculated for the small flume fluctuates around 20 L/s. In contrast to the rules stated for the PFM005764 gauging station, periods of missing discharge data were reduced by using the discharge calculated for the large flume when small-flume data were missing.

- **PFM005764:**
  - The discharge was set equal to the discharge calculated for the small flume if the small-flume discharge was less than 20 L/s.
  - The discharge was set equal to the discharge calculated for the large flume if the small-flume discharge was above 20 L/s and if the large-flume discharge was above 16 L/s.
- **PFM002669:**
  - The discharge was set equal to the discharge calculated for the small flume if the small-flume discharge was less than 20 L/s.
  - The discharge was set equal to the discharge calculated for the large flume if both small- and large-flume discharges were above 20 L/s.

Table 2-3. Levelled small-flume bottom elevations and elevations to signify zero discharge.

Gauging station	Bottom elevation (m, RHB 70) of upstream edge	Elevation (m, RHB 70) signifying zero discharge
PFM005764 (up to Aug. 25, 2014)	0.903	0.903 (0.990 prior to Sep. 13, 2006, when the observation well was lowered)
PFM005764 (from Aug. 26, 2014)	0.924	0.924 (station refurbished)
PFM002667 (up to Aug. 16, 2018)	1.502	1.518
PFM002667 (single flume, from Aug. 30, 2018)	1.580	1.580
PFM002668 (single flume)	4.287	4.296
PFM002669 (up to Sep. 14, 2015)	5.852	5.872
PFM002669 (from Sep. 15, 2015)	5.441	5.441 (station refurbished)

3 Results of stream monitoring

3.1 General

The results are stored in Sicada where they are traceable by the Activity Plan number. Only data stored in the primary database are accepted for further interpretation and modelling.

3.2 Results of field work

According to the activity plan (see Table 1-2) the gauging stations are to be inspected at least once a week. If needed, stations and stream reaches immediately upstream and downstream of the stations are to be cleaned from debris, vegetation, snow and ice, and EC sensors are to be cleaned using hydrochloride. Moreover, manual measurements of the water depth at the upstream edge of each flume are to be done at least every second week, and EC and temperature are to be measured manually once per month. Note that such measurements are not possible when water levels are low or flumes are dry, which implies that actual measurement intervals may be longer than stipulated.

During the hydrological year October 1, 2019–September 30, 2020, manual measurements of the water depth at the upstream edge of each flume using a folding rule were done on 8–9 occasions, whereas the depth to water was measured on 3 occasions in the PFM007564 observation well hosting the water-level bubbler (measurements were not possible when flumes were dry). Manual EC and temperature measurements, using a hand-held instrument (HACH HQ 14D), were done on 5–6 occasions (see above) during the 2019/2020 hydrological year.

The results of the manual measurements were stored in Lodis, which is SKB's database for manual measurements. Lodis data on water depths, EC and temperature were regularly transferred to HMS (but not to Sicada), where water depths are automatically transformed to water levels based on flume-bottom levels (cf Table A1-1 in Appendix 1). Specifically, manually measured water levels (based on measured water depths) were used for comparison with automatically measured water levels (see further details in Section 3.3.1).

3.3 Water level and discharge

3.3.1 Quality control

As a result of regular quality control, all water-level data have been approved for the whole data period of this report, i.e. up to and including September 30, 2020. Appendix 2 presents high-resolution water-level data from the four gauging stations during the 2019/2020 period. It is reminded that natural or deliberate flume movements are handled by calibration-constant adjustments, aiming to match manually measured in-flume water depths. Hence, the presented water levels are more or less incorrect in absolute terms.

The regular quality control concerns water-level data, neither EC nor temperature data (cf quality-control reports in Table 1-1). Once every week, it was checked that loggers were sending data and that all sensors were in function. Another check was performed four times during the data period of this report. Calibration constants were corrected (Table 3-1) in order to match automatically and manually measured water levels, i.e. water depths plus flume-bottom levels. On the occasions when water depths were measured manually, the status of the equipment was also checked and maintained if needed. The field maintenance included, for instance, removal of snow and ice and cleaning of EC sensors using hydrochloride (Section 3.2). The results of regular quality control are summarized in the following:

- **PFM005764:**
  - Small flume: Water-level data are error marked and hence missing due to unreasonable water-level fluctuations November, 2019–May 2020.
  - Large flume: Water-level data are error marked and hence missing due to unreasonable water-level fluctuations December, 10 2019–February 7, 2020, at which time the pressure transducer was replaced.

- **PFM002667:** Due to data logger problems, water-level data are occasionally missing during the period June–September 2020.
- **PFM002668:** Water-level data are error marked and hence missing during a period in November 2019, in January–February 2020 and in April 2020 due to technical problems with the Cube data logger. Water-level data are also missing a couple of days in May 2020 in connection to switch of the data logger. Due to data logger problems, water-level data are occasionally missing during the period June–September 2020.
- **PFM002669:** Water-level data are error marked and hence missing during a period in November 2019 due to low battery voltage in the Cube data logger, and in March 2020 due to technical problems with the data logger. Due to data logger problems, water-level data are occasionally missing during the period June–September 2020.

Apart from the regular quality control described above, a supplementary quality control was done of the whole 2019/2020 dataset, including EC and temperature data. Tables 3-1, 3-2 and 3-4 summarise the outcome of this quality control, in terms of data periods excluded from the HMS to Sicada data transferral, and reasons for the exclusions. Note that the quality control was performed on high-resolution data.

Table 3-1. Water-level data excluded from the HMS to Sicada data transferral, as a result of the supplementary quality control of the 2019/2020 dataset.

Gauging station (flume)	Dates and times (YYYY-MM-DD hh:mm)	Reason for exclusion (WL = water level)
PFM005764	No data excluded	
PFM002667	No data excluded	
PFM002668	No data excluded	
PFM002669 (small flume)	2020-09-11 07:30–2020-09-30 23:50	Likely due to low WL

3.3.2 Results of water-level monitoring

Water level data are stored in Sicada as Sicada Activity Type HY096–HMS monitoring surf. w level-small flume and HY097–HMS monitoring surface w level-big flume. Appendix 2 presents high-resolution water level data from the four gauging stations during the 2019/2020 period. During the period of this report, there are some water-level data gaps, i.e. data are missing in HMS, in particular for the gauging station PFM005764 but also for the other stations except PFM002667. Note that the quality control of the 2019/2020 dataset also results in some further data gaps (hourly values are missing) for station PFM002669, apart from data missing in HMS.

3.3.3 Flume and well levelling: Results and influence on discharge calculations

The gauging stations have been exposed to surface-water flow, debris and ice since 2004, which likely have influenced the stability of the flumes. In particular, the level of the bottom of the upstream edge of each flume, which is used to calculate the discharge, was levelled at time of installation. In order to check whether these levels are still valid, new levelling was done in June, September and October 2012 (Edvardson 2012), in June, August and September 2013 (SWECO 2013), in May and June 2014 (Edvardson 2014), in June 2015 (Edvardson 2015), in May 2016 (Ohrzén 2016), and in May–June 2017 (Hermansson 2017). The results of the levelling at time of flume and well installations and at the 2012–2017 levelling campaigns, which have a stated level accuracy of ±2 mm, are shown in Table A1-2 and Table A1-3 in Appendix 1. As mentioned in Section 2.1, the levelling performed at time of installations had less accuracy compared to the recent levelling campaigns. This implies that actual vertical movements during the period from flume and well installations to subsequent levelling campaigns are uncertain.

As can be seen in Table A1-2 and Table A1-3 in Appendix 1, flume and well movements since the original levelling seem to be particularly large for gauging station PFM002667 (both flumes have raised c 0.06 m and both wells c 0.08–0.09 m). The large vertical movements at PFM002669 are due to that both flumes wells were reinstalled in 2007. For some flumes (e.g. PFM005754 and -2669) the 2012–2015 levelling results are inconsistent, primarily the results of the 2013 levelling campaign, an issue which is related to the actual inaccuracies of the levelling. It is therefore recommended that evaluations of levelling methods and associated accuracies are integrated parts of continued levelling campaigns.

As discussed further in the corresponding 2011–2012 and 2013 dataset reports (Werner 2014a, b), potential flume movements raise the question of the validity of the discharge equations and their associated parameters. It was shown that vertical flume movements likely have small effects on discharge calculations, provided that manual water-depth measurements in the flumes are done regularly and with high accuracy (Werner 2014a). Adjustments of calibration constants to fit automatic and manual water-level measurements reduce potential errors due to vertical flume movements. The validity of discharge equations and associated parameters due to e.g. unlevelled flumes perpendicular to the stream-flow direction can be checked by independent discharge measurements (cf Section 2.2).

3.3.4 Nonconformities

The activity plans (Table 1-2) state that manual water-depth measurements are to be performed at least every second week. However, due to low water levels or dry flumes such measurements were only possible at 8–9 occasions during the period October 1, 2019–September 30, 2020 (Section 3.2). It is important that sufficient resources are allocated so that routines stated in activity plans can be followed also in the future.

3.3.5 Calculated discharge

Data on calculated discharge are stored in Sicada as Sicada Activity Type HY098–HMS stream flow rate – hourly data. Appendix 3 presents hourly average (screened) discharge data from the four gauging stations during the 2019/2020 period, calculated based on the stage-discharge relationships of Table 2-1. Due to technical problems and as a result of quality control, hourly average discharge data are missing for totally 18 % of the time for the PFM005764 station, less than 1 % of the time for the PFM002667 station, 10 % of the time for the PFM002668 station, and 21 % of the time for the PFM002669 station. Average, minimum and maximum discharges, affected by the mentioned data gaps, are shown in Table 3-2.

Table 3-2. Average, minimum and maximum discharges (screened data, rounded to integers) during the hydrological year October 1, 2019–September 30, 2020. Note that the statistics are affected by data gaps, in particular for the PFM005764 and -2669 stations.

	PFM005764	PFM002667	PFM002668	PFM002669
Average discharge (L/s)	30	21	17	26
Median discharge (L/s)	12	9	6	12
Min. discharge (L/s)	0	0	0	0
Max. discharge (L/s)	187	111	83	117
Missing hourly values (%)	18.0	0.9	10.2	20.7

3.3.6 Follow-up of completed refurbishments and reconstructions

Follow-up of refurbishment and reconstruction of the PFM005764 station

As mentioned above, a water-level bubbler was installed in the observation well connected to the large flume at the PFM005764 station, to be monitored in parallel with pressure-sensor measurements. The intention is to investigate whether temperature, air pressure and/or moisture conditions inside the cottage above the large flume may influence measurements using a vented pressure sensor (Werner 2018a). Werner (2019) compared water-level time series for the pressure sensor and the water-level bubbler for an initial monitoring period, whereas a comparison for the 2018/2019 hydrological year was presented in Werner (2020). Due to installation issues, the water-level bubbler provided unreliable data during the first months after installation, whereas data are more reliable from April 2018 and onwards.

Figure 3-1 and Figure 3-2 present an updated comparison for the hydrological year 2019/2020 in terms of water level. In general, there is a close match between bubbler and pressure sensor measurements. As was also noted in Werner (2019, 2020), the ”straight line” in the end of the hydrological year (Figure 3-2) likely represents the lower measurement limit of the water-level bubbler. For the 2019/2020 hydrological year, the average difference between pressure sensor and bubbler water levels is −0.0008 m, ranging between −0.0136 m and 0.0108 m. Observe that instrument-specific calibration constants have been adjusted to maintain fits between manual and automatic water-level measurements (cf Table 3-1).

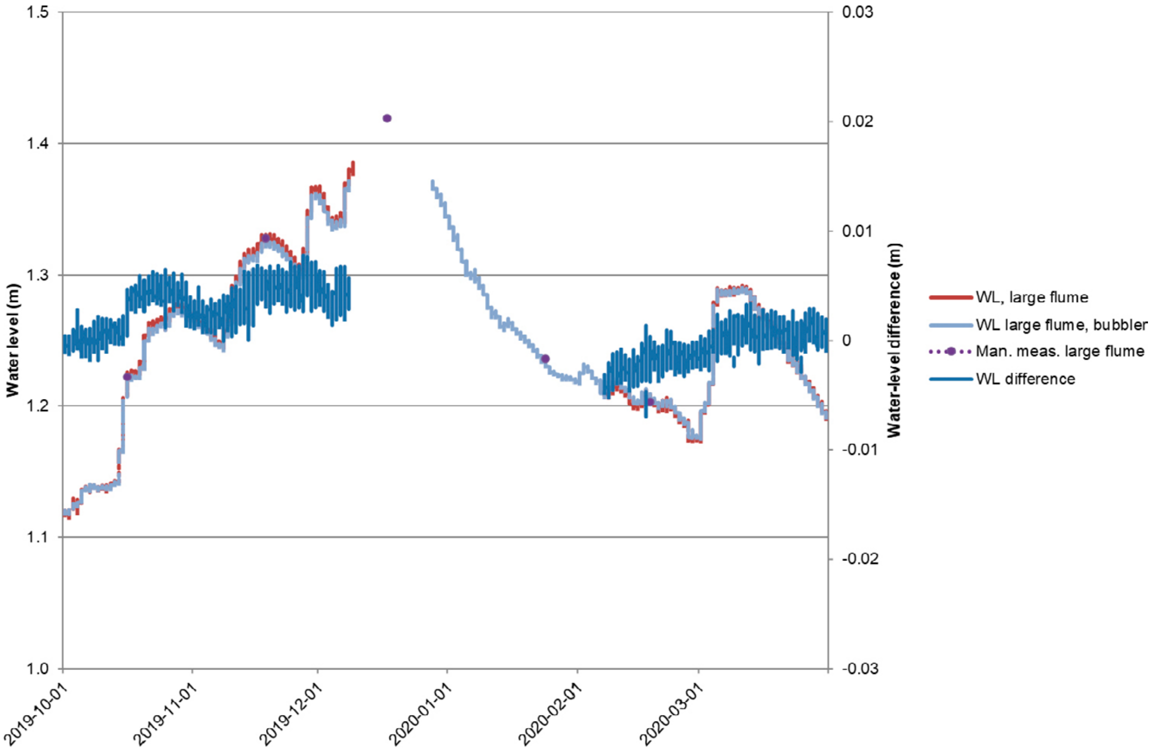

Figure 3-1. *Comparison of water-level time series for the pressure sensor and the water-level bubbler installed in the observation tube at the large flume at gauging station PFM005764 for the period October 1, 2019–Mar. 31, 2020. The plot also displays the water-level difference between the pressure sensor and the bubbler.*

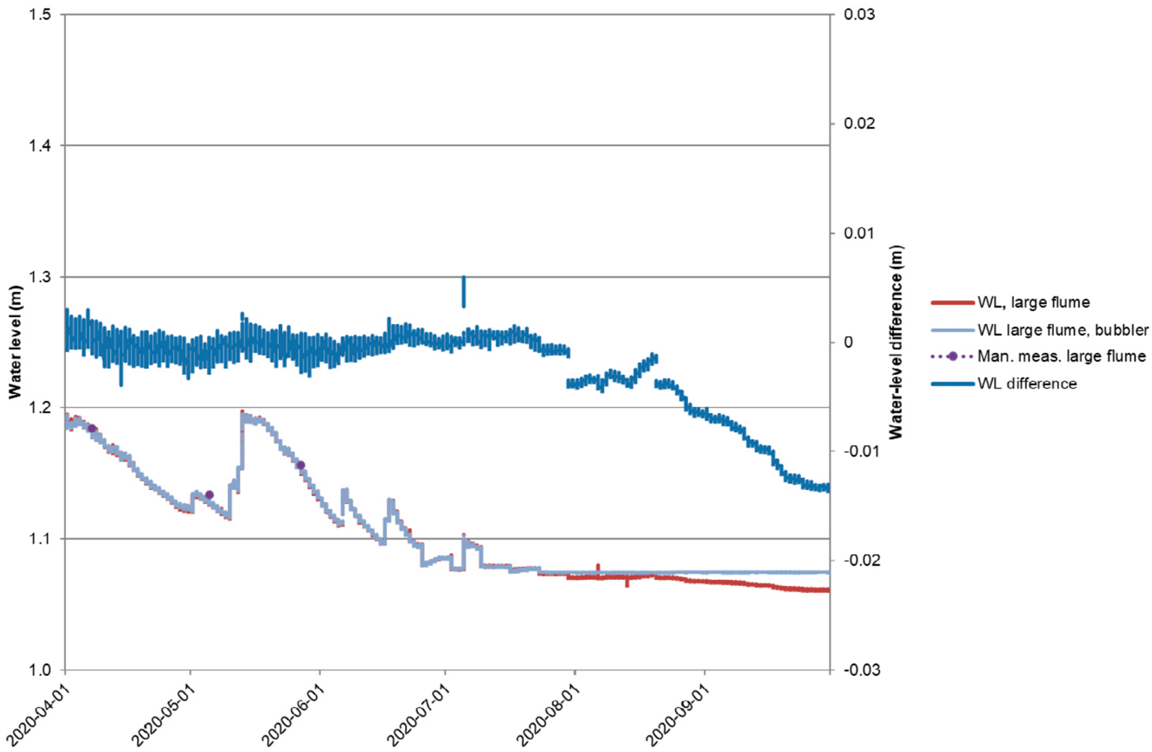

Figure 3-2. *Comparison of water-level time series for the pressure sensor and the water-level bubbler installed in the observation tube at the large flume at gauging station PFM005764 for the period Apr. 1–Sep. 30, 2020. The plot also displays the water-level difference between the pressure sensor and the bubbler.*

Follow-up of refurbishment and reconstruction of the PFM002667 station

As described in Werner (2019) the PFM002667 station was refurbished in August 2018. The objectives were to prepare the station for long-term monitoring and to relieve some issues related to the flat landscape. Prior to the refurbishment and reconstruction, the large flume at PFM002667 generally yielded realistic discharge values only up to c 55 L/s (e.g. Werner 2018a), and the small flume caused converging, supercritical flow and turbulence that disturbed the inflow to the large flume. Among other actions, the two flumes at the station were replaced by a single flume, and a small pond was excavated upstream of the flume to reduce the approach flow velocity and reduce risks for turbulence.

The new flume is designed using the WinFlume software (Wahl et al. 2000, Bergqvist 2019). The discharge range of the flume itself is 0–250 L/s, whereas the stage-discharge relationship (Table 2-1) at the given setting is considered to be applicable for the discharge range 0–150 L/s. According to WinFlume calculations, the mathematical error of the truncated stage-discharge relationship for the new flume is ±2.5 % at 20 L/s and ±4 % at 1 L/s (Bergqvist 2019). For CAD and WinFlume drawings of the flume, see Werner (2019). Levelling of the new flume subsequent to the PFM002667 refurbishment and reconstruction is presented in Hermansson (2019).

As was also noted in Werner (2020), the new flume and associated equipment appear to work satisfactorily. The maximum calculated discharge during the 2019/2020 hydrological year was 111 L/s; see Section 3.3), and no water-level data were excluded from HMS to Sicada transfer as a result of regular quality control (Section 3.2). Due to low water level, some EC and temperature data were excluded as a result of quality control of the 2019/2020 dataset (Section 3.4 and Section 3.5). Further evaluation of the refurbished and reconstructed PFM001267 station is recommended when longer time series are available.

3.4 Electrical conductivity

3.4.1 Quality control

Table 3-3. EC data excluded from the HMS to Sicada data transferral, as a result of the quality control of the 2019/2020 dataset.

Gauging station	Dates and times (YYYY-MM-DD hh:mm)	Reason for exclusion (WL = water level)
PFM005764	2020-03-06 12:20–12:27	Negative EC
PFM005764	2020-03-07	Negative EC
PFM005764	2020-04-01 11:58–12:08	Negative EC
PFM005764	2020-04-02 07:42–07:58	Negative EC
PFM005764	2020-07-24 07:15–2020-07-30 21:47	Low/negative EC (likely due to low WL)
PFM005764	2020-08-12 15:46–2020-09-30 23:30	Low/negative EC (likely due to low WL)
PFM002667	2020-06-26 17:50–2020-07-07:06:00	Low/zero EC (likely due to low WL)
PFM002667	2020-07-16 15:00–2020-09-30:23:30	Low/zero EC (likely due to low WL)
PFM002668	2020-03-14 04:10–2020-03-15 02:40	Zero EC
PFM002668	2020-03-23 02:50–2020-03-24 06:10	Zero EC
PFM002668	2020-03-31 21:40–2020-04-01 09:30	Zero EC
PFM002668	2020-05-03 23:50–2020-05-15 13:11	Zero EC
PFM002668	2020-06-16 04:30	Single EC peak
PFM002668	2020-06-25 11:00–2020-07-05 18:30	Low/zero EC (likely due to low WL)
PFM002668	2020-07-16 19:10–2020-07-30 18:20	Low/zero EC (likely due to low WL)
PFM002668	2020-08-03 15:10–2020-09-30 23:30	Low/zero EC (likely due to low WL)
PFM002669	2020-02-10 23:30–2020-2-11 00:20	Low/negative EC values (likely due to low WL)
PFM002669	2020-02-13 01:20–06:30	Low/negative EC values (likely due to low WL)
PFM002669	2020-03-02 02:20–11:30	Single outliers (likely due to low WL)
PFM002669	2020-06-18 01:03	Single outliers (low/negative EC values)
PFM002669	2020-07-14 11:50–12:20	EC drop
PFM002669	2020-07-18 03:00–2020-07-31 01:10	Low/zero EC
PFM002669	2020-08-03 13:00–2020-08-26 07:40	Zero EC
PFM002669	2020-09-07 11:10–2020-09-30 23:30	Zero EC

3.4.2 Results of EC monitoring

Electrical-conductivity data are stored in Sicada as Sicada Activity Type HY094–HMS Monitoring surface water EC. Appendix 4 presents high-resolution EC data from the four gauging stations during the 2019/2020 period, whereas average, minimum and maximum EC values (based on screened data) are shown in Table 3-4. As a result of the quality control of the 2019/2020 dataset (Section 3.4.2), EC data were excluded from the HMS to Sicada data transferral during periods with low or negative EC values.

Table 3-4. Average, minimum and maximum EC (screened data, rounded to integers) during the hydrological year October 1, 2019–September 30, 2020.

	PFM005764	PFM002667	PFM002668	PFM002669
Average EC (mS/m)	28.5	26.7	24.2	32.9
Min. EC (mS/m)	1.0	1.1	1.0	1.5
Max. EC (mS/m)	64.6	55.2	42.5	41.6

3.5 Temperature

3.5.1 Data availability and quality control

Table 3-5. Temperature data excluded from the HMS to Sicada data transferral, as a result of the quality control of the 2019/2020 dataset.

Gauging station	Dates and times (YYYY-MM-DD hh:mm)	Reason for exclusion (WL = water level)
PFM005764	2020-07-24 07:15–2020-07-31 21:30	Fluctuating temperatures (likely due to low WL)
PFM005764	2020-08-12 00:00–2020-09-30 23:30	Fluctuating temperatures (likely due to low WL)
PFM002667	2020-06-25 00:00–2020-07-07 06:00	Fluctuating temperatures (likely due to low WL)
PFM002667	2020-07-16 00:00–2020-09-30 23:30	Fluctuating temperatures (likely due to low WL)
PFM002668	2020-03-14 04:10–2020-03-15 02:40	Temperature drop
PFM002668	2020-03-23 02:50–2020-03-24 06:10	Temperature drop
PFM002668	2020-03-31 21:40–2020-04-01 09:30	Temperature drop
PFM002668	2020-05-03 23:50–2020-05-15 13:11	Zero temperatures
PFM002668	2020-06-25 00:00–2020-07-05 23:30	Fluctuating temperatures (likely due to low WL)
PFM002668	2020-07-16 00:00–2020-09-30 23:30	Fluctuating temperatures (likely due to low WL)
PFM002669	2020-07-18 00:00–2020-07-31 23:40	Fluctuating temperatures (likely due to low WL)
PFM002669	2020-08-03 00:00–2020-08-26 07:40	Fluctuating temperatures (likely due to low WL)
PFM002669	2020-09-07 11:10–2020-09-30 23:30	Fluctuating temperatures (likely due to low WL)

3.5.2 Results of temperature monitoring

Temperature data are stored in Sicada as Sicada Activity Type HY093–HMS Monitoring river water temperature. Appendix 5 presents high-resolution water-temperature data from the four gauging stations during the 2019/2020 period, whereas average, minimum and maximum temperature values (based on screened data) are shown in Table 3-6. As a result of the quality control of the 2019/2020 dataset, temperature data were excluded from the HMS to Sicada data transferral during periods with high or fluctuating temperature values. This includes a high-temperature period for gauging station PFM002668 (Appendix 5), which explains the relative low maximum temperature for that station.

Table 3-6. Average, minimum and maximum temperature (screened data, rounded to integers) measured at the gauging stations PFM005764, -2667, -2668 and -2669 during the hydrological year October 1, 2019–September 30, 2020. The statistics are affected by data gaps.

	PFM005764	PFM002667	PFM002668	PFM002669
Average temp. (°C)	8	6	7	7
Min. temp. (°C)	−0.1	−0.1	−0.1	−0.1
Max. temp. (°C)	25	25	22	22

4 Results of other hydrology-related monitoring

4.1 General

The stream monitoring described in this report is part of an extensive programme for monitoring of the rock and the surface system in Forsmark (SKB 2007). The monitoring provides data and information for various types of conceptual and quantitative modelling, which in turn form the basis for site descriptions, assessments of long-term radiological safety and environmental impact assessments. The present report and previous stream-monitoring reports (see Chapter 1) are focused on data reporting, i.e. to report and summarise the gathered monitoring data, and to put attention to data gaps, data uncertainties and required/performed changes of monitoring methods or installations. Moreover, recurrent monitoring-data evaluations are important for maintenance of the site understanding, and as a basis for identification of potential anthropogenic disturbances (Berglund and Lindborg 2017).

The following sections provide an overview of and use some results from other hydrology-related monitoring in Forsmark, as illustrative examples on integrated evaluations that may provide insight into near-surface hydrological interactions. Similar integrated evaluations were presented in the 2015, and 2015/2016–2018/2019 monitoring-data reports (Werner 2017, 2018a, b, 2019, 2020). For instance, these previous evaluations showed that stream discharge and ground- and surface-water levels increase in response to precipitation and/or minor snow-melt events during autumn and winter. It was also observed increasing stream discharge during early spring in response to snow and ice melt, and that increasing evapotranspiration during late spring and onwards leads to gradually decreasing responses of discharge and ground- and surface-water levels to precipitation events. Note that apart from stream-discharge data, the data presented in this chapter are obtained from the Sicada database, and that gathering and quality control of these data are not part of the present work.

In addition to corresponding data presentations and evaluations of this chapter, Werner (2020) presented key findings from SKB's and SMHI's long-term meteorological and hydrological monitoring in Forsmark and surrounding areas. For instance, the comprehensive data compilation and analysis of Werner (2020) covered long-term variability patterns and trends of precipitation, potential evapotranspiration (PET), air temperature, sea level and stream discharge in a regional perspective. The plan is to make similar, updated data compilations and analyses also in the future.

4.2 Overview of meteorological and other hydrology-related monitoring

4.2.1 Meteorological monitoring and monitoring of winter parameters

Meteorological parameters are monitored by SKB at the Labbomasten automatic meteorological station (PFM006281, see Figure 4-1), which is operated by SMHI (Swedish Meteorological and Hydrological Institute) on behalf of SKB. The monitoring comprises precipitation, air temperature, barometric pressure, wind direction and wind speed, relative humidity and global radiation. The monitoring also includes calculated parameters, specifically precipitation corrected for e.g. wind losses and calculation of potential evapotranspiration. For redundancy and quality control, the Labbomasten station is also equipped with instruments that were moved when the previously operated Högmasten station (PFM010700) was decommissioned in June 2015. The present report uses results of meteorological monitoring reported in Jones (2021).

Monitoring of winter parameters is conducted by SKB and comprises regular measurements of snow depth and snow weight, and observations of ice freeze and ice breakup (Figure 4-1). Specifically, snow depth and snow weight are measured at three locations representing open land (AFM000071) and forest glades (AFM000072 and AFM001172 at Jungfruholm). Moreover, ice-freeze and ice-breakup observations comprise Lake Eckarfjärden (AFM000010), a pond (AFM001426), and two sea bays (AFM000075 and AFM001449). The present report uses results of monitoring of winter parameters reported in Höglund (2020).

Figure 4-1. *Locations of the Labbomasten meteorological station (PFM006281) and winter-time observations of snow depth/weight and ice cover. The Högmasten meteorological station (PFM010700) was taken out of operation in June 2015.*

4.2.2 Surface-water level and temperature monitoring

The surface-water level monitoring at Forsmark comprises the surface-water level gauges listed in Table 4-1 (see overview map in Figure 4-2). The present report uses results of monitoring reported in Wass (2021). In addition, automatic water-temperature monitoring was done in natural and constructed ponds during the period Apr.–Oct. 2020. For further details on the water-temperature monitoring, see Section 4.4.

According to Table 4-1, the current report includes surface-water level data from a number of recently installed surface-water level gauges in which monitoring was initiated during summer/autumn 2019 or early 2020. These installations are part of a programme to update the scope of surface-water level and groundwater level monitoring in Forsmark (Johansson and Werner 2019). Specifically, recently initiated surface-water level monitoring includes gauges installed in lakes (SFM000172, -178 and -186) and gauges installed in ponds (PFM008262/-8263, SFM000170 and -184).

Table 4-1. List of surface-water level gauges (dates are given as YYYY-MM-DD). Pond id's refer to those of Hamrén and Collinder (2010). For some gauges, uncertainties related to the level of the top of casing ("ToC uncertainties") imply that data periods available for the present report are short or just a few data days.

Gauge id	Initiation of monitoring	Comments
PFM010038	2003-05-22	SKB sea-level gauge
PFM010039	2003-01-01	SMHI sea-level gauge (not shown in this report)
SFM0039	2003-04-30	Lake Norra Bassängen
SFM0040	2003-05-16	Lake Bolundsfjärden (not shown in this report, data only available 2019-10-01–08 due to ToC uncertainties)
SFM0041	2003-04-29	Lake Eckarfjärden; terminated 2011-02-28, gauge removed and replaced by SFM000127
SFM0042	2004-02-05	Lake Fiskarfjärden (not shown in this report, data only available 2019-10-01–07 due to ToC uncertainties)
SFM0043	2003-04-28	SKB sea-level gauge; terminated 2005-11-07, gauge destroyed by ice
SFM0064	2004-04-21	Lake Gällsboträsket (not shown in this report, data only available 2019-10-01–06 due to ToC uncertainties)
SFM0066	2004-05-06	Lake Lillfjärden; terminated 2006-12-04, gauge destroyed by ice
SFM000111	2009-04-28	Pond 7
SFM000113	2009-04-28	Pond 14 (Norra Labbofjärden) (for the present report, data only available to 2019-12-04 due to ToC uncertainties)
SFM000115	2009-04-28	Pond 16
SFM000117	2009-04-30	Pond 18 (Kungsträsket)
SFM000119	2009-05-07	Lake Tjärnpussen
SFM000127	2011-03-03	Lake Eckarfjärden; replacement for SFM0041 (not shown in this report, data only available 2019-10-01–06 due to ToC uncertainties)
SFM000128	2012-06-29	Constructed pond 11f
SFM000129	2012-06-29	Constructed pond 11g
SFM000130	2012-06-29	Constructed pond 19a
SFM000131	2012-06-29	Constructed pond 66a
SFM000136	2014-05-20	Constructed pond 6b
SFM000137	2014-05-20	Constructed pond 17a
PFM004513	2009-03-20	Man. gauging scale on well SFM000118 (data are only stored in the Lodis database and not available in Sicada for the present report)
SFM000156	2016-03-15	Pond 12
PFM008262, PFM008263	2020-02-14	Pond 122 (two gauging scales observed by an automatic wildlife camera, PFM008098)
SFM000170	2019-08-12	Pond 23
SFM000172	2019-08-15	Lake Puttan
SFM000178	2019-06-05	Lake Gunnarsboträsket
SFM000184	2019-09-23	Pond at Djupsundsdelarna
SFM000186	2019-09-24	Lake Vambörsfjärden (for the present report, data are only available to 2020-03-31 due to ToC uncertainties)

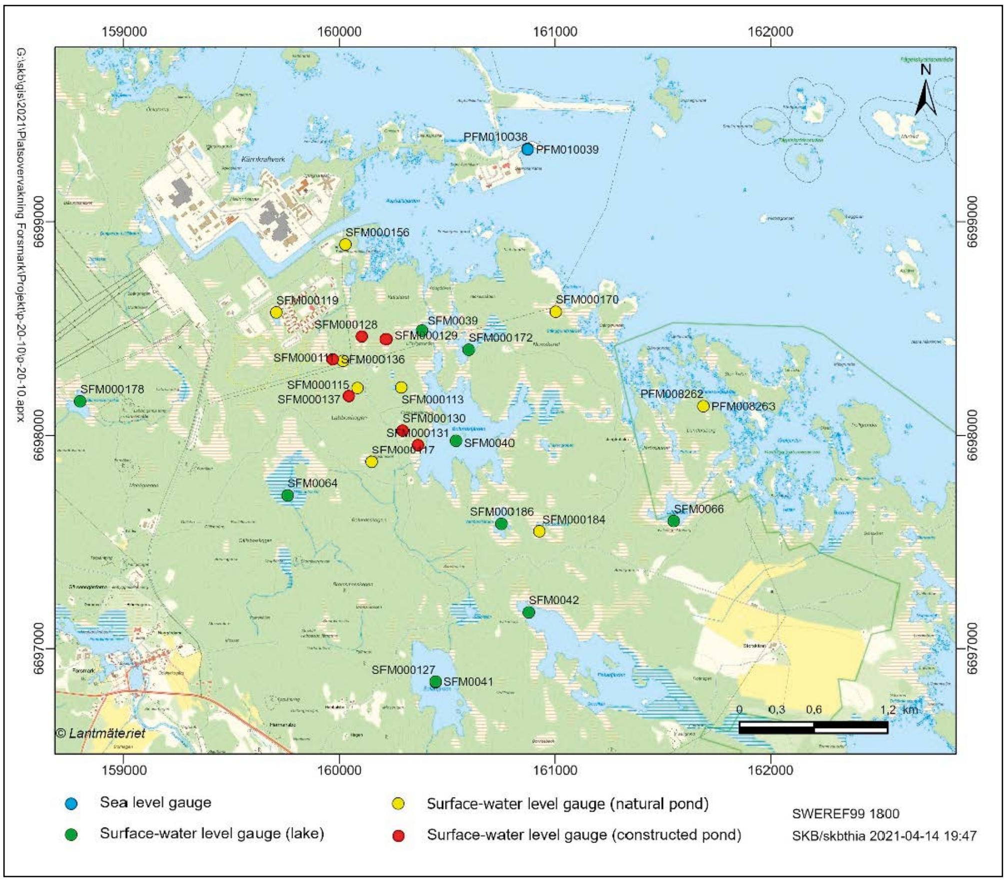

Figure 4-2. *Locations of surface-water level gauges in lakes and natural and constructed ponds, and SKB's (PFM010038) and SMHI's (PFM010039) sea-level gauges. SFM0066 was destroyed by ice in 2006.*

The installations and ongoing surface-water level monitoring at the remote pond 122 at Dundersborg near the coastline can be regarded as a methodology test. As can be seen in in Figure 4-3, the surface-water level of the pond is monitored using two gauging scales (PFM008262 and -8263), on which water-level readings (scale resolution 0.02 m) are observed by an automatic wildlife camera (PFM008098, Bolyguard SG880MK-18mHD). The camera is programmed to take an image of the scales each 8th hour, and images can be remotely downloaded from the camera by GSM telephony. The gauging scales are knocked down into the bottom of the pond manually using a rubber sledgehammer. The overall reason for this installation and monitoring setup is the difficult access to the remote Dundersborg location using a conventional track-driven drilling rig.

Figure 4-3. *Photo of the wildlife camera (PFM008098, left), the gauging scale PFM008262 (middle) and the supplementary gauging scale PFM008263 (right) in pond 122.*

As shown in Figure 4-4, the pond 122 water-level monitoring was initiated in mid-February 2020 using the PFM008262 gauging scale. A supplementary gauging scale (PFM008263) was installed next to the PFM008262 scale in the second half of April 2020. Surface-water levels (m, RH 2000) are calculated based on readings of the vertical distance between the levelled top of each scale and the water level. Moreover, surface-water depths at the location of the gauging scales are calculated based on the pond-bottom elevation and calculated surface-water levels. As can be seen in Figure 4-4, the currently available pond 122 dataset includes observations of surface-water levels for the period February 14–June 8, 2020. This observation period is followed by a data gap (due to technical reasons) and thereafter observations of dry conditions (i.e., zero surface-water depth) from mid-August to the beginning of November 2020. It is noted that the scales are installed in a natural pit in the pond bottom, implying that the whole pond is dry when the surface-water depth at the scale location is zero.

Based on the experiences so far from the pond 122 installations and monitoring, it is recommended to strive for more stable gauging-scale installations (Figure 4-3) and an improved camera/data transfer solution.

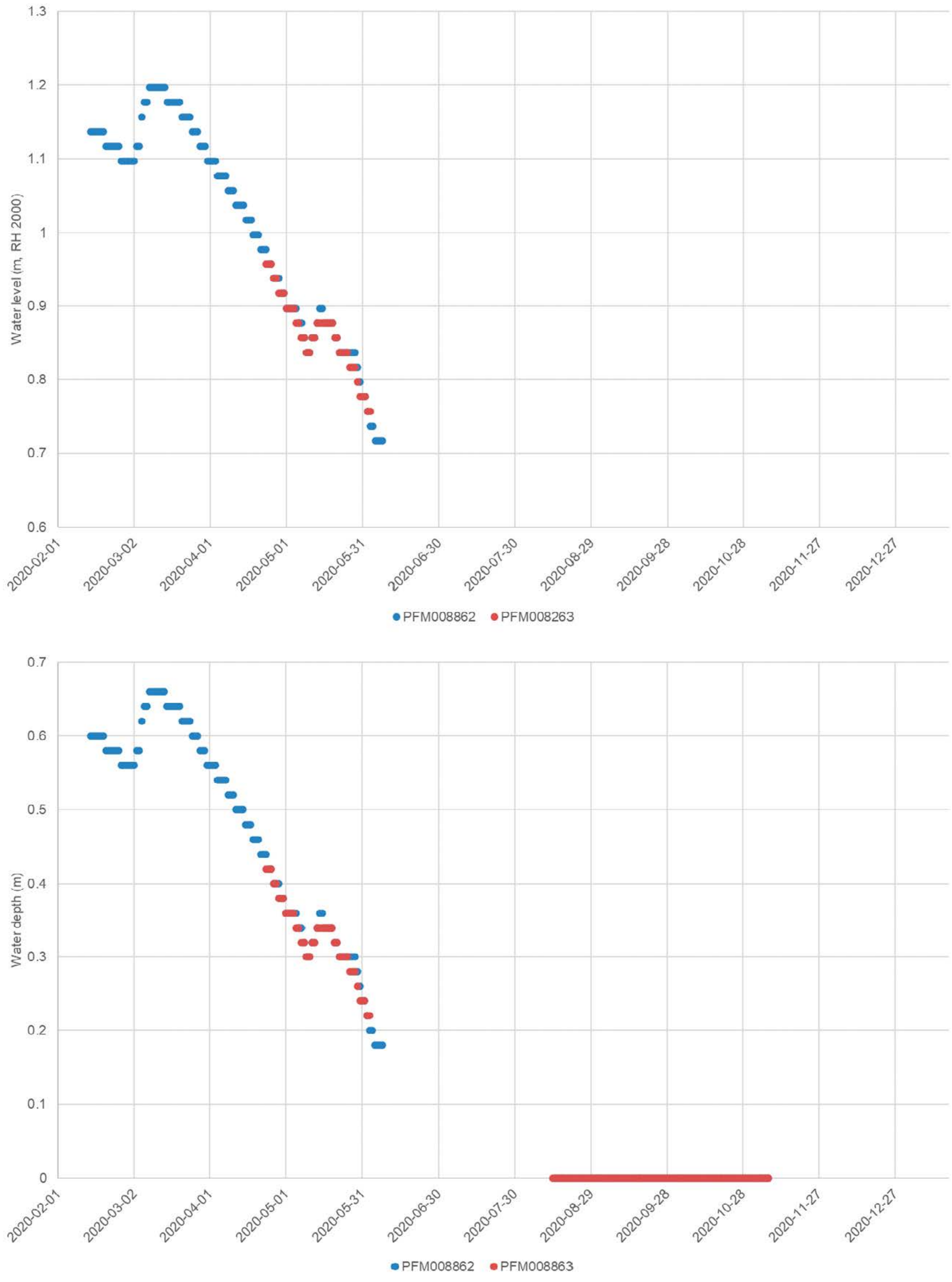

Figure 4-4. *Daily average surface-water levels (upper plot) and surface-water depth (lower plot) in pond 122. Note that during the Aug.–Nov. 2020 period, the water depth was zero at both flumes (only PFM008863 is visible in the plot).*

4.3 Integrated evaluation of surface-water level and stream-discharge monitoring data

Figure 4-5 and Figure 4-6 plot daily average surface-water levels (except PFM008262 and -8263) for gauges with data available for the data period of this report. Figure 4-5 includes sea level measured at the SKB gauging station. During the 2019/2020 hydrological year, the average of daily average sea levels was 0.21 m and the median was 0.19 m, where the maximum and the minimum daily average sea level was 0.81 and −0.22 m, respectively. The figures display an overall variation pattern in terms of rising surface-water levels during autumn, early winter and early spring, and decreasing levels during late spring and summer. It is also noted that the sea level may rise above thresholds and influence surface-water levels of near-coastal lakes and ponds (e.g. SFM0039 in Lake Norra Bassängen and SFM000156 in pond 12).

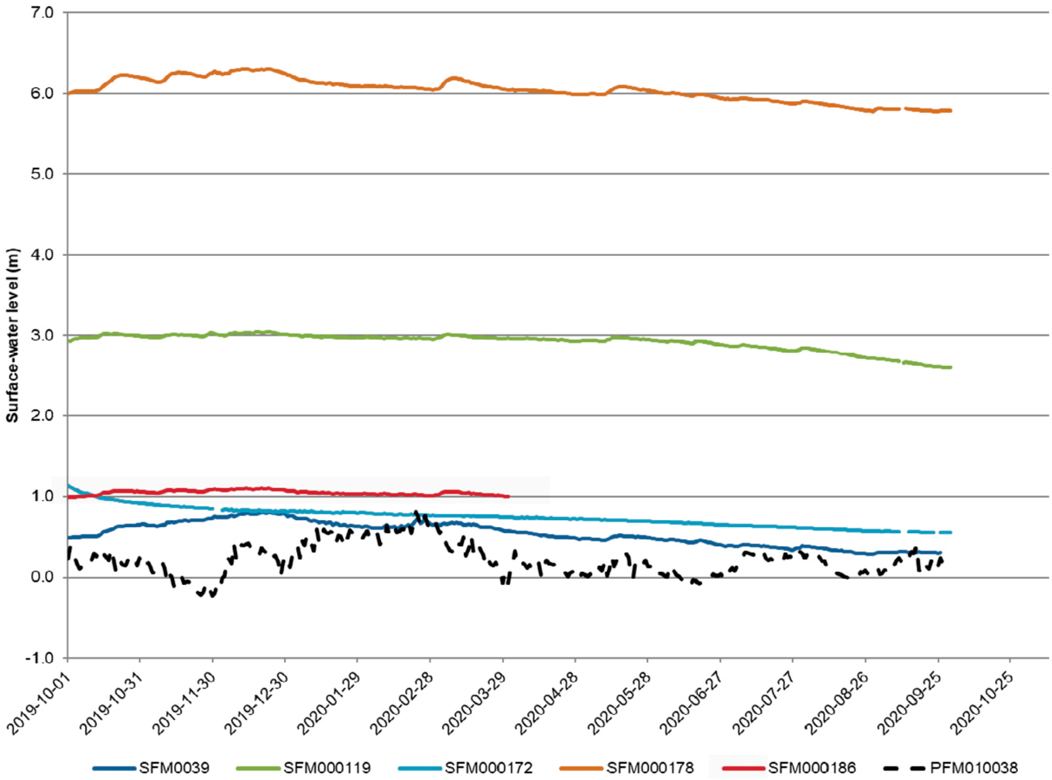

Figure 4-5. Daily average surface-water levels (m, RH 2000) in lakes and sea level measured at the SKB gauging station (cf Table 4-1).

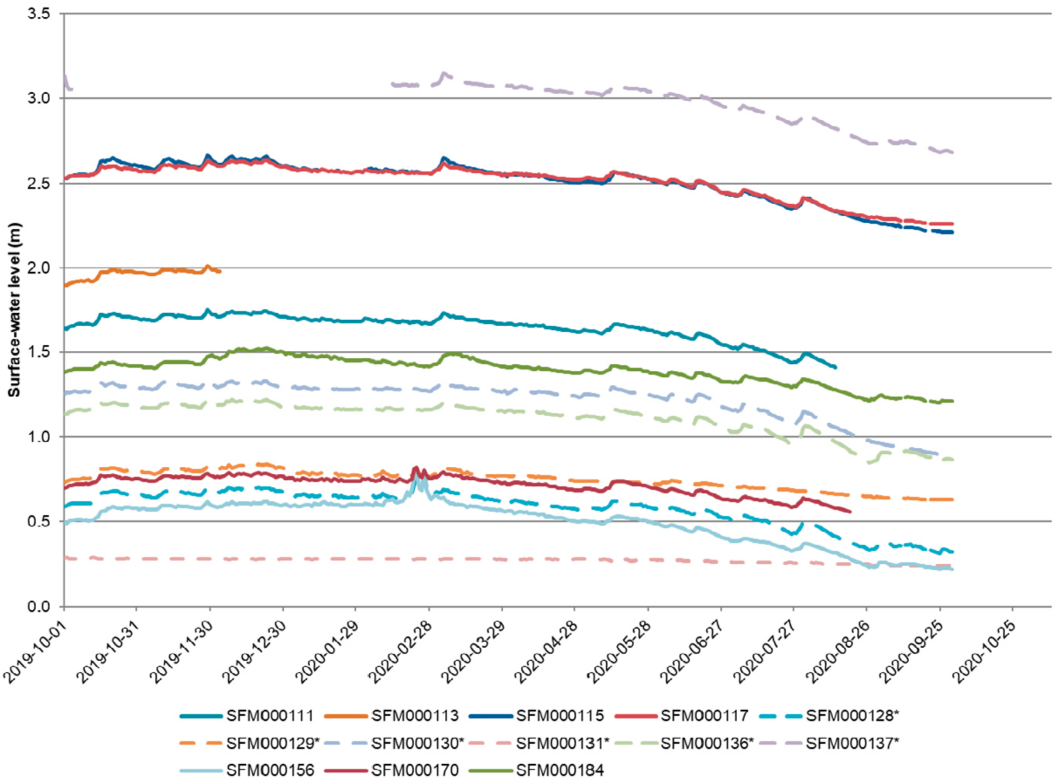

Figure 4-6. *Daily average surface-water levels (m, RH 2000) in natural (solid lines) and constructed (dashed lines) ponds (cf Table 4-1).*

According to Table 4-1, for the current report the data period for surface-water level gauge SFM000127, which is installed in Lake Eckarfjärden (upstream from stream-discharge gauging station PFM002668) is very short. It has previously been observed (e.g. Werner 2020) a high degree of co variation between surface-water levels and stream discharge, with rising surface-water level and stream discharge during autumn, early winter and early spring, and decreasing level and discharge during late spring and summer. The influence of precipitation events and periods on surface-water levels and stream discharge is illustrated in Figure 4-7 and Figure 4-8. Specifically, these figures demonstrate the rise of surface-water levels and stream discharges during periods of increasing cumulative precipitation sums.

The large influence of ice melt on surface-water levels and stream discharge is shown in Figure 4-9, which indicates the ice-covered period in Lake Eckarfjärden (upstream of PFM002668). It is interesting to note that there was no snow coverage during winter 2019/2020 (Höglund 2020), and hence no influence of snow melt on surface-water levels and stream discharge. In Figure 4-9, surface-water levels and the PFM002668 stream discharge reach annual maxima at the end of the ice-covered period in the middle of April, when precipitation is relatively modest (cf Figure 4-8). As shown in Figure 4-10, surface-water levels decrease during late spring (after the end of the spring-melt period) and during summer. During this period, evapotranspiration processes become gradually more active, driven by day temperatures of some 10–20 °C during May and June, and around 15–25 °C during July and August.

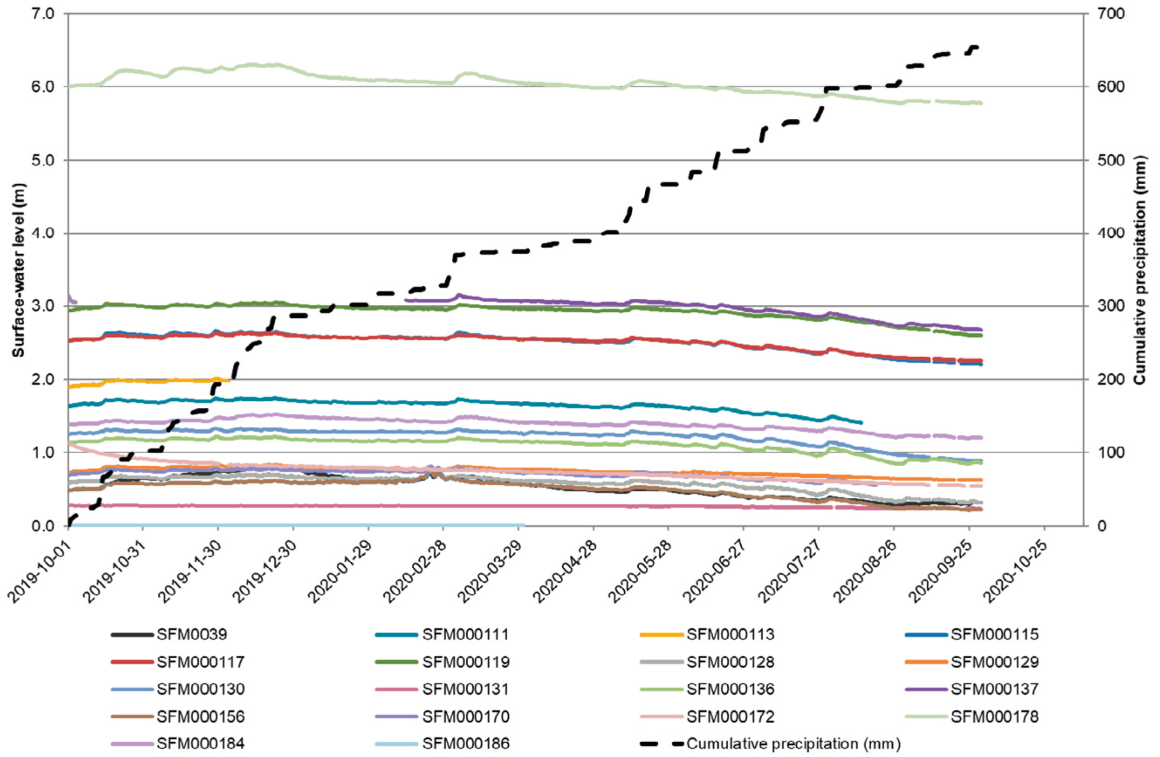

Figure 4-7. *Daily average surface-water levels (m, RH 2000) and cumulative sum of corrected precipitation at the Labbomasten meteorological station.*

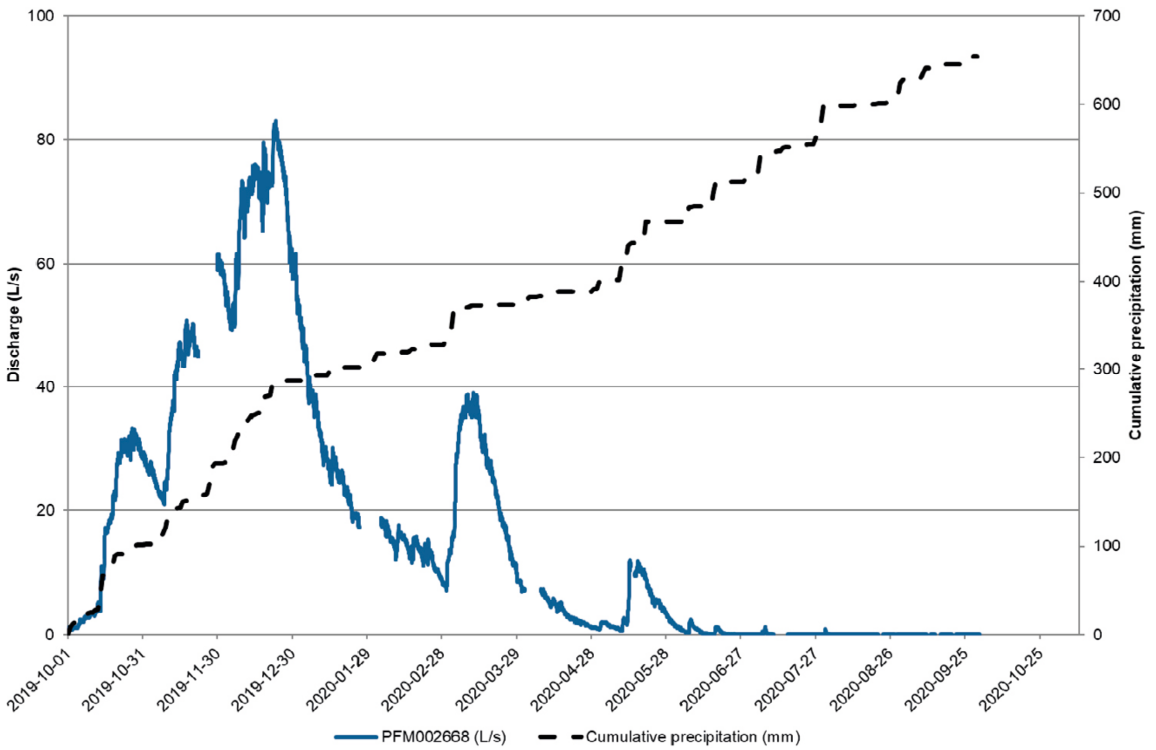

Figure 4-8. *Daily average stream discharge at gauging station PFM002668 and cumulative sum of corrected precipitation at the Labbomasten meteorological station.*

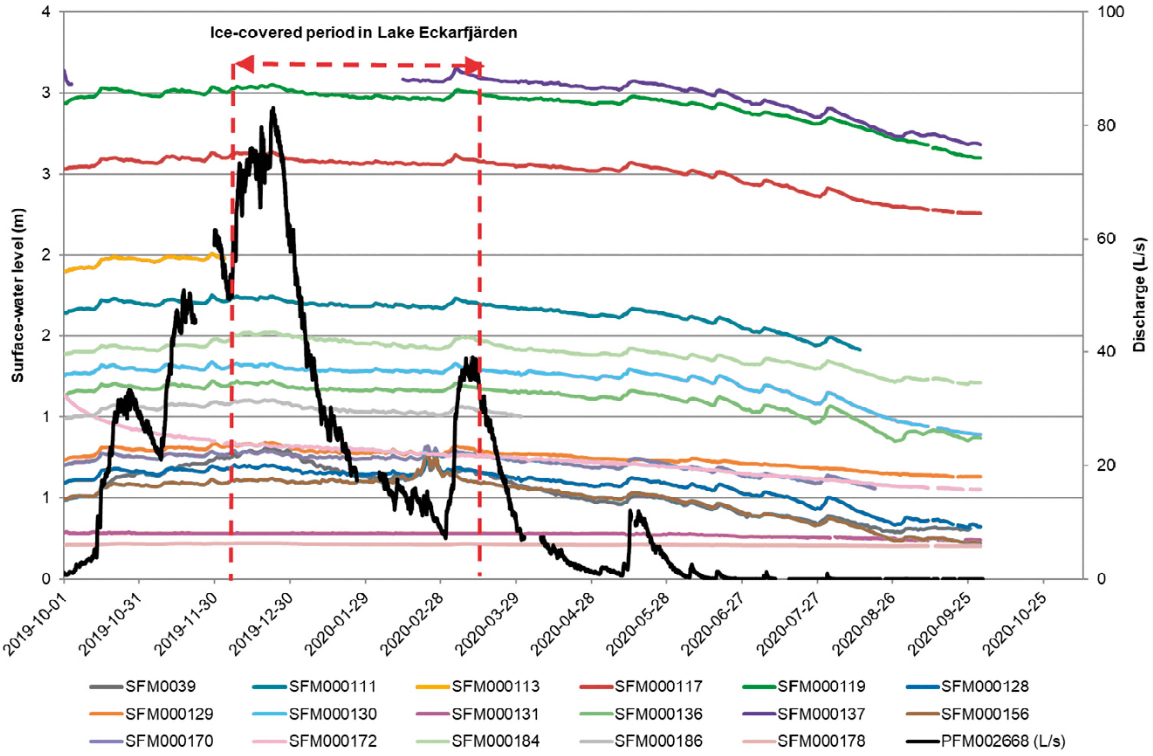

***Figure 4-9.** Daily average surface-water levels (m, RH 2000) and discharge at stream-gauging station PFM002668. The figure also indicates the ice-covered period in Lake Eckarfjärden (upstream of PFM002668).*

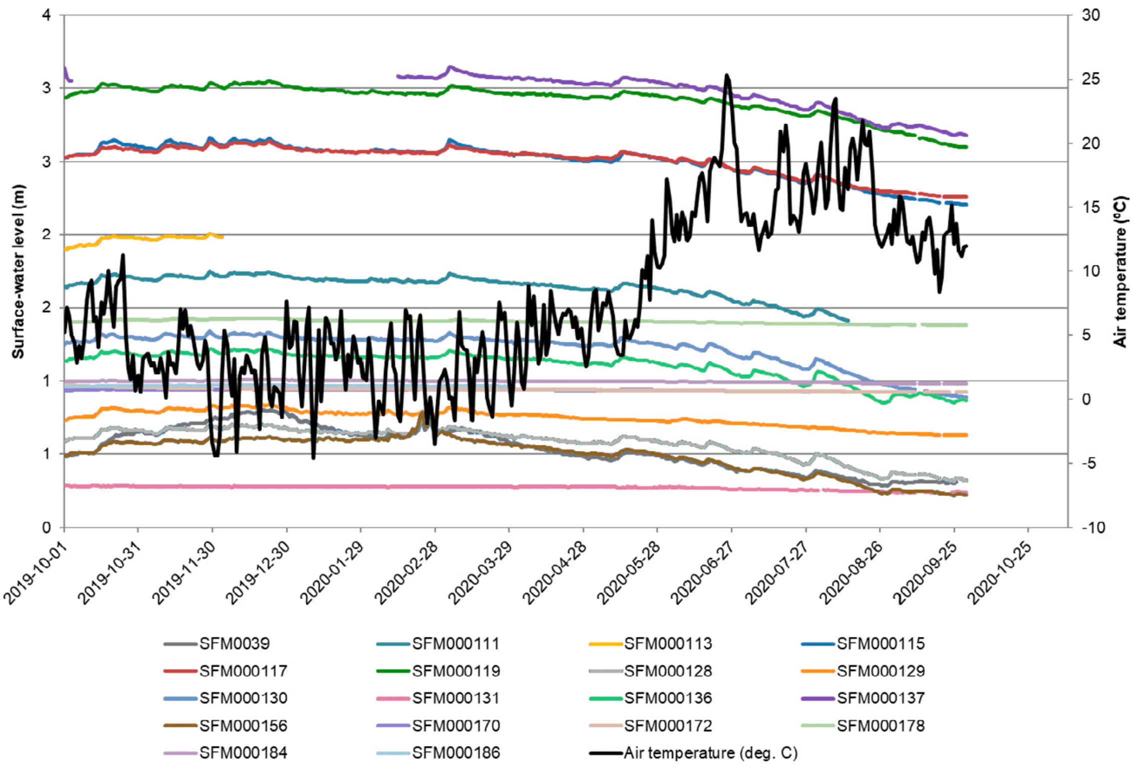

***Figure 4-10.** Daily average surface-water levels (m, RH 2000) and daily average air temperature at the Labbomasten meteorological station.*

4.4 Evaluation of surface-water temperature monitoring

4.4.1 Evaluation of 2020 monitoring campaign data

Automatic water-temperature monitoring was done in twelve natural ponds and one constructed pond during the period April 25–October 14, 2020 (Borgiel et al. 2021), see Figure 4-11. Water-temperature monitoring, also in other ponds, was conducted during the period Apr.–Oct. each year 2016–2019 (Borgiel et al. 2017, 2018, 2019, 2020). For summaries and evaluations of these previous monitoring campaigns, see Werner (2018a, 2019, 2020). Monitoring and evaluations of water temperatures are part of the background information required to evaluate the suitability of the monitored ponds for pool-frog reproduction from a water-temperature perspective.

The 2020 measurements are summarized in Table 4-2 and Table 4-3. Water temperatures were measured automatically (once per hour) using temperature sensors with integrated data loggers (Mini-Diver), at a constant depth of 0.05 m below the water surface. As mentioned above, somewhat different sets of ponds have been monitored during the 2016–2019 monitoring campaigns (Table 4-2). Specifically, PFM007870–73 (Lake Tjärnpussen, and ponds 12, 15 and 18) were added in the 2017 monitoring campaign, whereas PFM007764 (pond 7), PFM007768 (one location in pond 14) and PFM007769 (pond 16) were not monitored in 2017.

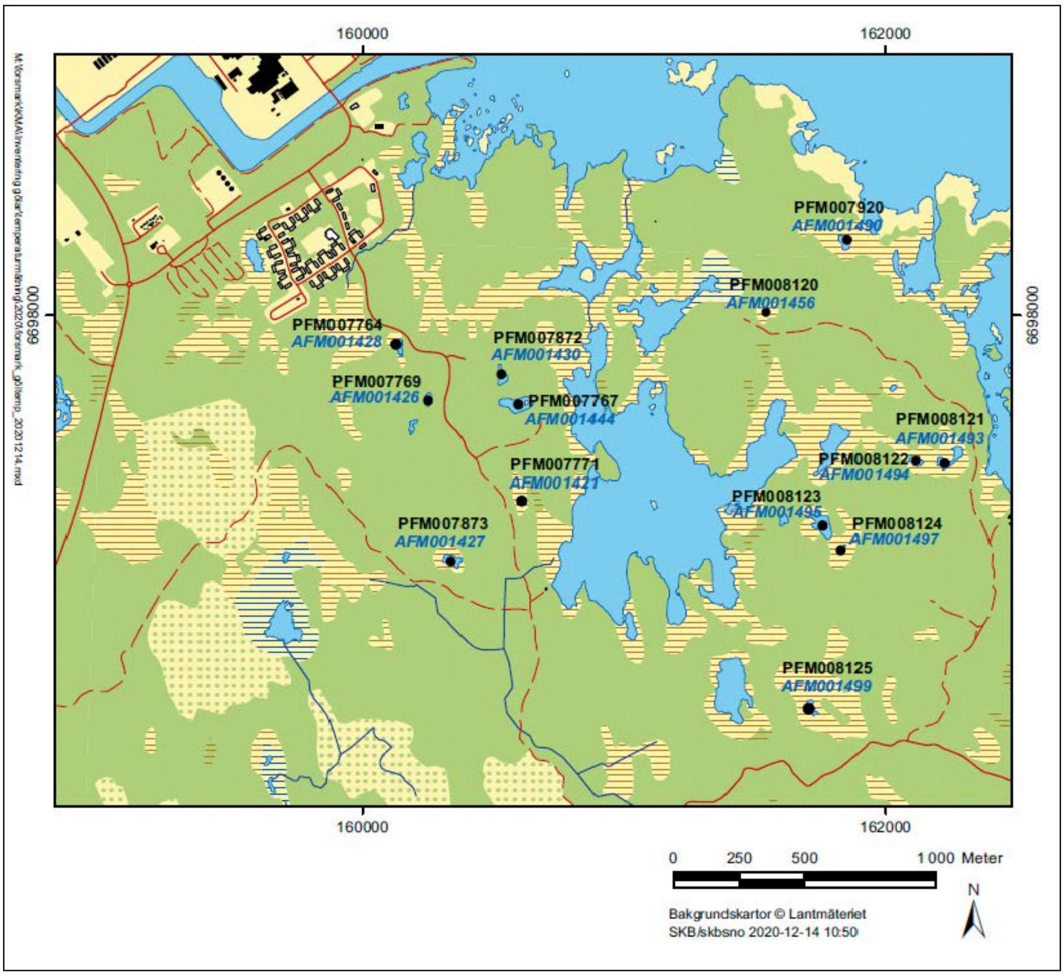

Figure 4-11. *Locations of automatic water-temperature measurements during 2020 (Borgiel et al. 2021).*

Table 4-2. Automatic water-temperature monitoring in twelve natural ponds and one constructed pond during the period Apr. 25–Oct. 14, 2020 (Borgiel et al. 2021).

Location id (automatic water-temp. meas.)	Pond id (alias)	Comments
PFM007764	AFM001428 (7), natural pond	Also monitored during 2016, 2018 and 2019
PFM007767	AFM001444 (14), natural pond	Also monitored during 2016–2019
PFM007769	AFM001426 (16), natural pond	Also monitored during 2016, 2018 and 2019
PFM007771	AFM001421 (19a), pond constructed in 2012	Also monitored during 2016–2019
PFM007872	AFM001430 (15), natural pond	Also monitored during 2017–2019
PFM007873	AFM001427 (18), natural pond	As above
PFM007920	AFM001490 (318), natural pond	Also monitored during 2018–2019
PFM008120	AFM001456 (22), natural pond	Also monitored during 2019
PFM008121	AFM001493 (377), natural pond	As above
PFM008122	AFM001494 (378), natural pond	As above
PFM008123	AFM001495 (380), natural pond	As above
PFM008124	AFM001497 (383), natural pond	As above
PFM008125	AFM001499 (388), natural pond	As above

Table 4-3. Summary of results of automatic water-temperature measurements in ponds.

Location id (PFM00-) (pond id)	Temp. (°C)				Temp. > 19 °C	
	Av.	Max	Min	Std. dev.	Time frac., full data period	Deg. hrs. (°C·h), May 15–Sep. 30
7764 (7)	16.93	32.31	5.76	5.51	0.34	6040
7767 (14)	18.15	31.88	7.23	5.27	0.44	7477
7769 (16)	16.18	30.50	5.06	5.13	0.29	4264
7771 (19a*)	17.21	31.04	6.46	5.24	0.38	5761
7872 (15)	16.86	31.30	5.99	5.30	0.35	5424
7873 (18)	17.39	32.49	5.69	5.43	0.38	6447
7920 (318)	17.68	31.18	8.14	4.65	0.41	5693
8120 (22)	16.05	31.09	5.95	4.84	0.26	3722
8121 (377)	-	-	-	-	-	-
8122 (378)	17.86	31.83	6.66	5.23	0.42	6851
8123 (380)	17.57	30.63	7.06	5.02	0.41	6027
8124 (383)	17.19	31.22	5.21	5.35	0.37	5861
8125 (388)	17.37	30.94	6.36	5.02	0.39	5693

Av. = average, std. dev. = standard deviation, time frac. = fraction of time, deg. hrs. = degree hours (temperatures above 19 °C). *Constructed pond. The sensor/logger at location id PFM008221 (pond 377) was lost during the monitoring campaign, and no data are therefore available.

According to Table 4-3, the ponds demonstrate rather similar temperature characteristics in terms of overall average temperatures (c 16–18 °C), maximum temperatures (c 30–32 °C) and standard deviations (c 4.7–5.4 °C), whereas there is broader range in terms of minimum temperatures (c 5.1–8.1 °C). During the 2020 monitoring period, the average water temperature was highest in the natural pond AFM001444 (pond 14), and lowest in the natural pond AFM001456 (pond 22), see Figure 4-12. It is also noted that the constructed pond monitored in 2020 (AFM001421, pond 19a) demonstrates an average water temperature similar to those of the natural ponds (cf Werner 2018a, 2019, 2020). The fraction of time with water temperatures above 19 °C, considered as threshold for pool-frog egg/tadpole development (Orizaola et al. 2010), and the cumulative degree-hours sum (degrees above 19 °C times time in hours, specifically for the period May 15–Sep. 30; see Figure 4-12) demonstrate some inter-pond variations (c 26–44 % and c 3700–7500 °C·h , respectively).

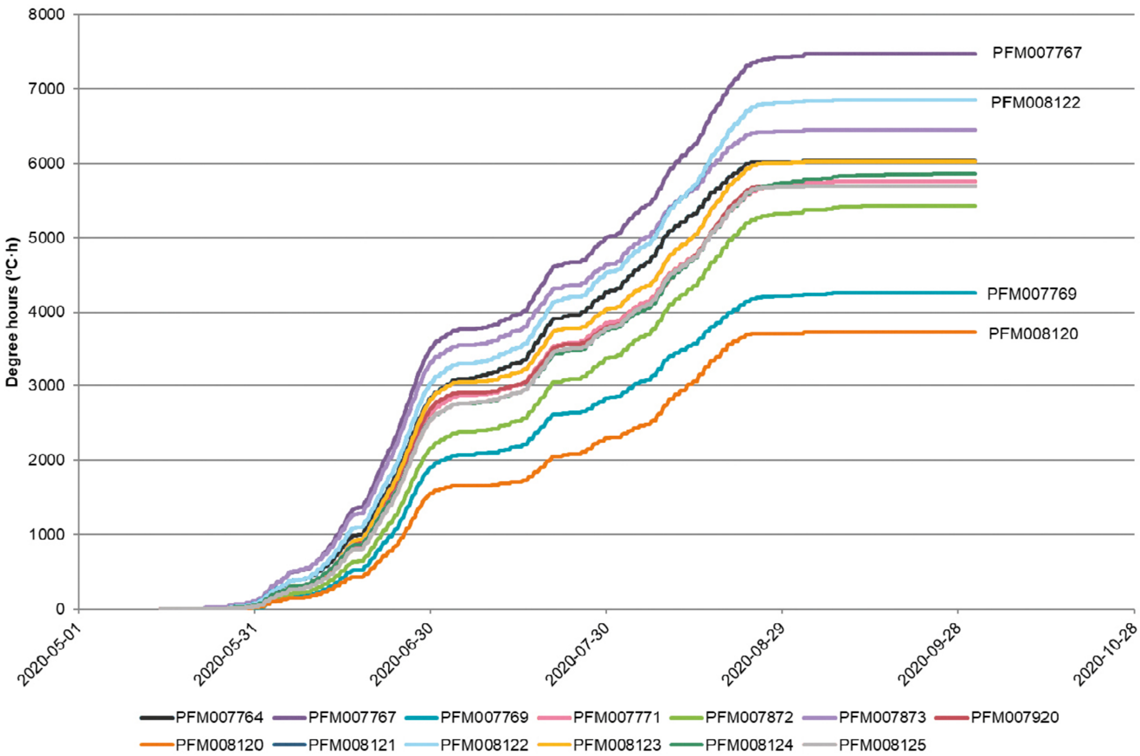

Figure 4-12. *Cumulative degree-hours sum (degrees above 19 °C times time in hours) for automatically measured water temperatures during the period May 15–Sep. 30, 2020.*

4.4.2 Scope and methods of continued monitoring campaigns

As mentioned above, the temperature-monitoring campaigns are part of the background information required to evaluate the suitability of the monitored ponds, including constructed ponds, for pool-frog reproduction from a water-temperature perspective. These objectives have been fulfilled by the five-year monitoring campaigns 2016–2020, which motivates a review of scope and methods for continued water-temperature monitoring campaigns. This section provides some background information for such a review. Specifically, the section investigates the possibilities to reduce the number of ponds to be monitored, or even replace the water-temperature monitoring by calculations based on air-temperature measurements. These possibilities are in the following investigated by linear-regression analyses of the pond-water temperature dataset and the same-time air temperature dataset from the Labbomasten meteorological station (PFM006281; see Section 4.2.1).

As shown in the example plot in Figure 4-13 (PFM007763) there is a relatively high degree of correlation between pond-water temperature and air temperature (cf Werner 2018a). According to Table 4-4, high-resolution (hourly) pond-water and air-temperature data demonstrate correlation coefficients (r) in the range 0.75–0.86, whereas r is in the range 0.84–0.93 in terms of daily averages. Table 4-4 also presents linear regression (LR) models for calculation of daily average pond-water temperatures based on daily average air temperatures (Labbomasten), and also the associated standard error of each regression.

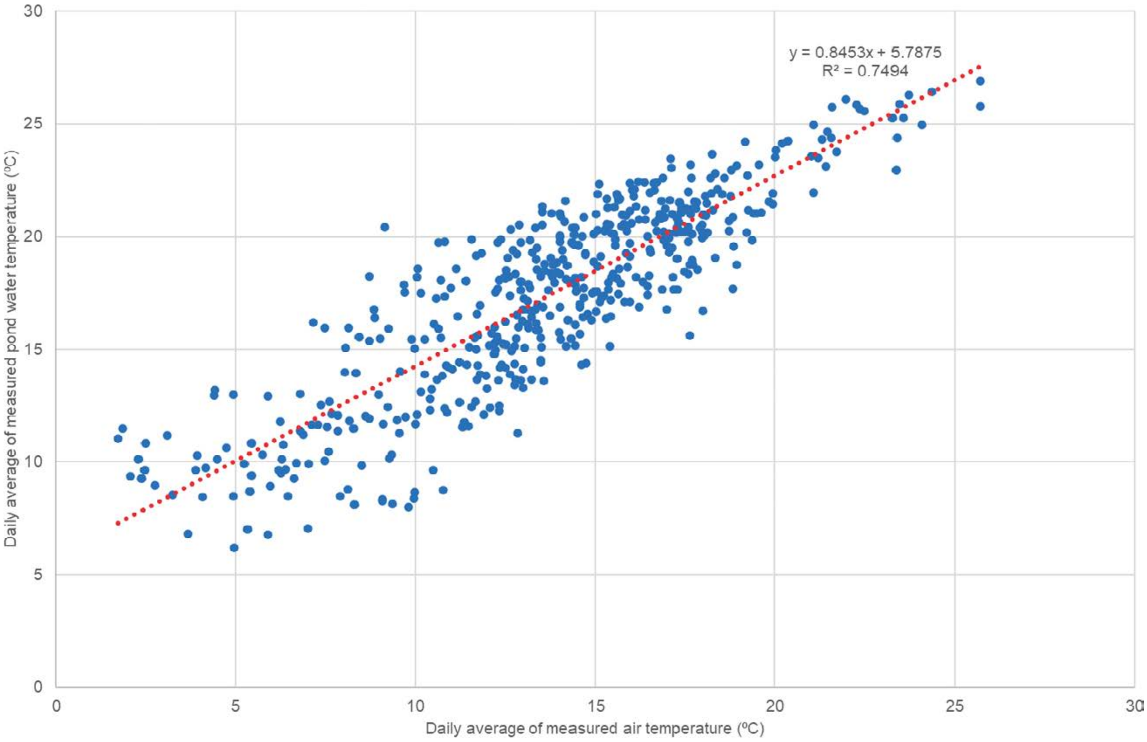

Figure 4-13. *Example plot of daily averages of measured pond water temperature (PFM007763) versus daily averages of measured air temperature at Labbomasten.*

Table 4-4. Results of pond-water and air-temperature regression analyses.

Location id (PFM00-) (pond id)	Data period(s)	Correl. coeff. (r)		LR model	Standard error of regression
		High res. (hourly) data	Daily av.		
7763 (6b)	2016–2018	0.79	0.87	7763 = 5.788 × LM + 0.845	2.152
7764 (7)	2016, 2018–2019	0.83	0.89	7764 = 5.241 × LM + 0.889	2.120
7765 (11f)	2016–2018	0.81	0.88	7765 = 4.961 × LM + 0.893	2.152
7766 (11g)	2016–2018	0.81	0.87	7766 = 5.538 × LM + 0.871	2.214
7767 (14)	2016–2019	0.76	0.87	7767 = 5.924 × LM + 0.906	2.416
7768 (14)	2016	0.75	0.84	7768 = 5.230 × LM + 0.904	2.442
7769 (16)	2016, 2018–2019	0.82	0.90	7769 = 4.254 × LM + 0.895	2.028
7770 (17a)	2016–2018	0.79	0.86	7770 = 5.902 × LM + 0.872	2.320
7771 (19a)	2016–2019	0.81	0.88	7771 = 5.597 × LM + 0.871	2.114
7772 (66a)	2016–2018	0.79	0.86	7772 = 5.597 × LM + 0.882	2.268
7870 (8)	2017–2018	0.75	0.85	7870 = 5.652 × LM + 0.877	2.457
7871 (12)	2017–2018	0.80	0.88	7871 = 6.066 × LM + 0.828	2.032
7872 (15)	2017–2019	0.82	0.91	7872 = 5.328 × LM + 0.871	1.935
7873 (18)	2017–2019	0.78	0.88	7873 = 6.526 × LM + 0.851	2.190
7920 (318)	2018–2019	0.80	0.90	7920 = 5.961 × LM + 0.866	2.106
8120 (22)	2019	0.86	0.91	8120 = 6.737 × LM + 0.727	1.526
8121 (377)	2019	0.84	0.91	8121 = 6.610 × LM + 0.827	1.722
8122 (378)	2019	0.83	0.91	8122 = 6.881 × LM + 0.827	1.759
8123 (380)	2019	0.81	0.91	8123 = 6.702 × LM + 0.832	1.766
8124 (383)	2019	0.85	0.92	8124 = 6.299 × LM + 0.835	1.707
8125 (388)	2019	0.85	0.93	8125 = 6.428 × LM + 0.817	1.569

Figure 4-15 shows daily averages of pond-water temperature, calculated using the relevant LR model of Table 4-4, versus daily averages of measured pond water temperature at PFM007763. The red lines delineate calculated and measured temperatures above/below 19 °C, i.e. the threshold for pool-frog egg/tadpole development. Hence, data points in the upper right and lower left quartiles are those for which both calculated and measured pond-water temperatures are above and below 19 °C, respectively. On the other hand, the relatively few data points in the upper left and lower right quartiles are those for which calculated pond-water temperatures are above and below 19 °C, respectively, and the opposite for measured temperatures.

According to Figure 4-16 and Figure 4-17, there is a tendency for calculated temperatures to be above measurements in the beginning and end of the annual monitoring campaigns, and the opposite in the middle of the campaigns. This behaviour is likely due to that the temperature of air, which has much less heat capacity compared to water and is used to calculate the pond-water temperature using the LR model based on whole data periods, rises more quickly in spring and also demonstrates faster cooling in autumn, compared to pond water.

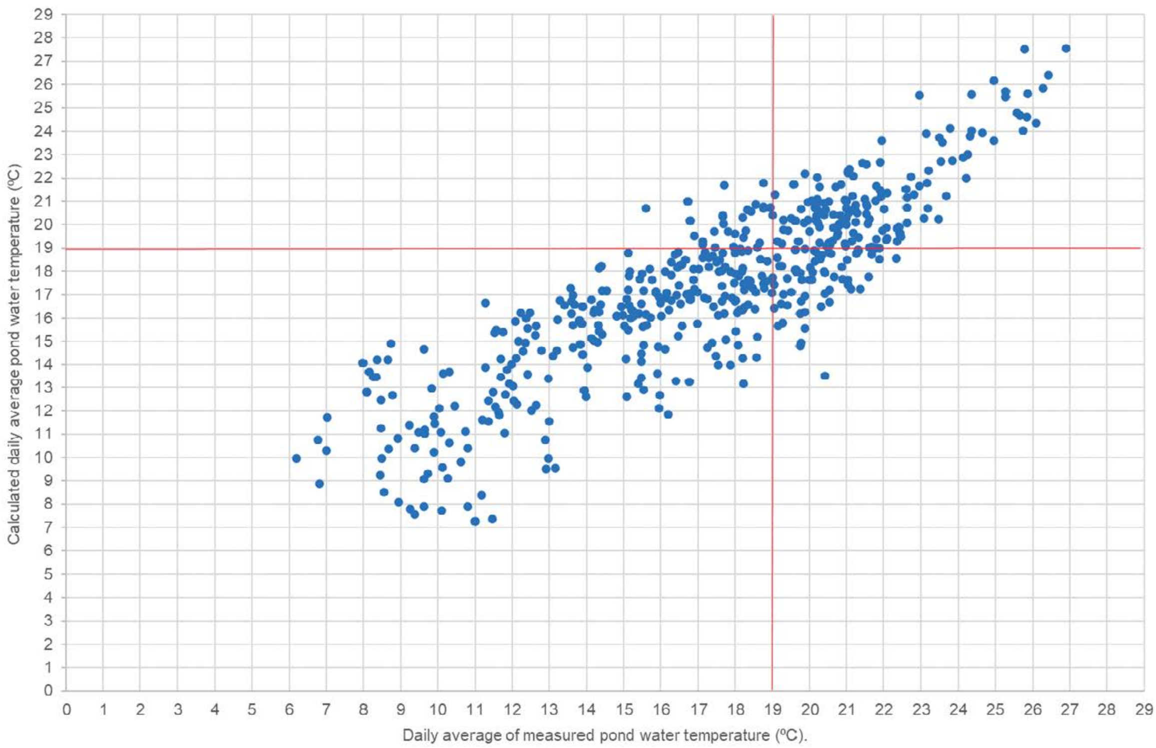

Figure 4-14. *Example plot (PFM007763) of calculated daily averages of pond-water temperature versus daily averages of measured pond-water temperature.*

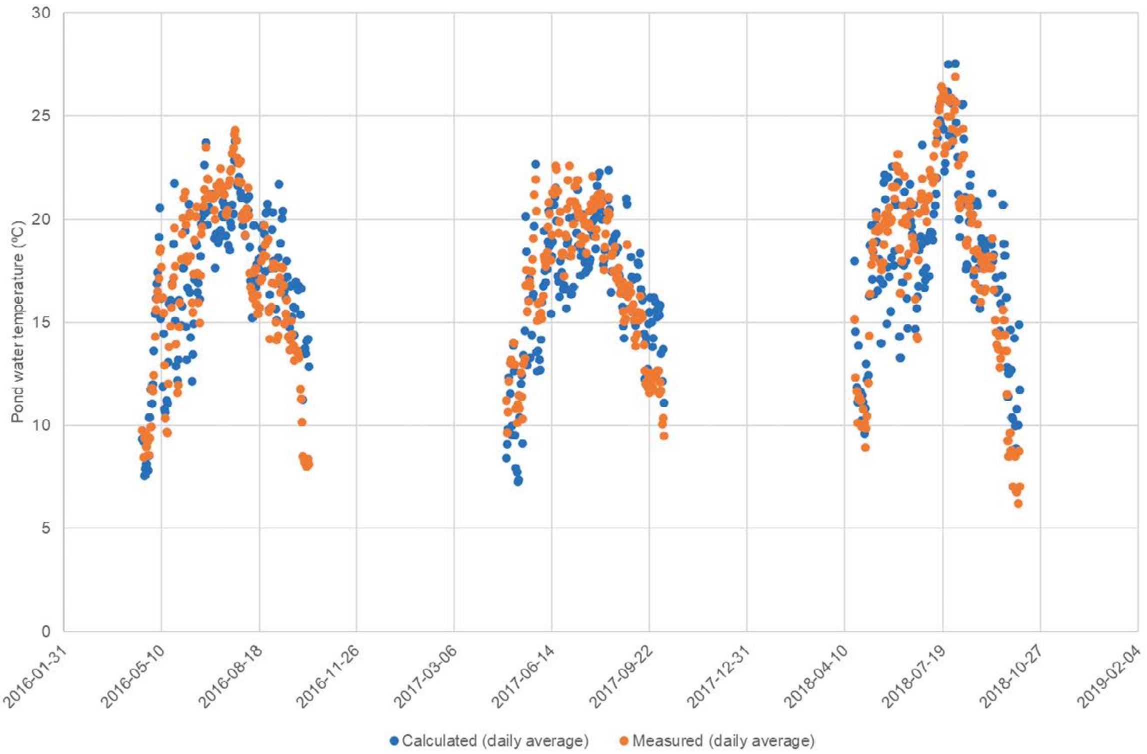

Figure 4-15. *Example plot (PFM007763) of daily averages of calculated and measured pond-water temperature.*

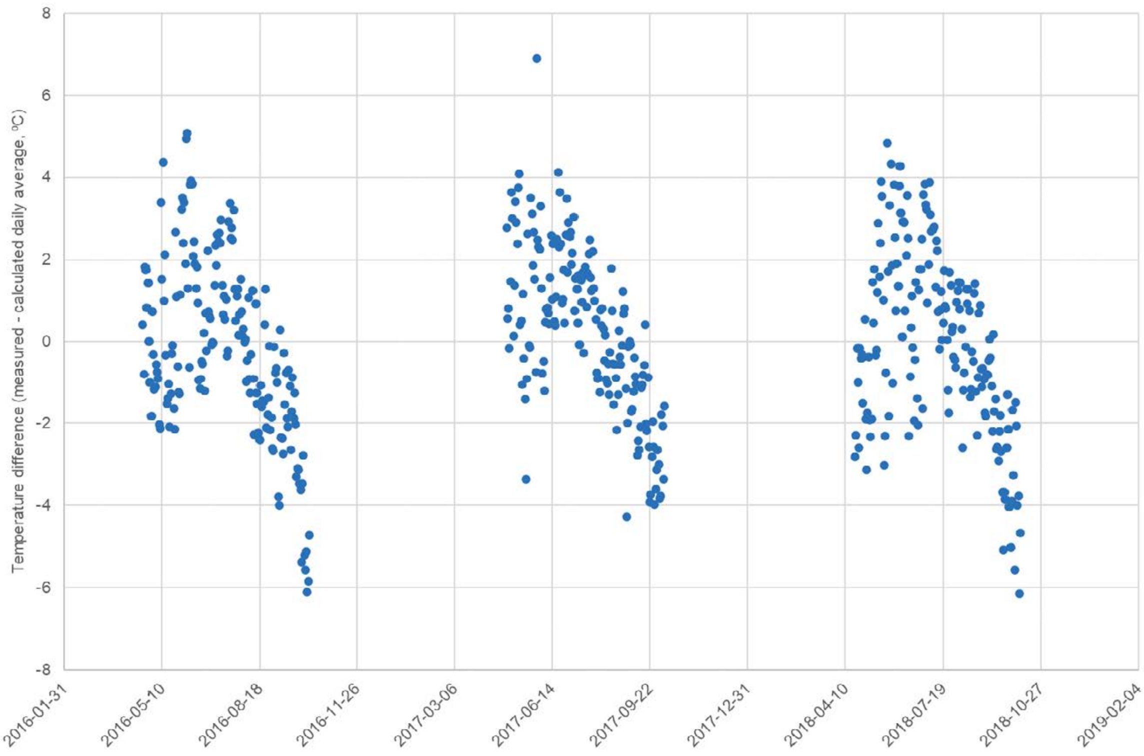

Figure 4-16. *Example plot (PFM007763) of differences between daily averages of measured and calculated pond-water temperatures.*

The LR models of Table 4-4 are developed based on all available pond-water temperature data 2016–2019. As demonstrated above, due to the seasonal behaviour of the air temperature and large differences in air and water heat capacities, these LR models inevitably lead to typical patterns of over- and under representations of pond-water temperatures. As a complement to the analyses above, it was also tested to perform linear-regression analyses on monthly basis for PFM007763, i.e. to develop LR models for individual months (Table 4-5). According to Table 4-5, standard errors of the regressions are below or much below those using all data in the regression.

Table 4-5. Results of PFM007763 pond-water and air-temperature regression analyses for individual months (data period 2016–2018).

Month	LR model	Standard error of regression
April	7763 = 0.426 × LM + 8.010	0.796
May	7763 = 0.654 × LM + 8.634	2.037
June	7763 = 0.541 × LM + 11.534	1.431
July	7763 = 0.599 × LM + 11.468	0.942
August	7763 = 0.735 × LM + 7.073	1.167
September	7763 = 0.826 × LM + 3.939	1.369

Moreover, from the water temperature dataset it is noted that pond-water temperature cross correlations are high, with day-to-day correlation coefficients in the order of r = 0.98−1.00. Hence, as an alternative to calculations of pond-water temperatures based on air-temperature data, pond-water temperatures may be calculated based on temperature data from a reduced set of ponds. The test was also in this case performed using daily average water temperatures for PFM007763 (data period 2016–2018). Moreover, the approach was tested using a proxy in terms of daily average temperatures (below denoted T_{all}) for all ponds monitored during the 2016–2018 campaigns. As illustrated in Figure 4-17, the analysis yields the LR model T_{all} = 1.034 × PFM007763 – 0.457 (standard error of the regression = 0.332). Figure 4-18 shows resulting "site-average" temperatures calculated using this LR model versus averages of daily average pond-water temperatures.

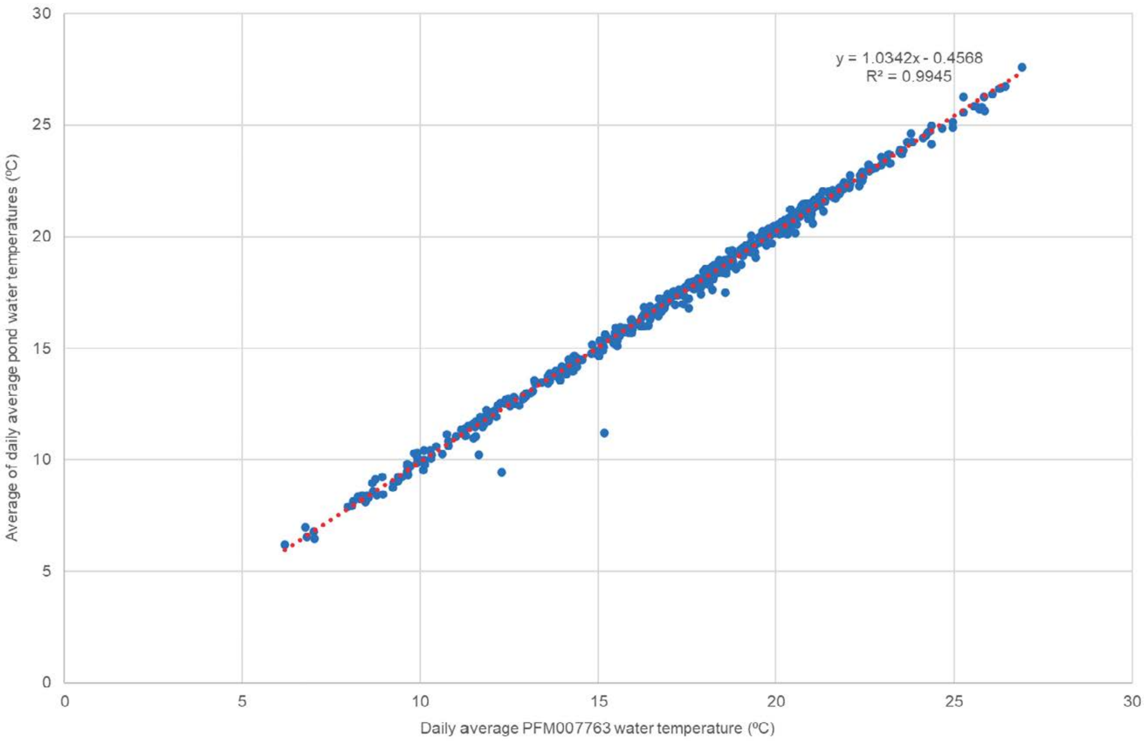

Figure 4-17. *Plot of averages of daily average pond-water temperatures versus daily averages of the PFM007763 water temperature during the 2020 monitoring campaign.*

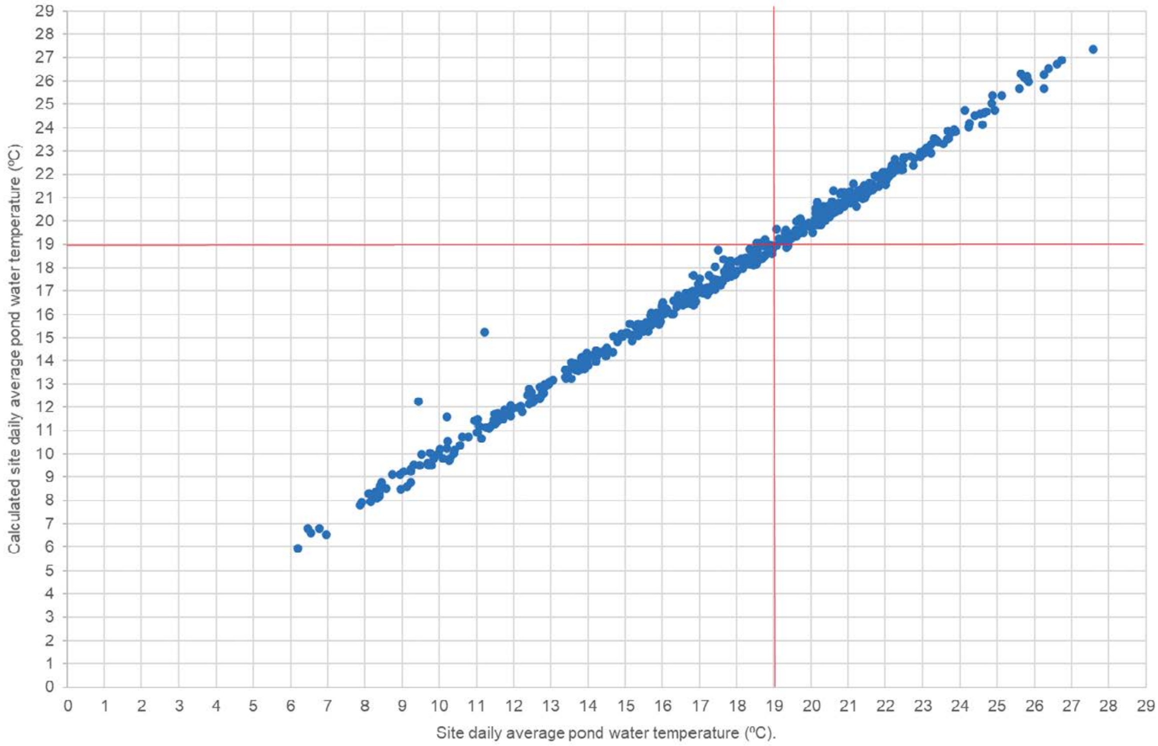

***Figure 4-18.** Plot of temperatures calculated using the LR model developed for the PFM007763 daily average water temperature versus averages of daily average pond-water temperatures.*

The outcomes of the analyses and associated LR models above are tested in Figure 4-19 to 4-30 using pond-water (Borgiel et al. 2021) and air-temperature data (Jones 2021) gathered during the 2020 pond-monitoring campaign. Specifically, the figures show plots of differences between daily averages of measured pond-water temperature, and temperatures calculated using the LR model developed for daily averages of air temperature and the LR model developed for the PFM007763 daily average water temperature, respectively. As PFM007763 (pond 6b) was not monitored during the 2020 campaign, the latter calculations were done using PFM007767 temperature data (pond 14).

As shown in these figures, deviations from measurements are generally smaller using the pond-water temperature based LR model compared to the air-temperature based LR model. Moreover, the pond-water temperature based LR model demonstrates systematic rather than inter-seasonal deviations from measurements associated with the air-temperature based LR model (cf Figure 4-17 and Figure 4-18 above). These systematic deviations are likely due to that the LR model is developed for averages of daily average pond-water temperatures (some ponds demonstrate large deviations from the across-pond average). These systematic deviations can likely be reduced substantially by development of pond-specific LR models.

The air temperature in Forsmark is presently measured only at one location (Labbomasten), whereas air temperatures tend to vary across a site (cf Werner 2018a). Depending on their locations, the ponds are to different degrees exposed to factors affecting their water temperature such as solar radiation and wind (the Labbomasten temperature sensor has a solar-radiation protection), and the ground conditions at Labboasten also differ from those in the vicinity of the ponds. Moreover, air and water have very different heat capacities, which in combination with differences in e.g. pond sizes, depths and water residence times makes an air-temperature based calculation approach difficult.

Based on the above, it can hence be concluded that the best option likely is not to terminate the pond-water temperature monitoring campaigns. Rather, the number of ponds may be reduced in forthcoming monitoring campaigns, and water temperatures can then be calculated based on pond-specific LR models (that need to be developed). It is therefore recommended that such LR models are developed, and that the scope for continued water-temperature monitoring campaigns considers a reduced set of ponds to include in those campaigns.

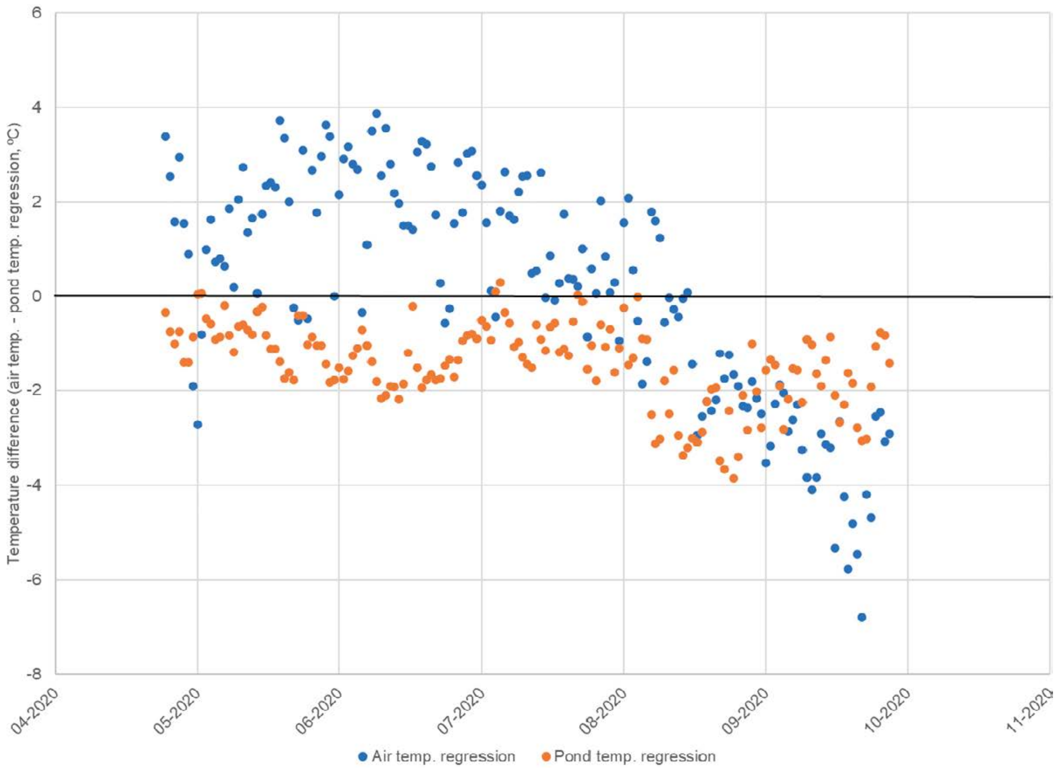

Figure 4-19. *PFM007764 plot (2020 campaign, MM-YYYY) of differences between daily averages of measured pond-water temperature, and temperatures calculated using the LR model developed for daily averages of air temperature (air temp. regression) and the LR model developed for the PFM007763 daily average water temperature (pond temp. regression), respectively.*

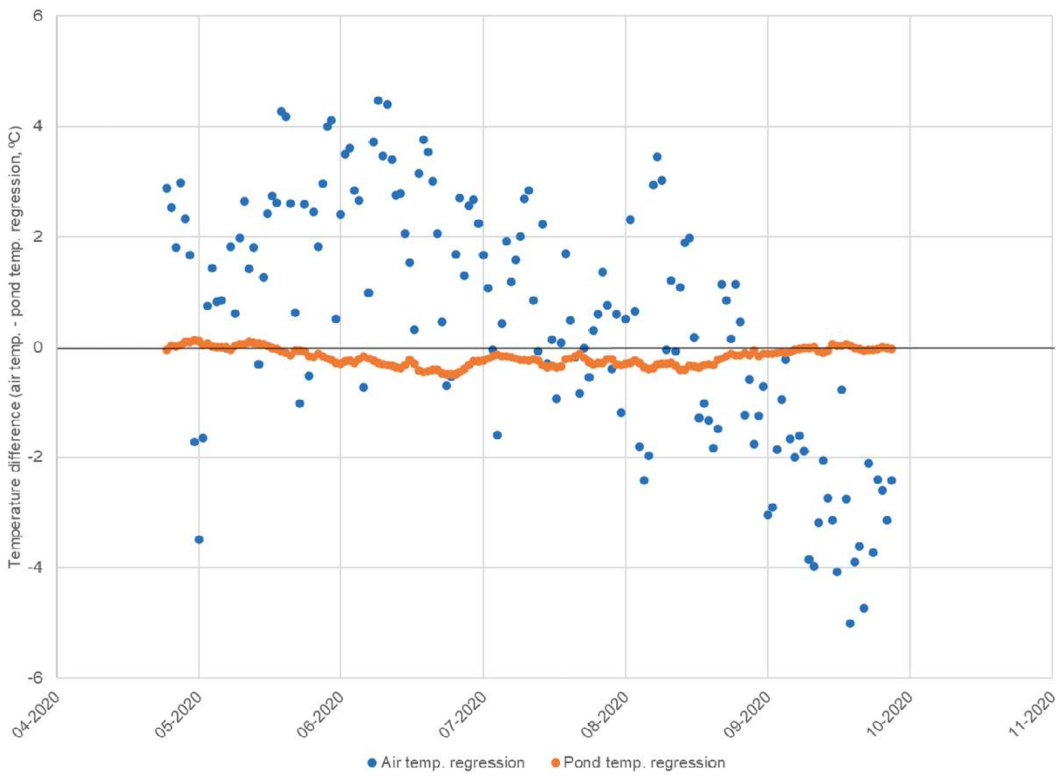

Figure 4-20. *PFM007767 plot (2020 campaign, MM-YYYY) of differences between daily averages of measured pond-water temperature, and temperatures calculated using the LR model developed for daily averages of air temperature (air temp. regression) and the LR model developed for the PFM007763 daily average water temperature (pond temp. regression), respectively.*

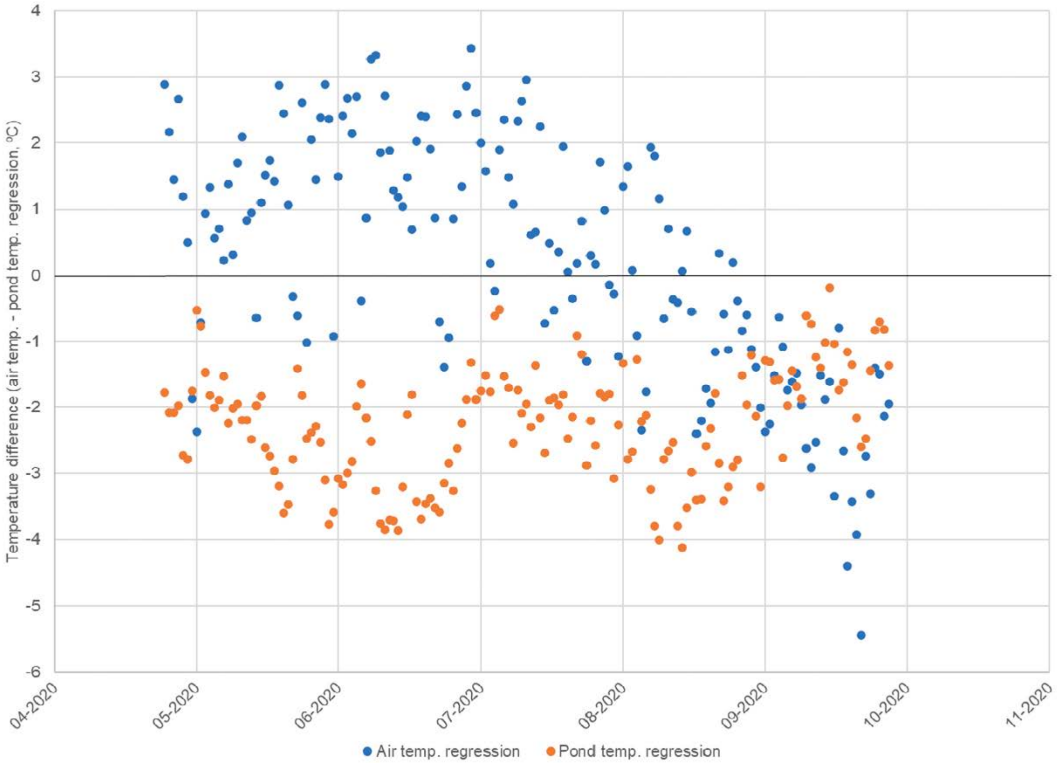

Figure 4-21. *PFM007769 plot (2020 campaign, MM-YYYY) of differences between daily averages of measured pond-water temperature, and temperatures calculated using the LR model developed for daily averages of air temperature (air temp. regression) and the LR model developed for the PFM007763 daily average water temperature (pond temp. regression), respectively.*

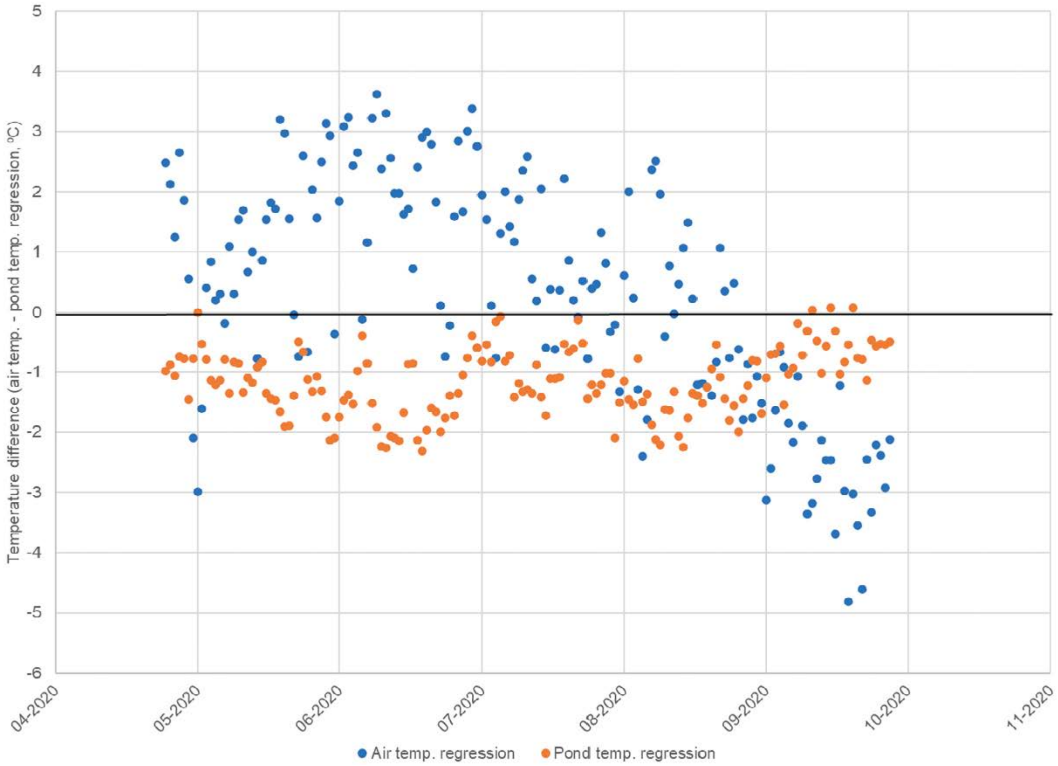

Figure 4-22. *PFM007771 plot (2020 campaign, MM-YYYY) of differences between daily averages of measured pond-water temperature, and temperatures calculated using the LR model developed for daily averages of air temperature (air temp. regression) and the LR model developed for the PFM007763 daily average water temperature (pond temp. regression), respectively.*

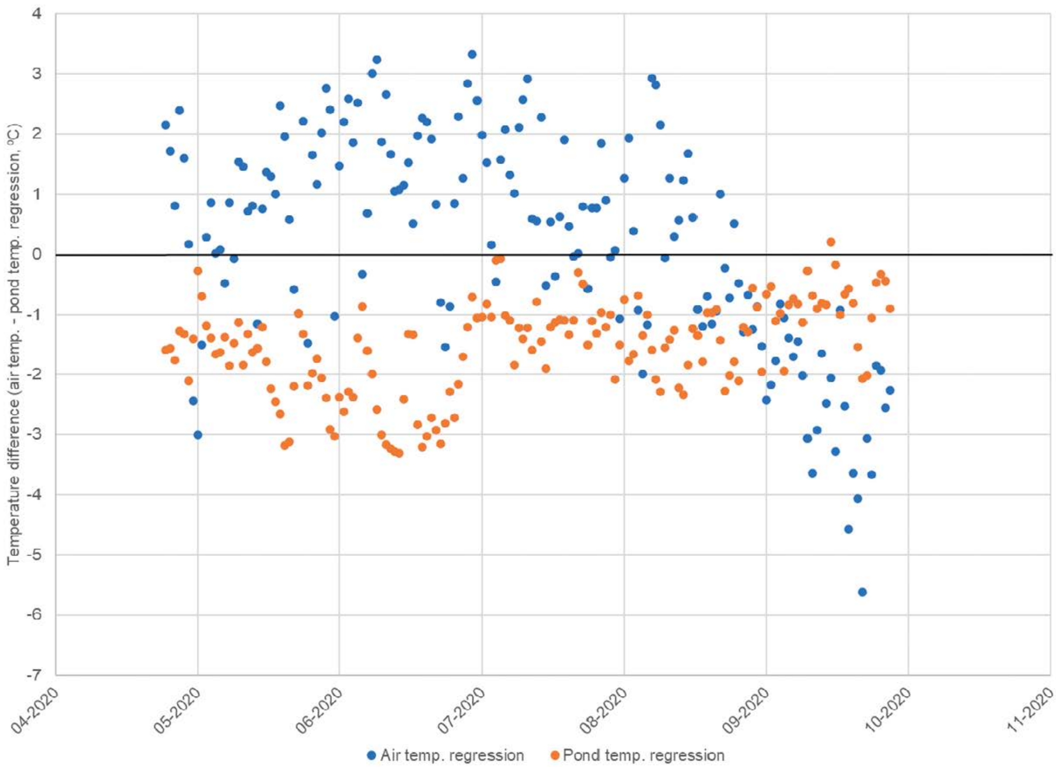

Figure 4-23. *PFM007872 plot (2020 campaign, MM-YYYY) of differences between daily averages of measured pond-water temperature, and temperatures calculated using the LR model developed for daily averages of air temperature (air temp. regression) and the LR model developed for the PFM007763 daily average water temperature (pond temp. regression), respectively.*

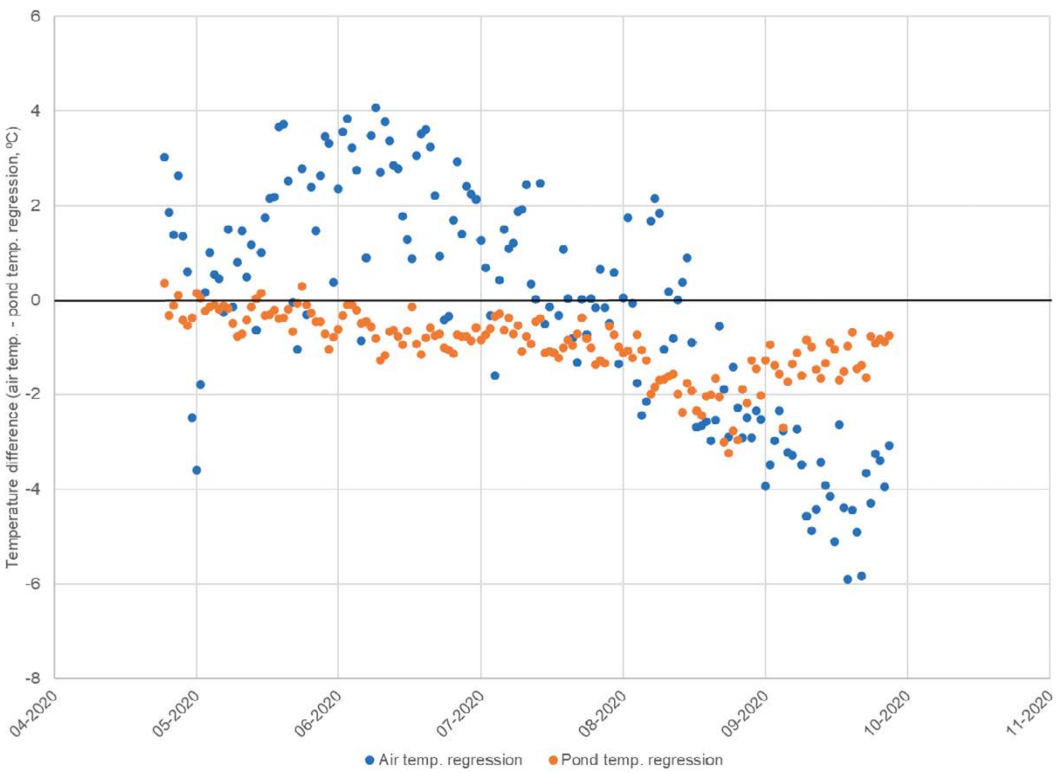

Figure 4-24. *PFM007873 plot (2020 campaign, MM-YYYY) of differences between daily averages of measured pond-water temperature, and temperatures calculated using the LR model developed for daily averages of air temperature (air temp. regression) and the LR model developed for the PFM007763 daily average water temperature (pond temp. regression), respectively.*

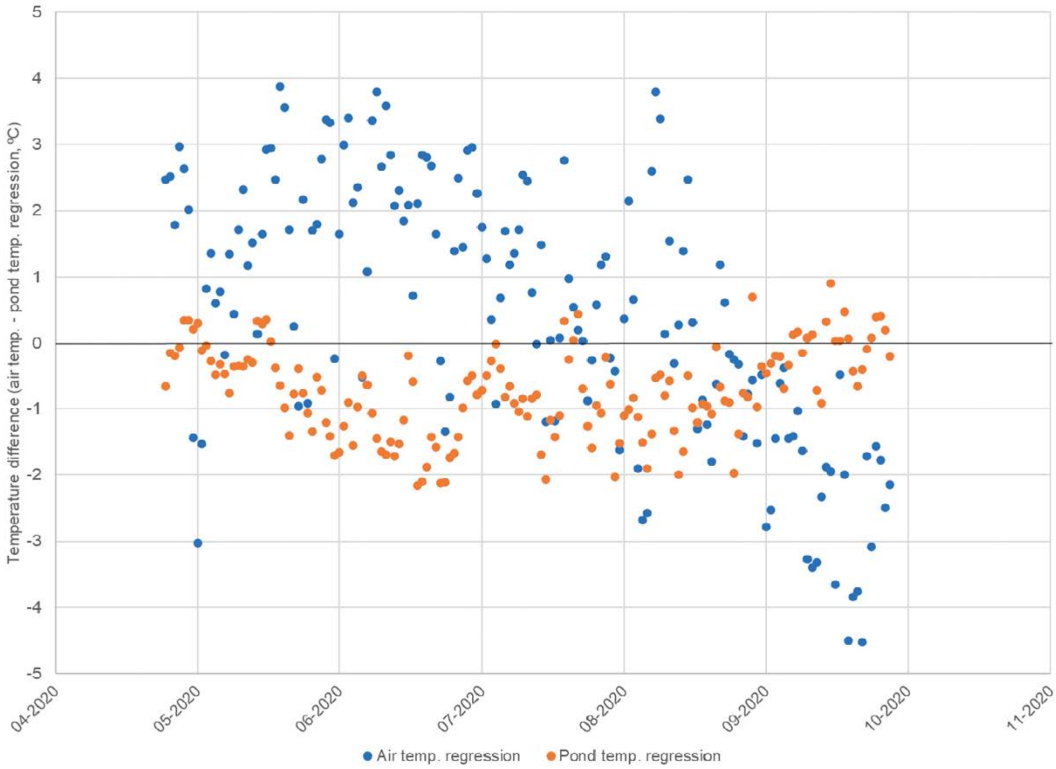

Figure 4-25. *PFM007920 plot (2020 campaign, MM-YYYY) of differences between daily averages of measured pond-water temperature, and temperatures calculated using the LR model developed for daily averages of air temperature (air temp. regression) and the LR model developed for the PFM007763 daily average water temperature (pond temp. regression), respectively.*

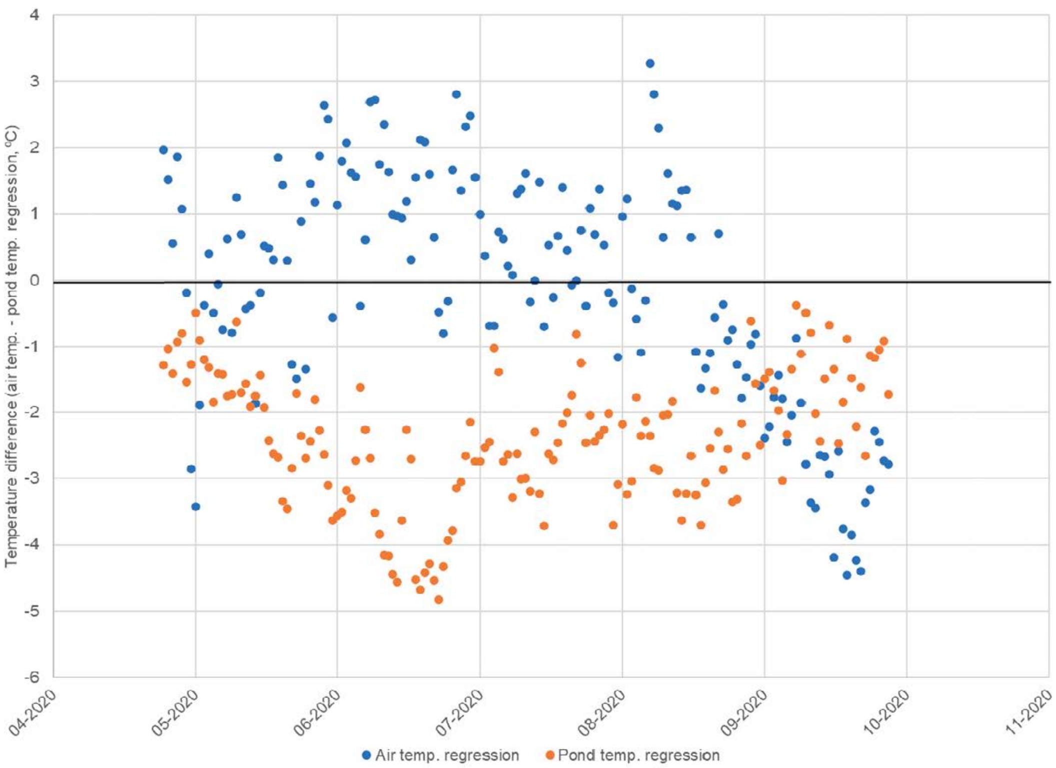

Figure 4-26. *PFM008120 plot (2020 campaign, MM-YYYY) of differences between daily averages of measured pond-water temperature, and temperatures calculated using the LR model developed for daily averages of air temperature (air temp. regression) and the LR model developed for the PFM007763 daily average water temperature (pond temp. regression), respectively.*

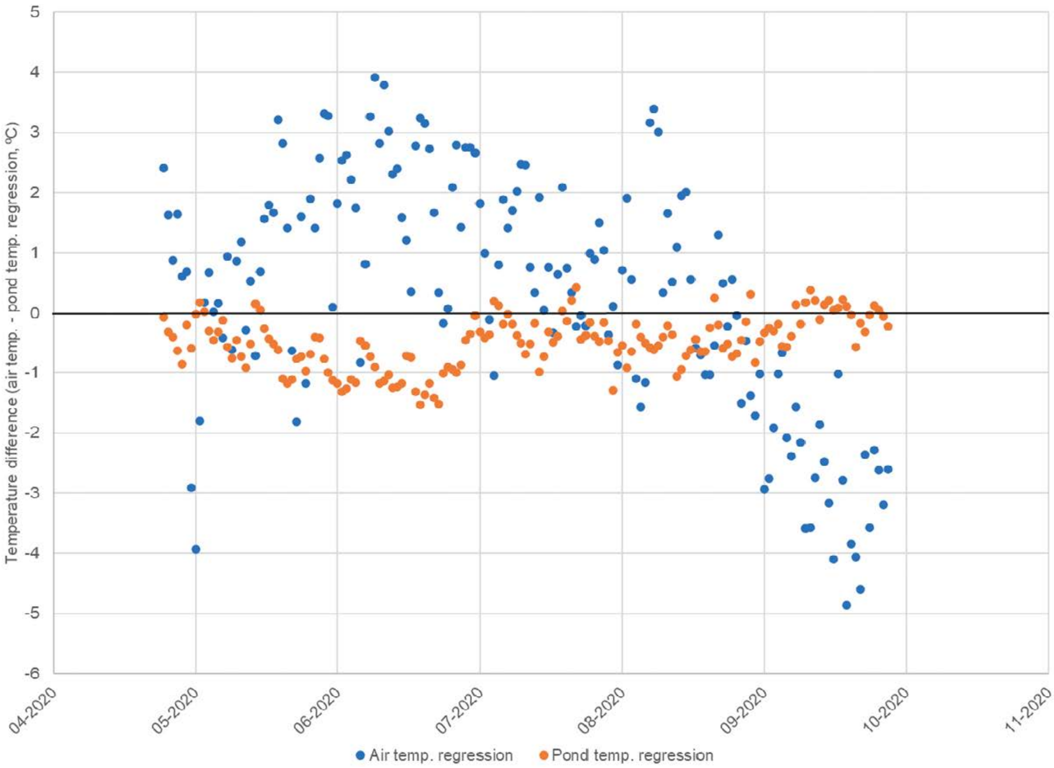

Figure 4-27. *PFM008122 plot (2020 campaign, MM-YYYY) of differences between daily averages of measured pond-water temperature, and temperatures calculated using the LR model developed for daily averages of air temperature (air temp. regression) and the LR model developed for the PFM007763 daily average water temperature (pond temp. regression), respectively.*

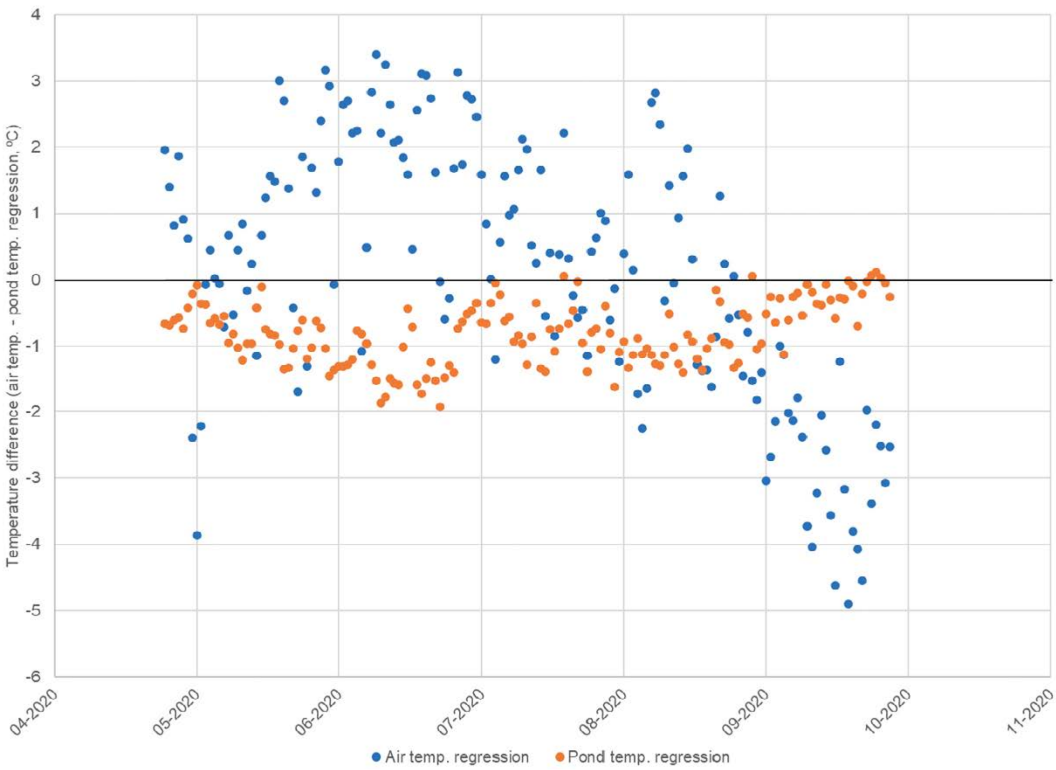

Figure 4-28. *PFM008123 plot (2020 campaign, MM-YYYY) of differences between daily averages of measured pond-water temperature, and temperatures calculated using the LR model developed for daily averages of air temperature (air temp. regression) and the LR model developed for the PFM007763 daily average water temperature (pond temp. regression), respectively.*

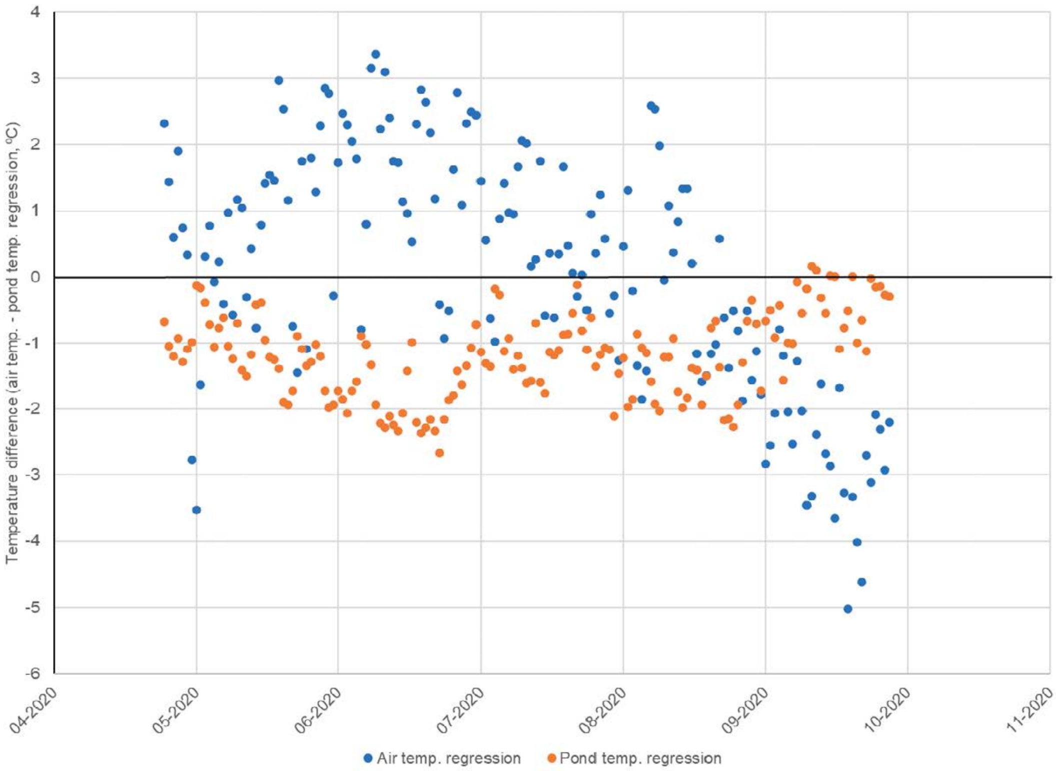

Figure 4-29. *PFM008124 plot (2020 campaign, MM-YYYY) of differences between daily averages of measured pond-water temperature, and temperatures calculated using the LR model developed for daily averages of air temperature (air temp. regression) and the LR model developed for the PFM007763 daily average water temperature (pond temp. regression), respectively.*

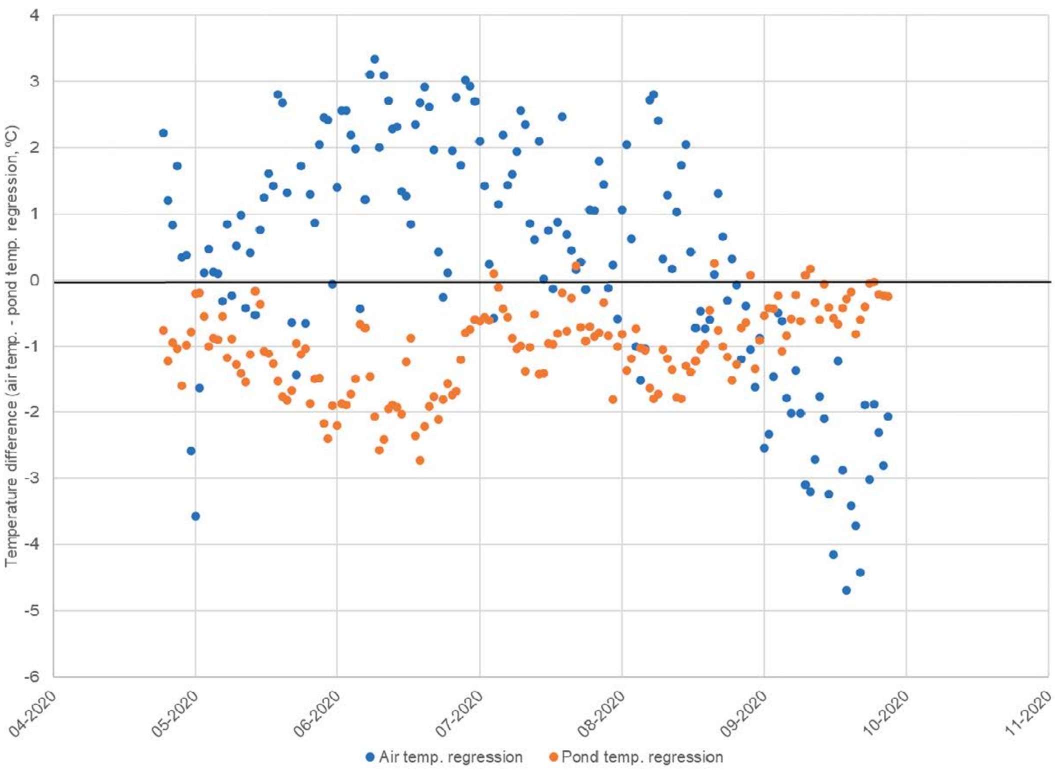

Figure 4-30. *PFM008125 plot (2020 campaign, MM-YYYY) of differences between daily averages of measured pond-water temperature, and temperatures calculated using the LR model developed for daily averages of air temperature (air temp. regression) and the LR model developed for the PFM007763 daily average water temperature (pond temp. regression), respectively.*

4.5 Monitoring of soil moisture and soil temperature

During the summer of 2017 sensors for soil moisture and soil temperature monitoring were installed in regolith at different depths below the ground surface at four locations (Figure 4-31 and Table 4-6), representing different regolith and evapotranspiration conditions (Hargelius et al. 2018, Werner 2018a): (1) Wetland (PFM007874–7875), (2) coniferous forest (PFM007876–7877), (3) coniferous forest on lime-rich soil (PFM007878–7879, and (4) open land (PFM007880–7881). The installed sensors (CS650 Soil Water Content Reflectometer, Onset Computer Corp.) measure volumetric soil-water content (water volume per unit volume of soil; Bilskie 2001) based on TDR (time domain reflectometry) technique. The sensors also measure EC and temperature, and they are connected to CR300 data loggers (Campbell Scientific Inc.).

In addition, during the summer of 2017 sensors (TMC6-HD and TMC20-HD, Onset Computer Corp.) for soil-temperature monitoring were installed in regolith at different depths below the ground surface at two locations, see Figure 4-31: (1) A clay area in the vicinity of a wetland (PFM007822; 8 sensors 0–140 cm below ground), and (2) a till-dominated area (PFM007823; 8 sensors 0–200 cm below ground). The sensors are connected to U12-008 data loggers (Onset Computer Corp.).

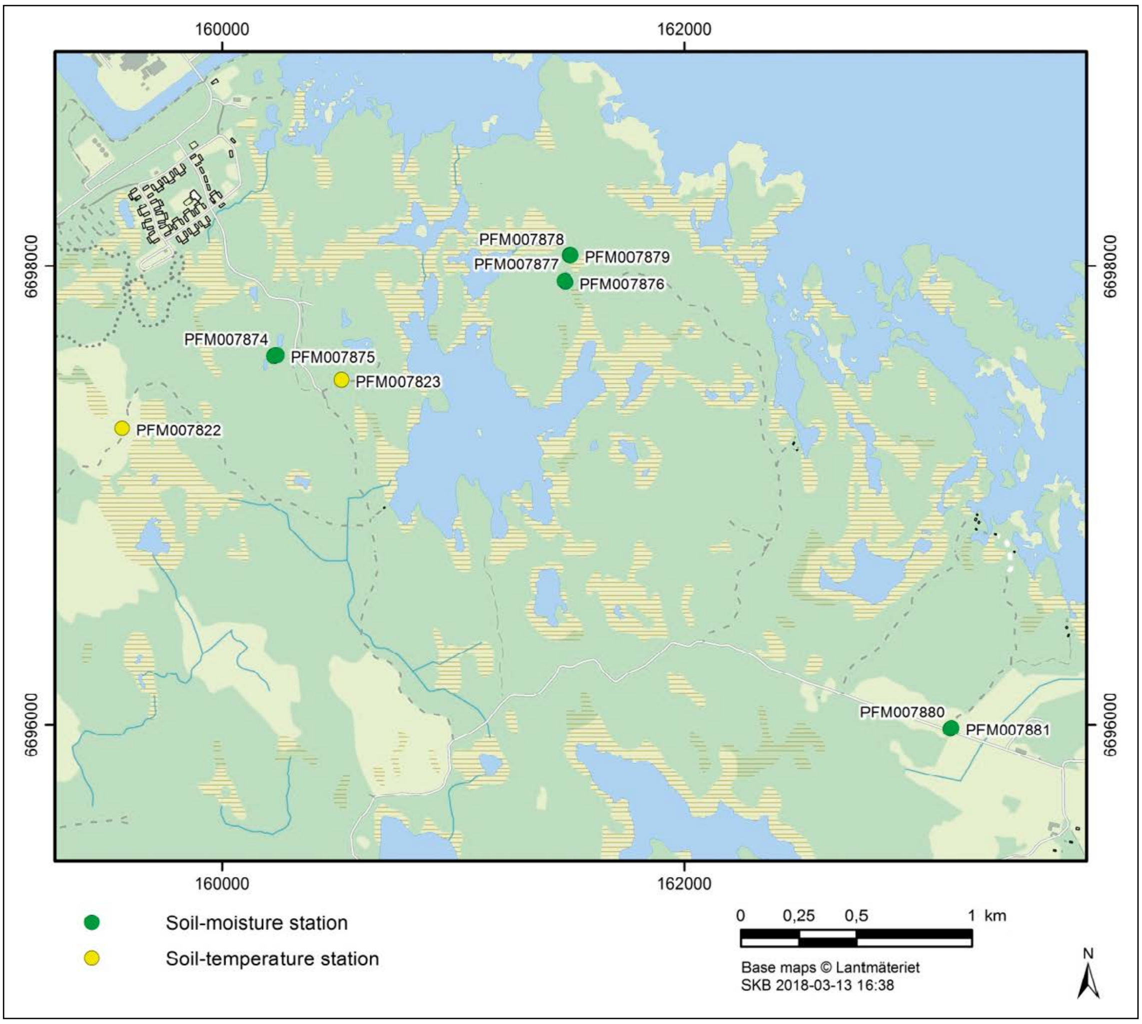

Figure 4-31. Locations of sensors for soil-moisture and soil-temperature monitoring.

Table 4-6. Installed soil moisture and temperature probes (Hargelius et al. 2018).

Location/station id	Regolith stratigraphy	Installation depth (m bgs)	Regolith type at installation depth
Wetland (station 4415)			
PFM007874	0–0.25 Humus 0.25–0.65 Till 0.65– Clay	0.15 0.25 0.60 0.75	Humus Till Clay Clay
PFM007875	0–0.15 Humus 0.15–0.50 Clay 0.50– Silty till	0.15 0.30 0.45 0.65	Humus Cay Clay Silty till
Coniferous forest (station 4413)			
PFM007876	0–0.15 Humus 0.15– Sandy till	0.07 0.10 0.25 0.45	Humus Humus Sandy till Sandy till
PFM007877	0–0.15 Humus 0.15– Sandy till	0.20 0.35 0.50 0.80	Sandy till Sandy till Sandy till Sandy till
Coniferous forest on lime-rich soil (station 4415)			
PFM007878	0–0.15 Humus 0.15–0.40 Sandy-silty till 0.40– Gravelly-sandy-silty-clayey till	0.10 0.42 0.70 0.85	Humus Sandy-silty-gravelly-clayey till Clayey-sandy-silty-gravelly till Clayey-sandy-silty-gravelly till
PFM007879	0–0.20 Humus 0.20– Gravelly-sandy-silty-clayey till	0.25 0.40 0.55 0.75	Humus Sandy-silty-gravelly-clayey till Clayey-sandy-silty-gravelly till Clayey-sandy-silty-gravelly till
Open land (station 4416)			
PFM007880	0–0.10 Humus 0.10–0.40 Sandy-gravelly till 0.40– Silty-clayey-gravelly till	0.10 0.40 0.70 0.90	Humus Sandy-gravelly till Silty-clayey-gravelly till Silty-clayey-gravelly till
PFM007881	0–0.10 Humus 0.10–0.30 Sandy-gravelly till 0.30– Silty-clayey-gravelly till	0.05 0.50 0.70 1.00	Humus Silty-clayey-gravelly till Silty-clayey-gravelly till Silty-clayey-gravelly till

Appendix 6 presents soil-moisture and soil-temperature data retrieved during the hydrological year 2019/2020, and some preliminary interpretations of the data. Table 4-7 summarizes soil-temperature data (soil-temperature sensors; Sicada activity type GT063 Temperature at different depth in the ground). Moreover, Table 4-8 provides a summary of soil-moisture and soil-temperature data (TDR sensors; Sicada activity type HY008 Soil moisture content (TDR)).

Table 4-7. Summary of results of soil-temperature monitoring during the 2019/2020 hydrological year (temperatures in °C). The measurement frequency is 3 hours.

Location id	Depth (m b gs)	Monitoring period	Average	St. dev.
PFM007822	0.00	2019-10-01–2020-09-30	5.91	5.12
	0.10	As above	6.00	4.13
	0.20	As above	6.21	3.56
	0.35	As above	6.29	3.20
	0.50	As above	6.39	2.88
	0.80	As above	6.32	2.37
	1.10	As above	6.45	1.99
	1.40	As above	6.43	1.77
PFM007823	0.00	As above	8.40	7.07
	0.20	As above	8.33	5.68
	0.40	As above	8.13	4.85
	0.75	As above	7.98	4.24
	1.00	As above	7.94	3.88
	1.25	As above	7.89	3.60
	1.50	As above	7.80	3.31
	2.00	As above	7.70	2.83

Table 4-8. Summary of results of soil moisture- and temperature monitoring during the 2019/2020 hydrological year. Freq. = measurement frequency, SWC = soil water content.

Location id	Monitoring period	Freq.	Depth (m b gs)	Average		St. dev.	
				Temp. (°C)	SWC (%)	Temp. (°C)	SWC (%)
PFM007874	2019-10-01–2020-09-30	10 mins	0.15	7.29	41.44	3.59	8.05
			0.25	7.30	9.79	3.18	2.11
			0.60	7.17	47.70	2.76	5.18
			0.75	7.25	49.19	2.64	1.73
PFM007875	As above	10 mins	0.15	7.36	45.90	3.90	17.82
			0.30	7.22	47.19	3.10	3.00
			0.45	7.29	49.15	3.44	2.11
			0.65	7.20	51.62	2.82	0.31
PFM007876	As above	1 h	0.07	7.23	19.79	3.67	14.70
			0.10	7.14	20.19	3.31	17.28
			0.25	7.25	24.92	3.88	15.84
			0.45	7.09	29.70	3.04	12.30
PFM007877	As above	1 h	0.20	7.26	12.57	4.02	7.38
			0.35	7.22	24.00	3.51	10.04
			0.50	7.23	27.70	3.38	12.17
			0.80	7.19	20.57	3.05	4.58
PFM007878	As above	1 h	0.10	7.61	18.85	3.75	7.29
			0.42	7.57	21.68	2.95	3.24
			0.70	7.59	21.46	2.66	2.90
			0.85	7.51	24.47	2.66	0.73
PFM007879	As above	1 h	0.25	7.56	23.86	3.58	9.70
			0.40	7.51	26.82	3.32	4.92
			0.55	7.47	32.99	3.12	9.46
			0.75	7.52	23.75	2.94	0.55
PFM007880	As above	10 mins	0.10	7.69	26.64	5.29	9.65
			0.40	7.66	20.52	4.66	7.78
			0.70	7.67	26.60	3.98	3.85
			0.90	7.62	24.98	3.78	2.97
PFM007881	As above	10 mins	0.05	8.00	28.54	5.72	10.80
			0.50	7.76	19.46	4.53	4.72
			0.70	7.69	20.88	4.06	4.02
			1.00	7.66	22.58	3.72	3.39

As exemplified in Figure 4-32 to Figure 4-35 (cf Appendix 6), measured soil temperatures demonstrate expected seasonal variations, with increasing temperatures during spring and decreasing temperatures during autumn. In addition, heating and cooling in response to seasonal air-temperature variations are faster close to the ground surface than at depth. In relation to near-surface soil temperatures, soil temperatures at depth show a time lag in response to seasonal air-temperature variations. Moreover, vertical soil-temperature gradients switch direction during the year. From autumn (say, end of September) up to late spring (say, end of March) soil temperatures at depth are higher than near-surface temperatures (the temperature gradient is directed upward). On the contrary, the temperature gradient is directed downward during the approximate period April–September (near-surface temperatures are higher than temperatures at depth).

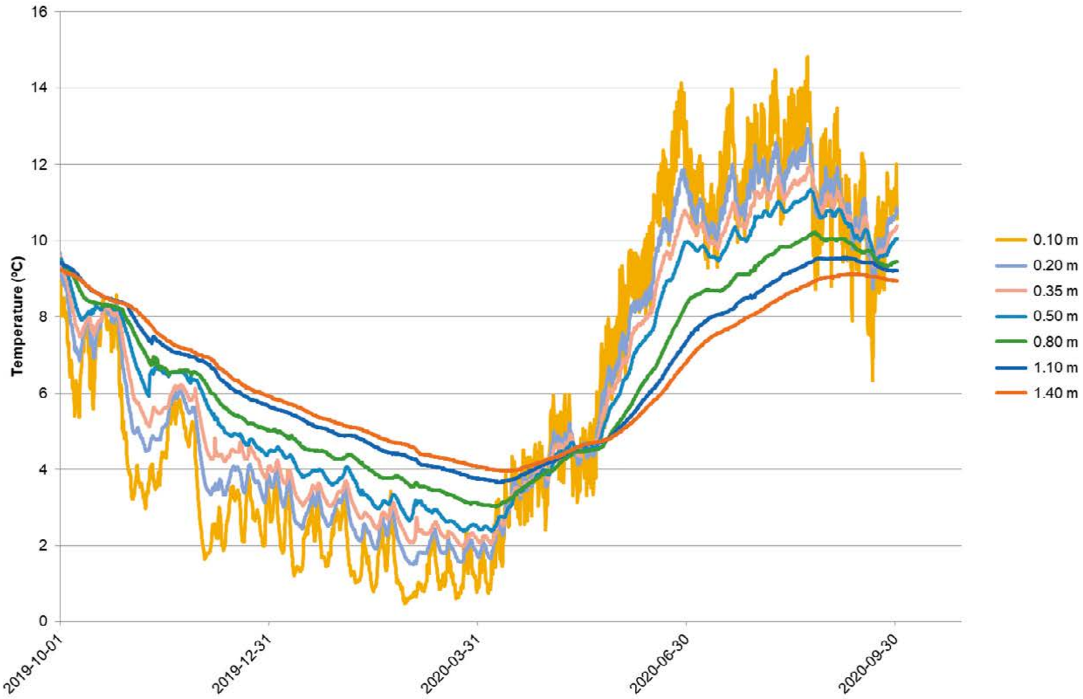

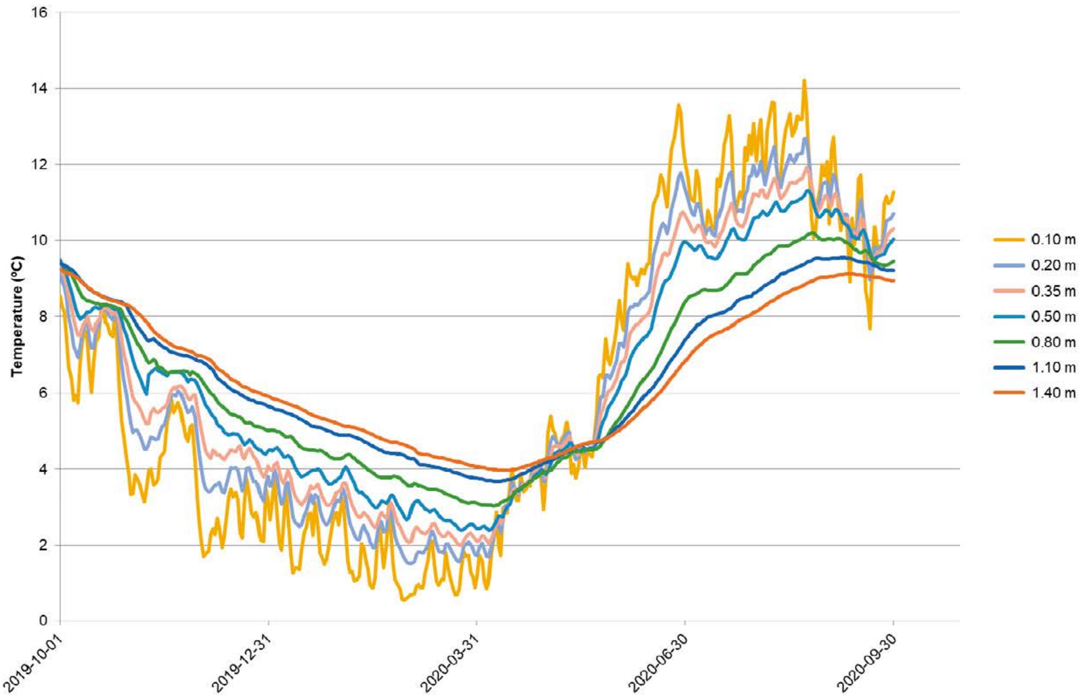

Figure 4-32. *Soil temperature at different depths below ground in PFM07822. Upper plot: High-resolution data (measurement interval 3 hours). Lower plot: Daily averages.*

According to soil-temperature data, there are no ground frost (soil temperatures equal to or below 0 °C) at the monitored locations (PFM007822-7823) during the 2019/2020 winter season. At PFM007880 and PFM007881, the lowest measured soil temperatures during the 2019/2020 winter season were close to but not quite 0 °C.

Near-surface soil temperatures demonstrate large temporal variations in response to short-term air-temperature variations, whereas soil temperatures at depth are more stable. As shown in Appendix 6, the same phenomenon is observed in terms of soil moisture, with generally larger temporal moisture variability close to the ground surface in response to short-term wetting (precipitation and snow melt) and drying (evapotranspiration) processes. At the TDR stations PFM007880 and -7881, the highest soil-water contents close to the ground surface are associated with soil-water temperatures slightly above 0 °C, likely attributed so melting of snow and ice. At the same time, the lowest soil-water temperatures are close to but not quite 0 °C (see above). This may be due to the so called zero-curtain effect (e.g. Kelley and Weaver 1969), which implies that release of latent heat slows down the phase transition from water to ice when air temperatures falls below zero.

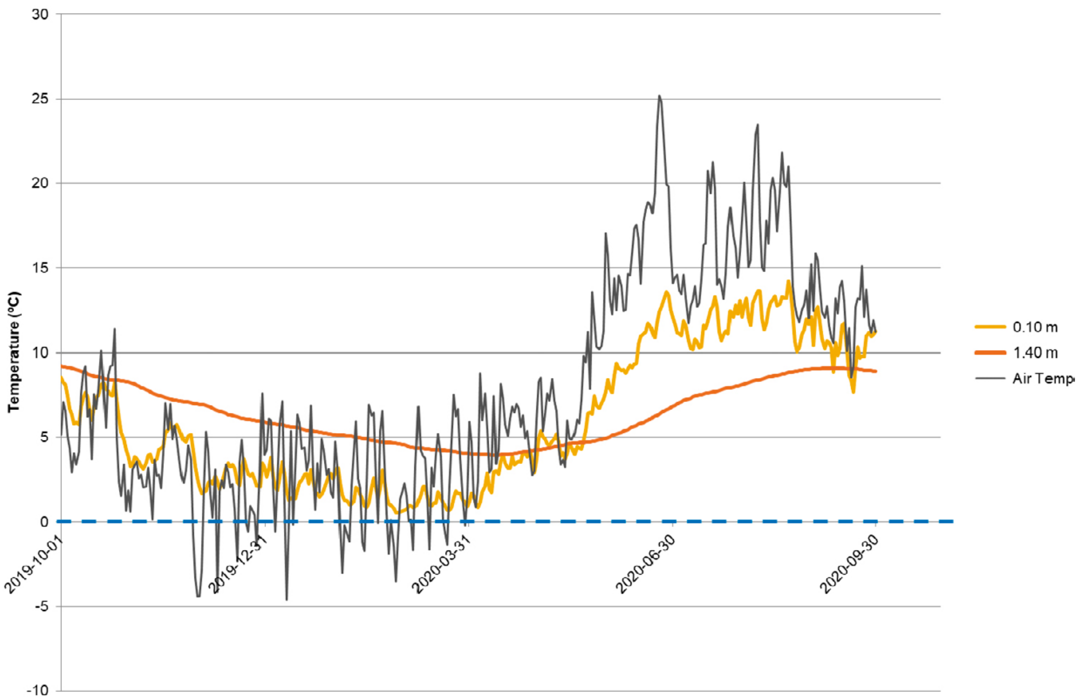

Figure 4-33. *Daily average soil temperatures at depths 0.10 and 1.40 m below ground surface at PFM07822. 0 °C is marked with a dashed line. For reference, the plot also shows daily average air temperature at the Labbomasten meteorological station (PFM006281) during the 2019/2020 hydrological year.*

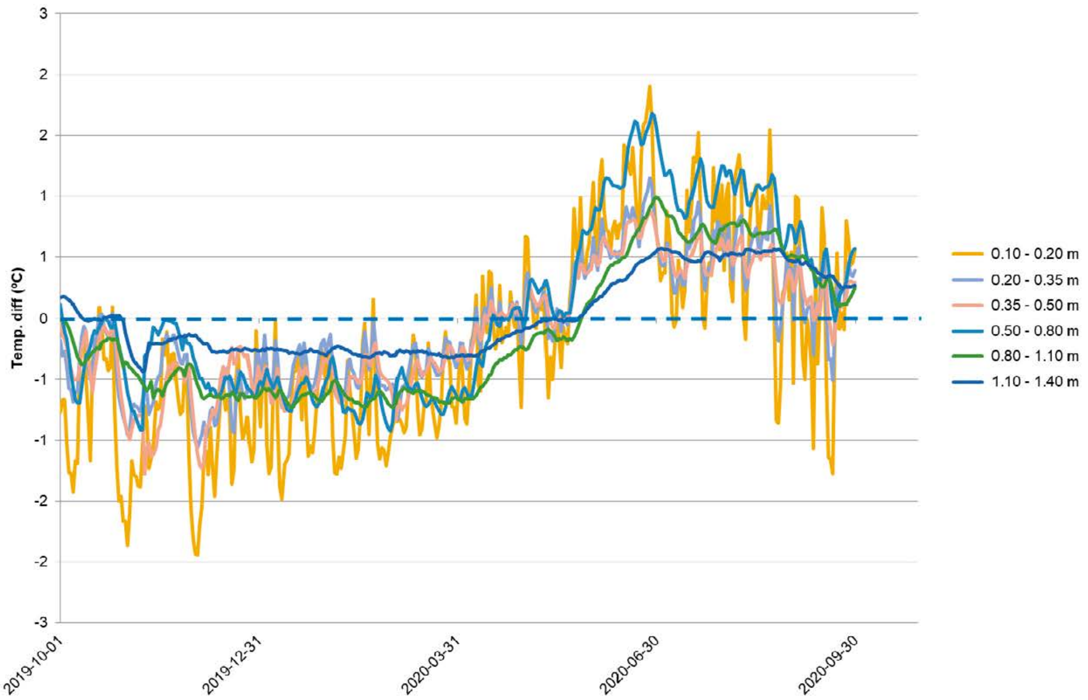

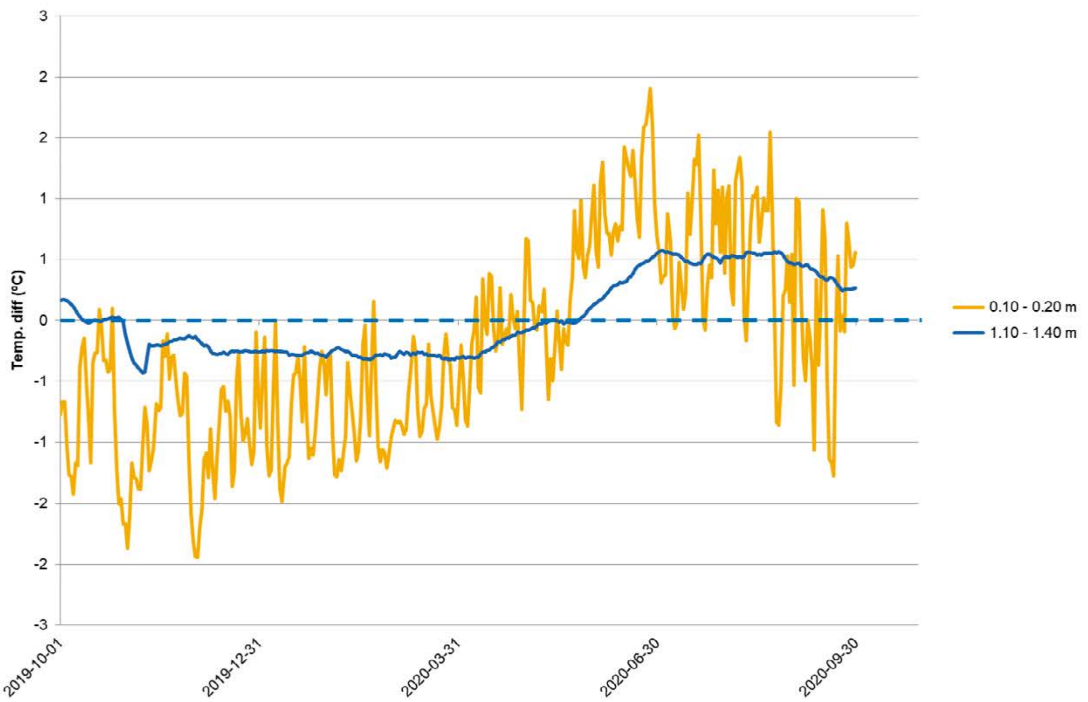

Figure 4-34. *Daily average soil-temperature differences between adjacent measurement depths below ground surface at PFM07822. Upper plot: All depths. Lower plot: Top and bottom measurement depths. 0 °C is marked with a dashed line.*

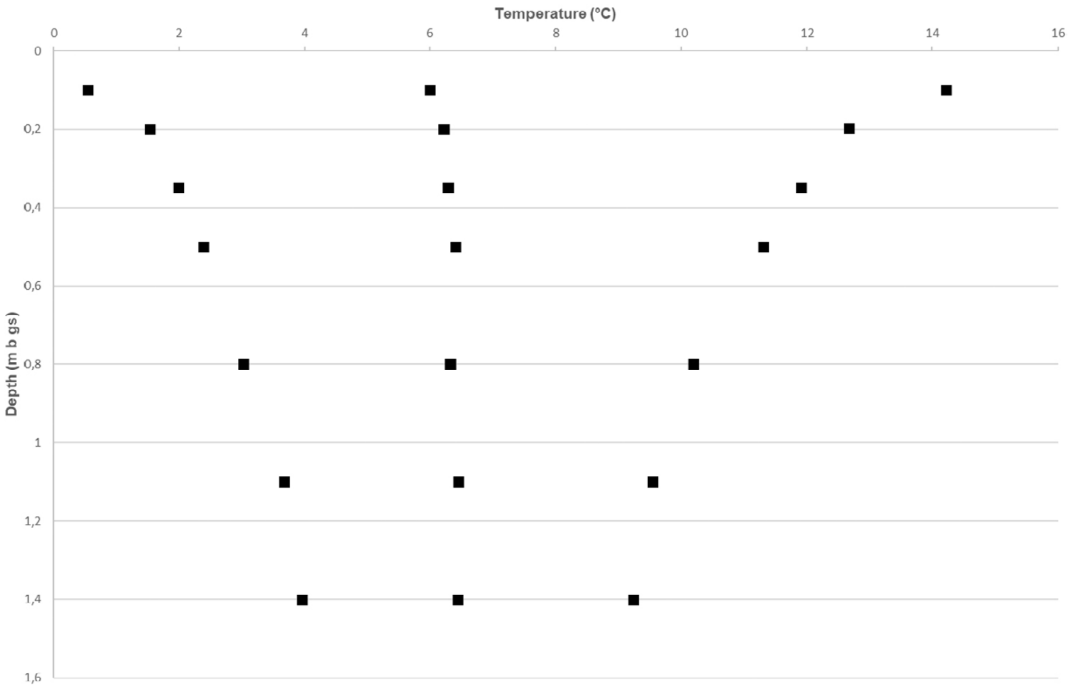

Figure 4-35. *Soil-temperature range (minimum, maximum, and average) at different measurement depths below ground surface at PFM07822.*

References

SKB's (Svensk Kärnbränslehantering AB) publications can be found at www.skb.com/publications. SKBdoc documents will be submitted upon request to document@skb.se.

Berglund S, Lindborg T (eds), 2017. Monitoring Forsmark – evaluation and recommendations for programme update. SKB TR-15-01, Svensk Kärnbränslehantering AB.

Bergqvist N, 2014a. Kontrollmätning Forsmark VP3 2013-12-16. SKBdoc 1445903 ver 1.0, Svensk Kärnbränslehantering AB. (In Swedish.)

Bergqvist N, 2014b. Kontrollmätning Forsmark VP3 2013-05-03. SKBdoc 1445923 ver 1.0, Svensk Kärnbränslehantering AB. (In Swedish.)

Bergqvist N, 2014c. Rapport från flödesmätning av mätrännor vecka 17 2014. 1445896 ver 1.0, Svensk Kärnbränslehantering AB. (In Swedish.)

Bergqvist N, 2019. Byte mätränna vid mätstation PFM002667 augusti 2018. SKBdoc 1699158 ver 1.0, Svensk Kärnbränslehantering AB. (In Swedish.)

Bergström S, 1993. Sveriges hydrologi – grundläggande hydrologiska förhållanden. SMHI, Norrköping. (In Swedish.)

Bilskie J, 2001. Soil water status: content and potential. App. Note 2S-I, Campbell Scientific, Inc., Logan, UT.

Borgiel M, Wallin A, Qvarfordt S, 2017. Mätning av ytvattentemperatur i gölar i Forsmark, 2016. SKB P-17-01, Svensk Kärnbränslehantering AB. (In Swedish.)

Borgiel M, Qvarfordt S, Wallin M, 2018. Mätning av ytvattentemperatur i gölar i Forsmark, 2017. SKB P-17-43, Svensk Kärnbränslehantering AB. (In Swedish.)

Borgiel M, Qvarfordt S, Wallin M, 2019. Mätning av ytvattentemperatur i gölar i Forsmark 2018. SKB P-19-01, Svensk Kärnbränslehantering AB. (In Swedish.)

Borgiel M, Qvarfordt S, Wallin M, 2020. Mätning av ytvattentemperatur i gölar i Forsmark 2019. SKB P-20-03, Svensk Kärnbränslehantering AB. (In Swedish.)

Borgiel M, Qvarfordt S, Wallin M, 2021. Mätning av ytvattentemperatur i gölar i Forsmark 2020. SKB P-21-01, Svensk Kärnbränslehantering AB. (In Swedish.)

Brunberg A-K, Carlsson T, Blomqvist P, Brydsten L, Strömgren M, 2004. Forsmark site investigation. Identification of catchments, lake-related drainage parameters and lake habitats. SKB P-04-25, Svensk Kärnbränslehantering AB.

Clemmens A J, Wahl T L, Bos M G, Replogle J A, 2001. Water measurement with flumes and weirs. ILRI Publ. 58, International Institute for Land Reclamation and Improvement, Wageningen, Netherlands.

Edvardson K, 2012. SKB avvägning jordrör/bäckrännor. Uppföljande avvägning av 14 jordrör, nybestämning av åtta jordrör samt lägen på sju bäckrännor. SWECO Infrastructure AB. SKBdoc 1395324 ver 1.0, Svensk Kärnbränslehantering AB. (In Swedish.)

Edvardson K, 2014. SKB höjdkontroll GV-rör, bäckrännor. Uppföljande höjdbestämning av 28 jordrör och sju bäckrännor, nybestämning av sju jordrör samt inmätning av strandlinjen i två nya gölar. SWECO Civil AB. SKBdoc 1444516 ver 1.0, Svensk Kärnbränslehantering AB. (In Swedish.)

Edvardson K, 2015. SKB höjdkontroll GV-rör, bäckrännor. Uppföljande höjdbestämning av 30 grundvattenrör och fem bäckrännor. SWECO Civil AB. SKBdoc 1593195 ver 1.0, Svensk Kärnbränslehantering AB. (In Swedish.)

Hamrén U, Collinder P, 2010. Vattenverksamhet i Forsmark. Ekologisk fältinventering och naturvärdesklassificering samt beskrivning av skogsproduktionsmark. SKB R-10-16, Svensk Kärnbränslehantering AB. (In Swedish.)

Hargelius M, Orbe R, Petrone J 2018. Installation och drift av fyra stationer för mätning av markvattenhalt i Forsmark. SKBdoc 1582426 ver 2.0, Svensk Kärnbränslehantering AB. (In Swedish.)

Hermansson N, 2017. Kontrollerande höjdbestämning av jordrör och bäckrännor i Forsmark 2017. Metria AB. SKBdoc 1601610 ver 1.0, Svensk Kärnbränslehantering AB. (In Swedish.)

Hermansson N, 2019. Kontrollerande höjdbestämning av jordrör och bäckrännor i Forsmark 2018. Metria AB. SKBdoc 1858639 ver 1.0, Svensk Kärnbränslehantering AB. (In Swedish.)

Höglund A, 2020. Registrering av snödjup/vatteninnehåll och tider för isläggning/islossning i Forsmark vintersäsongen 2019/2020. SKBdoc 1906075 ver 1.0, Svensk Kärnbränslehantering AB. (In Swedish.)

Johansson P-O, 2005. Forsmark site investigation. Installation of brook discharge gauging stations. SKB P-05-154, Svensk Kärnbränslehantering AB.

Johansson P-O, Juston J, 2007. Forsmark site investigation. Monitoring of brook levels, water electrical conductivities, temperatures and discharges from April 2004 until March 2007. SKB P-07-135, Svensk Kärnbränslehantering AB.

Johansson P-O, Juston J, 2009. Forsmark site investigation. Monitoring of brook water levels, electrical conductivities, temperatures and discharges from April 2007 until December 2008. SKB P-09-68, Svensk Kärnbränslehantering AB.

Johansson P-O, Juston J, 2011a. Forsmark site investigation. Monitoring of brook water levels, electrical conductivities, temperatures and discharges January–December 2009. SKB P-10-44, Svensk Kärnbränslehantering AB.

Johansson P-O, Juston J, 2011b. Forsmark site investigation. Monitoring of brook water levels, electrical conductivities, temperatures and discharges January–December 2010. SKB P-11-12, Svensk Kärnbränslehantering AB.

Johansson P-O, Werner K, 2019. Surface-water levels and groundwater levels in regolith at the Forsmark site. Monitoring programme updates prior to repository construction. SKB P-18-10, Svensk Kärnbränslehantering AB.

Jones J, 2021. Meteorological monitoring at Forsmark during the hydrological year October 2019 –September 2020. SKBdoc 1924269 ver 1.0, Svensk Kärnbränslehantering AB.

Kelley J J, Weaver D F, 1969. Physical processes at the surface of the arctic tundra. Arctic 22, 425–437.

Kilpatrick F A, Schneider V R, 1983. Use of flumes in measuring discharge. Techniques of Water-Resources Investigations of the United States Geological Survey. Book 3 – Applications of Hydraulics, Chapter A14.

Ohrzén S, 2016. SKB höjdkontroll GV-rör, bäckrännor. Uppföljande höjdbestämning av 40 grundvattenrör, fyra bäckrännor och en sjötröskel. SKBdoc 1552488 ver 1.0. SWECO Civil AB. Svensk Kärnbränslehantering AB. (In Swedish.)

Orizaola G, Quintela M, Laurila A, 2010. Climatic adaptation in an isolated and genetically impoverished amphibian population. Ecography 33, 730–737.

Robinson A R, 1966. Water measurement in small irrigation channels using trapezoidal flumes. Transactions – American Society of Agricultural Engineers 9, 382–388.

Robinson A R, 1968. Trapezoidal flumes for measuring flow in irrigation channels. ARS 41-140, Agricultural Research Service, United States Deptartment of Agriculture.

Ryman M, Strömbeck N, 2016. Luode teknisk delrapport. Redovisning av utförda flödesmätningar i naturliga vattendrag vid SKB's mätstationer utanför Forsmark. Luode Consulting Oy. SKBdoc 1538578 ver 1.0, Svensk Kärnbränslehantering AB. (In Swedish.)

Ryman M, Strömbeck N, 2018. Luode teknisk rapport. Redovisning av installation av mätutrustning samt utförda flödesmätningar i naturliga vattendrag vid SKB's mätstationer utanför Forsmark. Luode Consulting Oy. SKBdoc 1858240 ver 1.0, Svensk Kärnbränslehantering AB . (In Swedish.)

SKB, 2007. Forsmark site investigation. Programme for long-term observations of geosphere and biosphere after completed site investigations. SKB R-07-34, Svensk Kärnbränslehantering AB.

SWECO, 2013. SKB avvägning jordrör/bäckrännor. Uppföljande mätning av 29 jordrör, lägen på sju bäckrännor samt sju strandlinjer. SWECO Infrastructure AB. SKBdoc 1417299 ver 2.0, Svensk Kärnbränslehantering AB. (In Swedish.)

Wahl T L, Clemmens A J, Replogle J A, Bos M G, 2000. WinFlume – Windows-based software for the design of long-throated measuring flumes. 4th Decennial National Irrigation Symposium, 14–16 November, Phoenix, AZ.

Wass E, 2021. Monitoring Forsmark. Hydro Monitoring Program. Report for October 2019 – September 2020. SKBdoc 1956418 ver 1.0, Svensk Kärnbränslehantering AB.

Werner K, 2014a. Monitoring hydrology in Forsmark 2011–2012. Projekt Kärnbränsleförvaret, Slutförvarsanläggning för använt kärnbränsle – Monitoring of streams: Water level, discharge, electrical conductivity and temperature 2011–2012. SKBdoc 1437594 ver 2.0, Svensk Kärnbränslehantering AB.

Werner K, 2014b. Monitoring hydrology in Forsmark 2013. Monitoring of streams: Water level, discharge, electrical conductivity and temperature 2013. SKBdoc 1449116 ver 1.0, Svensk Kärnbränslehantering AB.

Werner K, 2015. Flödesmätningar i bäckar i Forsmark – mätningar med saltutspädningsmetoden 2014-12-09. SKBdoc 1467666 ver 1.0, Svensk Kärnbränslehantering AB. (In Swedish.)

Werner K, 2016. Monitoring hydrology in Forsmark 2014. Monitoring of streams: Water level, discharge, electrical conductivity and temperature 2014. SKBdoc 1520285 ver 1.0, Svensk Kärnbränslehantering AB.

Werner K, 2017. Monitoring hydrology in Forsmark 2015. Monitoring of streams: Water level, discharge, electrical conductivity and temperature. SKB P-17-27, Svensk Kärnbränslehantering AB.

Werner K, 2018a. Hydrological monitoring in Forsmark – surface waters, ground moisture and ground temperature October 1, 2016 – September 30, 2017. SKB P-17-44, Svensk Kärnbränslehantering AB.

Werner K, 2018b. Monitoring hydrology in Forsmark. Hydrological year October 1, 2015 – September 30, 2016. Monitoring of streams: Water level, discharge, electrical conductivity and temperature. SKB P-17-29, Svensk Kärnbränslehantering AB.

Werner K, 2019. Hydrological monitoring in Forsmark – surface waters, ground moisture and ground temperature October 1, 2017 – September 30, 2018. SKB P-19-08, Svensk Kärnbränslehantering AB.

Werner K, 2020. Hydrological monitoring in Forsmark – surface waters, ground moisture and ground temperature October 1, 2018– September 30, 2019. SKB P-20-10, Svensk Kärnbränslehantering AB.

Werner K, Norville J, Öhman J, 2014. Meteorological, hydrological and hydrogeological monitoring data from Forsmark – compilation and analysis for the SR-PSU project. SR-PSU Biosphere. SKB R-13-20, Svensk Kärnbränslehantering AB.

Appendix 1

Tables

Table A1-1 presents flume and observation-well coordinates, whereas Table A1-2 and Table A1-3 show results of levelling of flume-bottom levels and top of casing of observation wells, respectively.

Table A1-1. Flume and observation-well coordinates (Northing and Easting: RT 90 2.5 gon W 0:-15; elevation: RHB 70) used for calculation and adjustment of water levels and calculation of stream discharges (see also Section 3.4.3). Flume and/or well movements are handled by calibration-constant adjustments (cf Table 3-1). Note that after refurbishment in 2018, the PFM002667 station is levelled in the coordinate system RH 2000 (Hermansson 2019). Elevation in the RHB 70 system is calculated as RH 2000–0.185 m.

Id	Northing (m)	Easting (m)	Elevation (m)
PFM005764 (Nov. 27, 2003–Oct. 1, 2004)			
Small flume			
Top of obs. well	6698745.4	1631660.4	1.701
Flume bottom, upstream edge	6698747.6	1631658.9	0.577
Large flume			
Top of obs. well	6698752.1	1631666.5	1.740
Flume bottom, upstream edge	6698753.1	1631665.1	0.551
PFM005764 (Oct. 5, 2004–Aug. 25, 2014)			
Small flume			
Top of obs. well	6698745.4	1631660.9	2.190 (orig. levelling; lowered to 2.050 in Sep. 2006, handled by cal.- const. adjustment; Table 3-1)
Flume bottom, upstream edge	6698747.3	1631659.1	0.903
Large flume			
Top of obs. well	6698751.8	1631667.2	2.117
Flume bottom, upstream edge	6698753.0	1631666.0	0.895
PFM005764 (Aug. 26, 2014–)			
Small flume			
Top of obs. well	6698746.5	1631657.3	2.085
Flume bottom, upstream edge	6698747.8	1631656.0	0.924
Large flume			
Top of obs. well	6698754.1	1631666.6	2.131
Flume bottom, upstream edge	6698755.4	1631665.1	0.893
PFM002667 (Oct. 1, 2004–Aug. 16, 2018)			
Small flume			
Top of obs. well	6698263.0	1631595.5	2.679
Flume bottom, upstream edge	6698264.1	1631593.5	1.502
Large flume			
Top of obs. well	6698270.2	1631598.4	2.721
Flume bottom, upstream edge	6698271.0	1631596.5	1.511

Id	Northing (m)	Easting (m)	Elevation (m)
PFM002667 (Aug. 30, 2018–)			
Single flume			
Top of obs. well	6698270.5	1631598.0	2.771
Flume bottom, upstream edge	6698270.9	1631597.1	1.580
PFM002668			
Top of obs. well	6697474.9	1632066.9	5.482
Flume bottom, upstream edge	6697475.5	1632065.7	4.287
PFM002669 (Nov. 10, 2003–Sep. 14, 2015)			
Small flume			
Top of obs. well	6699047.4	1629371.7	6.994 (orig. levelling; reinstalled in Nov. 2007, handled by cal.-const. adjustment; Table 3-1)
Flume bottom, upstream edge	6699046.6	1629371.2	5.852 (orig. levelling; reinstalled in Nov. 2007, handled by cal.-const. adjustment; Table 3-1)
Large flume			
Top of obs. well	6699045.9	1629379.9	6.901 (orig. levelling; reinstalled in Nov. 2007, handled by cal.-const. adjustment; Table 3-1)
Flume bottom, upstream edge	6699043.9	1629379.1	5.843 (orig. levelling; reinstalled in Nov. 2007, handled by cal.-const. adjustment; Table 3-1)
PFM002669 (Sep. 15, 2015–)			
Small flume			
Top of obs. well	6699048.1	1629370.3	6.607
Flume bottom, upstream edge	6699048.9	1629370.6	5.441
Large flume			
Top of obs. well	6699047.3	1629379.5	6.501
Flume bottom, upstream edge	6699045.6	1629378.5	5.431

Table A1-2. Results of the levelling of bottom levels (m) of upstream edges of flumes at time of flume installations (2004) and in 2012–2018. Using the notation of the levelling reports, points B and C refer to each flume-bottom corner (single point C in the 2018 levelling of PFM002667). The flumes at PFM002669 were reinstalled in 2007, and the PFM005764, PFM002669 and PFM002667 stations were refurbished in Aug. 2014, Aug.–Sep. 2015 and Aug. 2018, respectively. The results of the 2013 levelling are inconsistent. Note that PFM002667 was not included in the 2016 levelling campaign, and that PFM002668 was not included in the 2016 and 2017 campaigns. The data in the table are not stored in Sicada. Dates are given as YYYY-MM-DD.

Gauging station and flume)	Point B (RHB 70)	Point C (RHB 70)	Average (RHB 70)	Level change (m)
PFM005764				
Original levelling (2004-04-30):				
Small flume	0.577	Used for discharge calc. 2003-11-27–2004-10-01		
Large flume	0.551	As above		
Levelling after reconstruction (2004-11-09):				
Small flume	0.903	Station reconstructed in Oct. 2004 Used for discharge calc. 2004-10-05–2014-08-25 and as ref. level for man. meas. in HMS 2004-11-03–2014-08-25 (obs. well ToC was used up to 2004-11-03)		
Large flume	0.895	As above		
2012:				
Small flume	0.911	0.908	0.910	-
Large flume	0.889	0.896	0.893	-
2013:				
Small flume	0.894	0.892	0.893	−0.017 (level change since 2012)
Large flume	0.885	0.890	0.888	−0.004 (as above)
2014:				
Small flume	0.909	0.908	0.909	−0.002 (as above)
Large flume	0.891	0.898	0.895	+0.002 (as above)
Levelling after reconstruction (2015):				
Small flume	0.924	0.923	0.924	Refurbished Aug. 2014 Used for discharge calc. and as ref. level for man. meas. in HMS 2014-08-26–
Large flume	0.889	0.897	0.893	As above
2016:				
Small flume	0.924	0.923	0.924	0 (level change since refurbishment)
Large flume	0.889	0.896	0.893	0 (as above)
2017:				
Small flume	0.928	0.927	0.928	+0.004 (as above)
Large flume	0.893	0.899	0.896	+0.004 (as above)

Gauging station and flume)	Point B (RHB 70)	Point C (RHB 70)	Average (RHB 70)	Level change (m)
PFM002667				
Original levelling (2004-11-09):				
Small flume	1.502	Used for discharge calc. 2004-12-08– and as ref. level for man. meas. in HMS 2004-11-03– (the obs. well ToC was used up to 2004-11-03)		
Large flume	1.511	As above		
2012:				
Small flume	1.565	1.564	1.565	-
Large flume	1.566	1.569	1.568	-
2013:				
Small flume	1.570	1.570	1.570	+0.005 (level change since 2012)
Large flume	1.572	1.576	1.574	+0.006 (as above)
2014:				
Small flume	1.568	1.568	1.568	+0.003 (as above)
Large flume	1.570	1.573	1.572	+0.004 (as above)
2015:				
Small flume	1.566	1.566	1.566	+0.001 (as above)
Large flume	1.567	1.570	1.569	+0.001 (as above)
2017:				
Small flume	1.569	1.568	1.569	+0.004 (as above)
Large flume	1.570	1.573	1.572	+0.004 (as above)
Levelling after reconstruction (2018):				
Single flume	-	-	1.580 (single levelling point denoted C acc. to the levelling report)	Refurbished Aug. 2018 Used for discharge calc. and as ref. level for man. meas. in HMS 2018-08-30–
PFM002668				
Original levelling (2004-11-10):				
	4.287	Used for discharge calc. 2004-12-08– and as ref. level for man. meas. in HMS 2004-11-03 (the obs. well ToC was used up to 2004-11-03)		
2012:				
	4.282	4.278	4.280	-
2013:				
	4.286	4.282	4.284	+0.004 (level change since 2012)
2014:				
	4.283	4.279	4.281	+0.001 (as above)
2015:				
	4.282	4.278	4.280	0 (as above)

Gauging station and flume)	Point B (RHB 70)	Point C (RHB 70)	Average (RHB 70)	Level change (m)
PFM002669				
Original levelling (2004-11-10):				
Small flume	5.852		Used for discharge calc. 2004-12-08–2015-09-14 and as reference point in HMS 2004-11-03–2015-09-14 (obs. well before that)	
Large flume	5.843		As above	
2012:				
Small flume	5.438	5.439	5.439	-
Large flume	5.425	5.431	5.428	-
2013:				
Small flume	5.443	5.444	5.444	+0.005 (level change since 2012)
Large flume	5.433	5.440	5.437	+0.008 (as above)
2014:				
Small flume	5.440	5.441	5.441	+0.002 (as above)
Large flume	5.427	5.435	5.431	+0.002 (as above)
Levelling after refurbishment (2016):				
Small flume	5.441	5.441	5.441	Refurbished Aug.–Sep. 2015
Large flume	5.428	5.433	5.431	Used for discharge calc. and as ref. level for man. meas. in HMS 2015-09-15–
2017:				
Small flume	5.442	5.443	5.443	+0.001 (level change since refurbishment)
Large flume				Not levelled

Table A1-3. Results of the levelling of top of casing of observation wells (m) at flumes in 2012–2018. Using the notation of the levelling reports, point I refer to the well ToC (point A in the 2018 levelling of PFM002667). The wells at PFM002669 were reinstalled in 2007, and the PFM005764, PFM002669 and PFM002667 stations were refurbished in Aug. 2014, Aug.–Sep. 2015 and Aug. 2018, respectively. The results of the 2013 levelling and the 2012 levelling of PFM002668 (likely measurement error) are inconsistent. Note that PFM002667 was not included in the 2016 levelling campaign, and that PFM002668 was not included in the 2016 and 2017 campaigns. Unless stated otherwise, data are not stored in Sicada. Dates are given as YYYY-MM-DD.

Gauging station and well	Original levelling	Comment on original levelling
	Point I (RHB 70)	Level change since original levelling (m)
PFM005764		
Original levelling (2004-04-30):		
Small flume	1.701 (stored in Sicada)	Used as ref. level for man. meas. in HMS 2003-03-01–2004-10-04
Large flume	1.740	As above
Levelling after reconstruction (2004-11-09):		
Small flume	2.190 (stored in Sicada)	Station reconstructed in Oct. 2004 Used as ref. level for man. meas. in HMS 2004-10-05–2004-11-02 (flume-bottom level is used after 2004-11-02)
Large flume	2.117	As above
Levelling after lowering of well (2006-09-13):		
Small flume	2.050 (stored in Sicada)	Well lowered to eliminate the zero-discharge issue (cf Table 3-2)
2012:		
Small flume	2.059	-
Large flume	2.141	-
2013:		
Small flume	2.064	+0.005 (level change since 2012)
Large flume	2.147	+0.006 (as above)
2014:		
Small flume	2.058	−0.001 (as above)
Large flume	2.144	+0.003 (as above)
Levelling after refurbishment (2015):		
Small flume	2.085 (stored in Sicada)	Station refurbished in Aug. 2014
Large flume	2.131	Station refurbished in Aug. 2014
2016:		
Small flume	2.085	0 (level change since refurbishment)
Large flume	2.132	+0.001 (as above)
2017:		
Small flume		Not levelled
Large flume	2.133	+0.002 (level change since refurbishment)
PFM002667		
Original levelling (2004-11-09):		
Small flume	2.679 (stored in Sicada)	Used as ref. level for man. meas. in HMS 2004-10-01–2004-11-02 (flume-bottom level is used after 2004-11-02)
Large flume	2.721	As above
2012:		
Small flume	2.769	-
Large flume	2.804	-

Gauging station and well	Original levelling	Comment on original levelling
	Point I (RHB 70)	**Level change since original levelling (m)**
2013:		
Small flume	2.787	+0.018 (level change since 2012)
Large flume	2.823	+0.019 (as above)
2015:		
Small flume	2.770 (stored in Sicada)	+0.001 (as above)
Large flume	2.804	0 (as above)
2017:		
Small flume		Not levelled
Large flume		Not levelled
Levelling after refurbishment (2018):		
Single flume	2.771 (point A)	Station refurbished in Aug. 2018
PFM002668		
Original levelling (2004-11-10):		
	5.482 (stored in Sicada)	Used as ref. level for man. meas. in HMS 2004-10-01–2004-11-02 (flume-bottom level is used after 2004-11-02)
2012:		
	5.128 (likely measurement error)	-
2013:		
	5.497	-
2015:		
	5.479 (stored in Sicada)	−0.003 (level change since 2012)
PFM002669		
Original levelling (2004-11-10):		
Small flume	6.994 (stored in Sicada)	Used as ref. level for man. meas. in HMS 2004-10-01–2004-11-02 (flume-bottom level is used after 2004-11-02)
Large flume	6.901	As above
2012:		
Small flume	6.605 (well reinstalled in 2007)	-
Large flume	6.509 (as above)	-
2013:		
Small flume	6.631	+0.026 (level change since 2012)
Large flume	6.532	+0.023 (as above)
2014:		
Small flume	6.609	+0.004 (as above)
Large flume	6.510	+0.001 (as above)
Levelling after refurbishment (2016):		
Small flume	6.607	Refurbished Aug.–Sep. 2015
Large flume	6.501	Refurbished Aug.–Sep. 2015
2017:		
Small flume		Not levelled
Large flume		Not levelled

Appendix 2

Water level

Figures A2-1 to A2-8 show water level time-series plots for the flumes at gauging stations PFM005764, -2667, -2668 and -2669 for the period October 1, 2019–September 30, 2020. The plots also show manually measured water levels (flume-bottom elevation + manually measured water depth), and data periods excluded (SCREEN) from the data transfer to the Sicada database as a result of the quality control of the 2019/2020 water-level dataset.

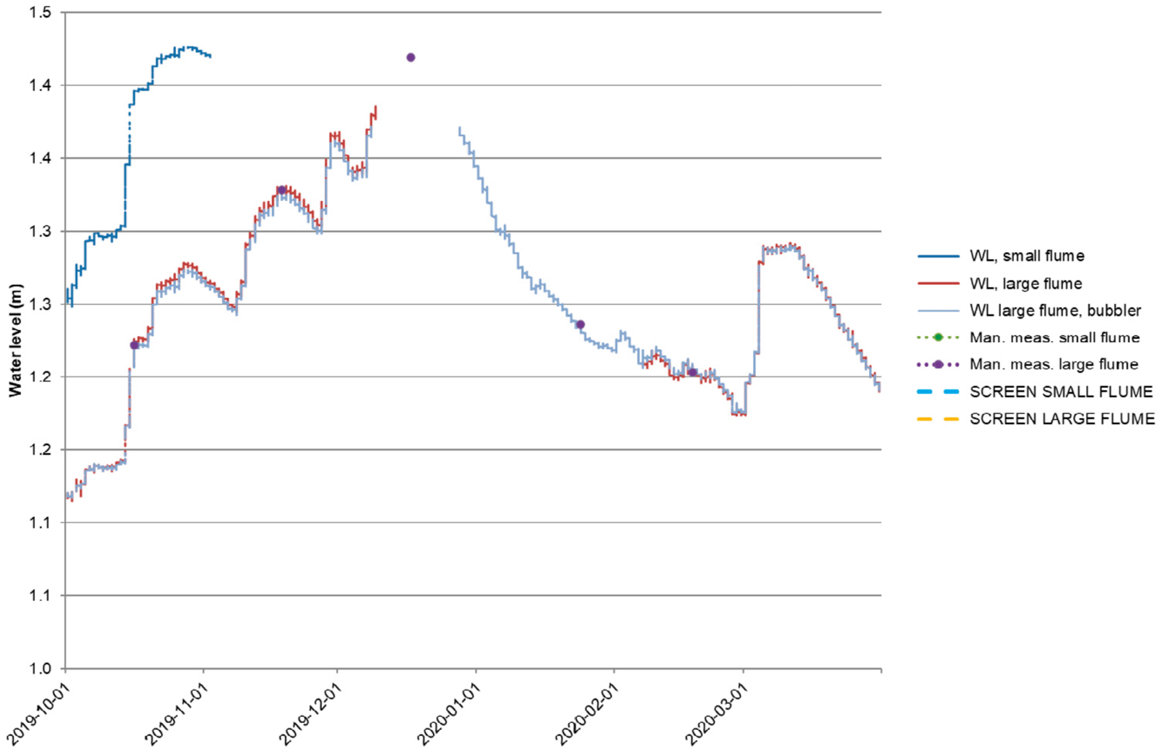

Figure A2-1. *Water-level time series for the flumes at gauging station PFM005764 for the period Oct. 1, 2019–Mar. 31, 2020.*

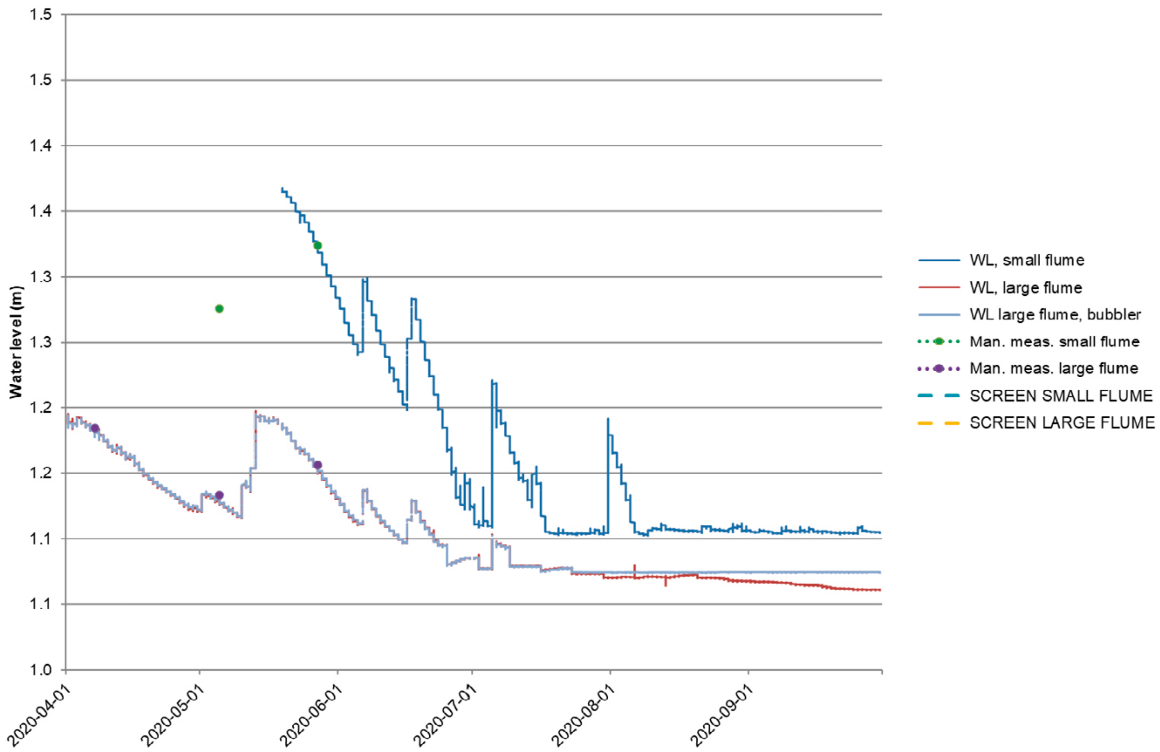

Figure A2-2. *Water-level time series for the flumes at gauging station PFM005764 for the period Apr. 1–Sep. 30, 2020.*

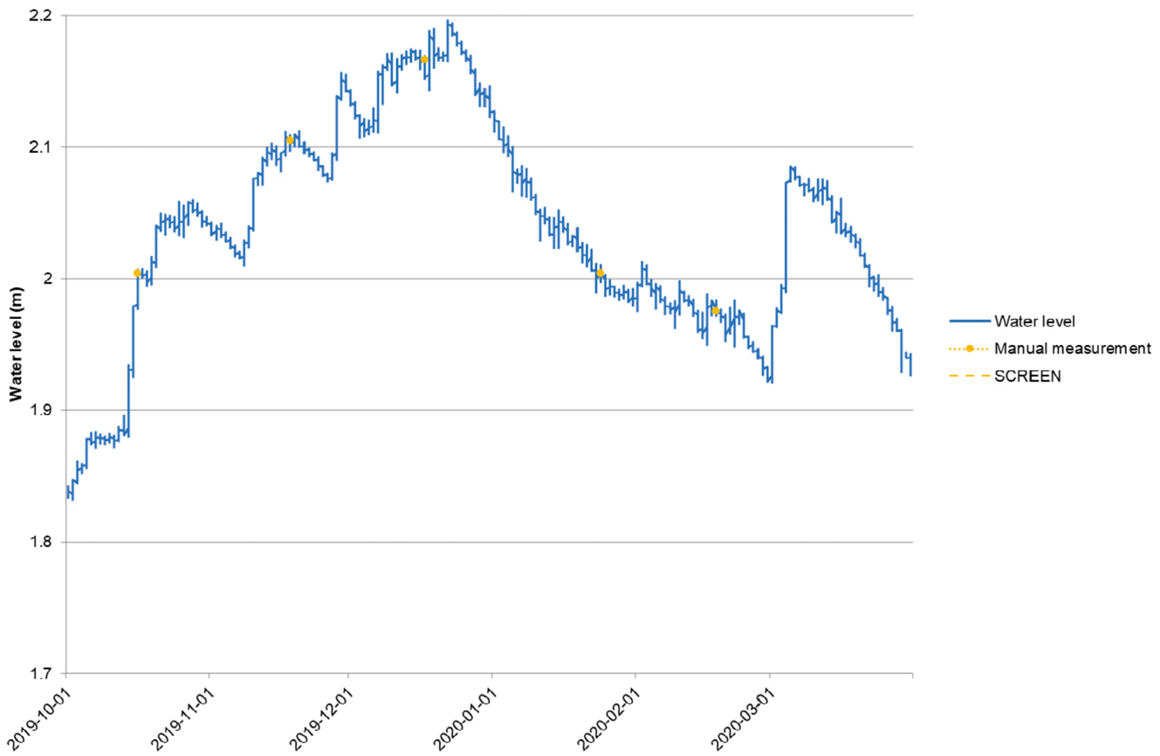

Figure A2-3. *Water-level time series for the flume at gauging station PFM002667 for the period Oct. 1, 2019–Mar. 31, 2020.*

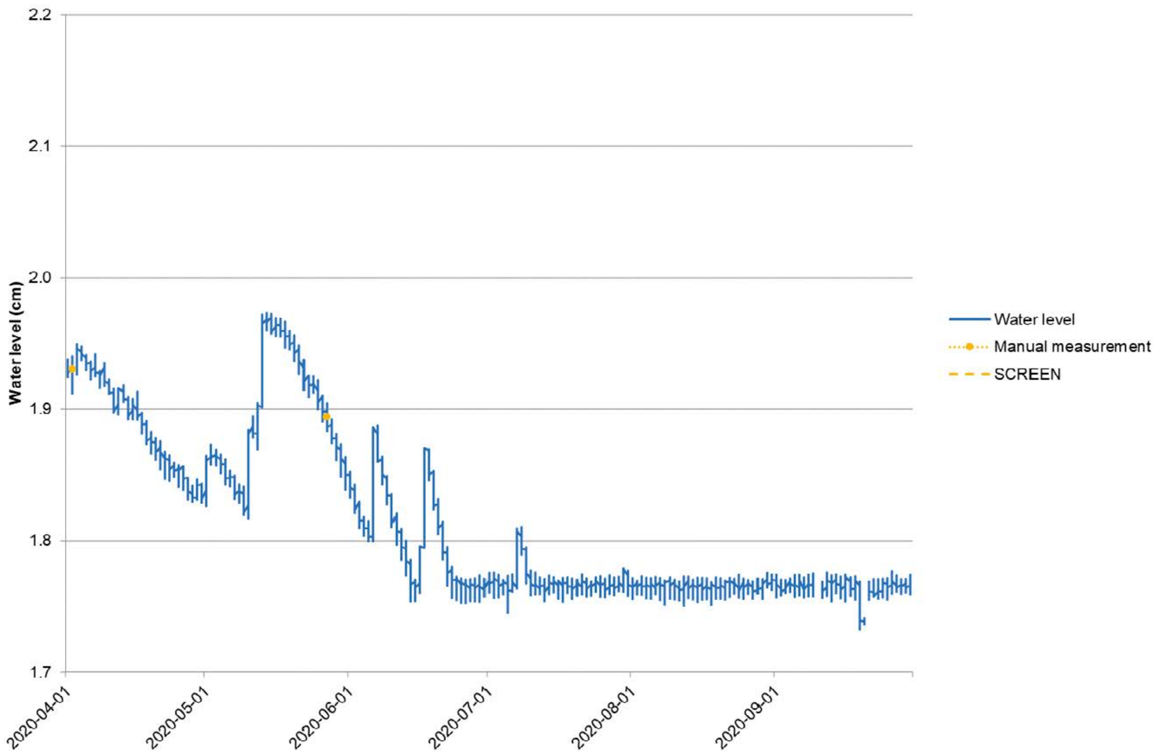

Figure A2-4. *Water-level time series for the flume at gauging station PFM002667 for the period Apr. 1–Sep. 30, 2020.*

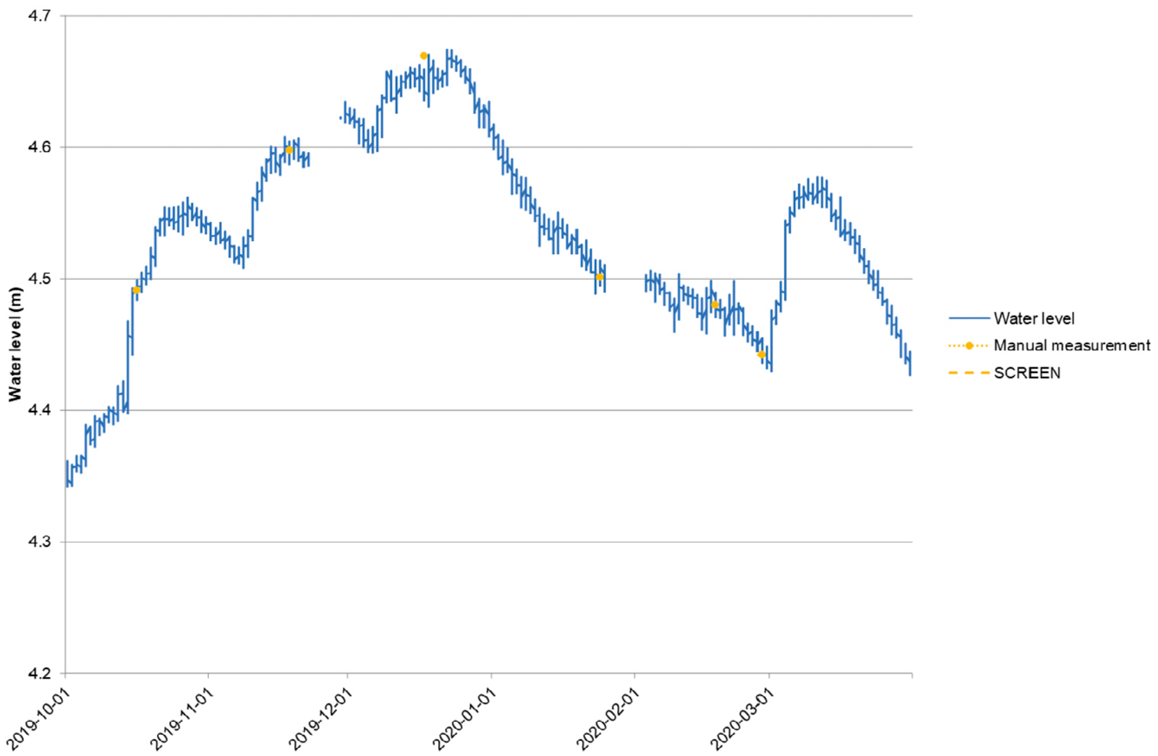

Figure A2-5. *Water-level time series for the flume at gauging station PFM002668 for the period Oct. 1, 2019–Mar. 31, 2020.*

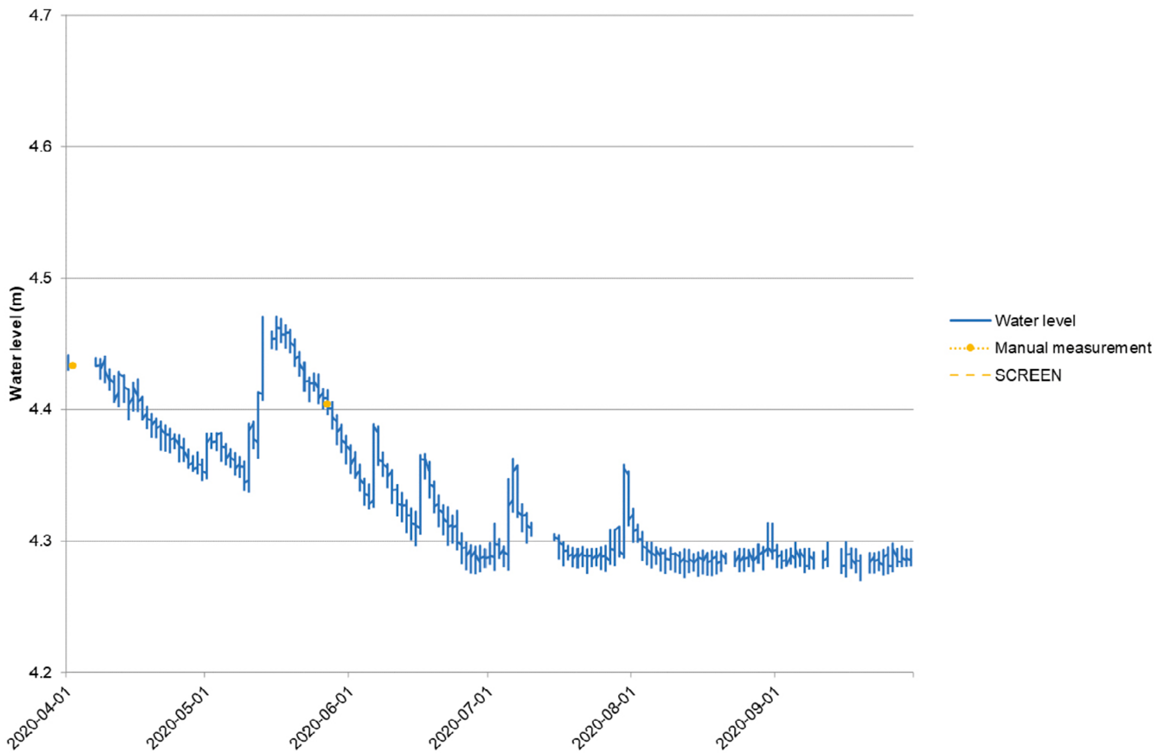

Figure A2-6. *Water-level time series for the flume at gauging station PFM002668 for the period Apr. 1–Sep. 30, 2020.*

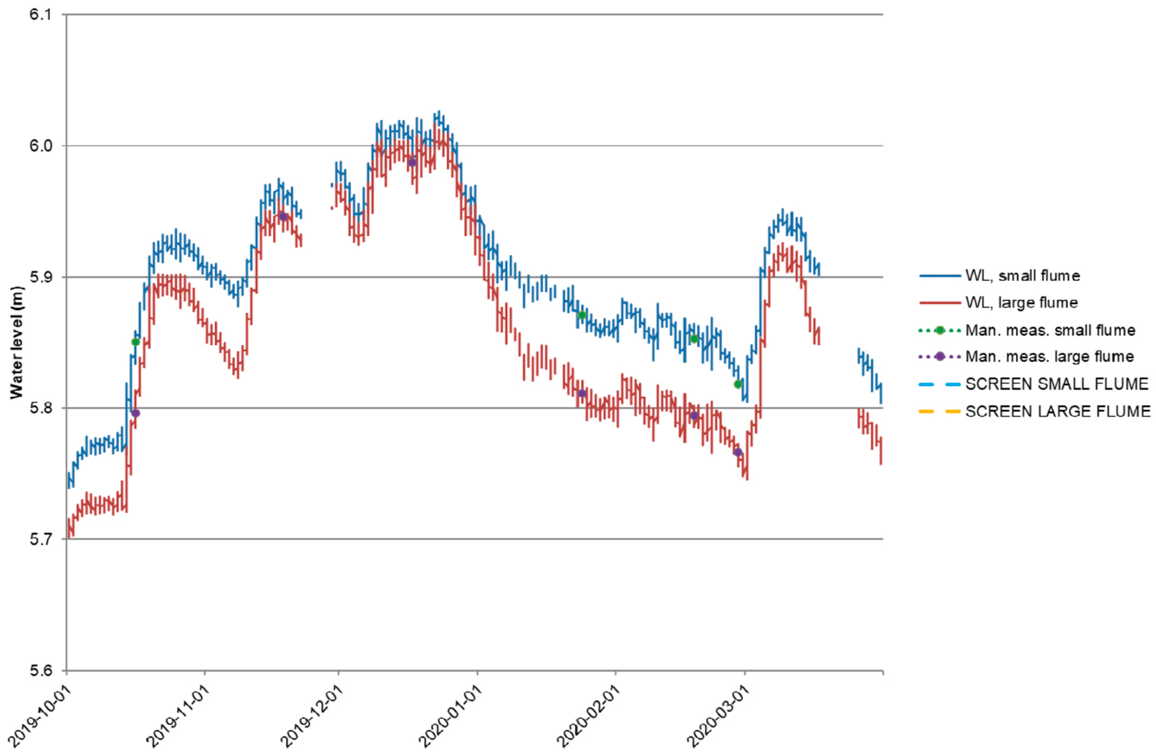

Figure A2-7. *Water-level time series for the flumes at gauging station PFM002669 for the period Sep. 1, 2019–Mar. 31, 2020.*

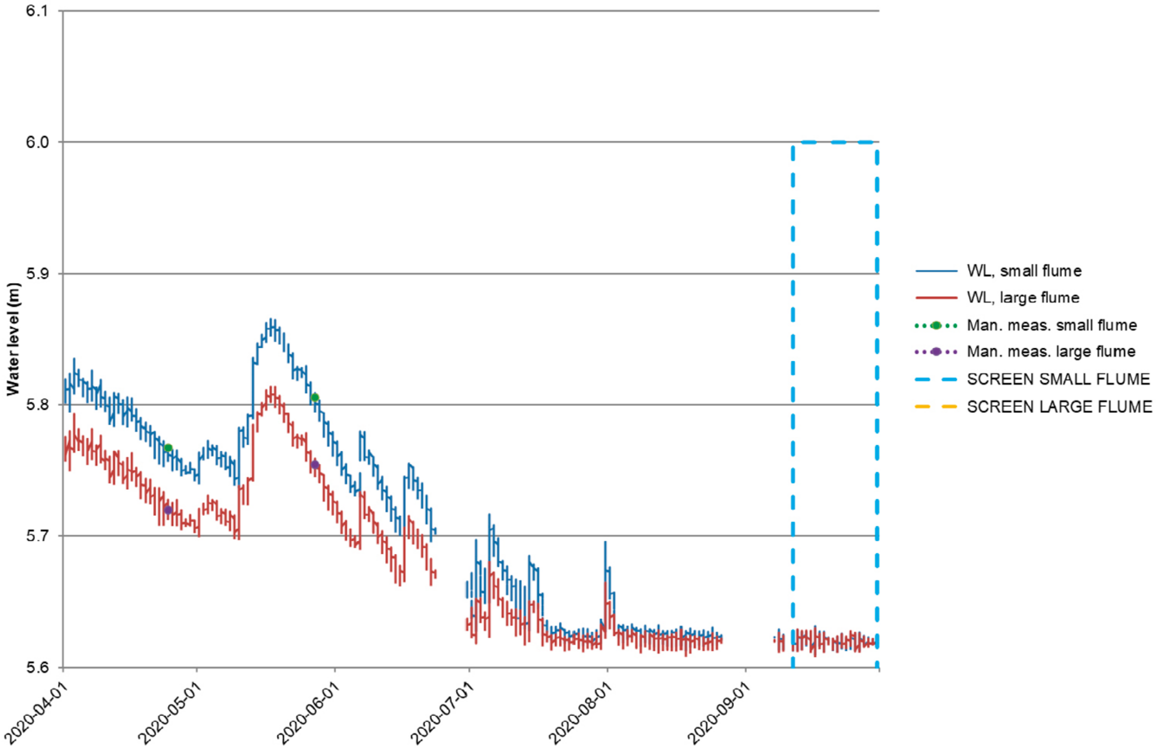

Figure A2-8. *Water-level time series for the flumes at gauging station PFM002669 for the period Apr. 1–Sep. 30, 2020.*

Calculated discharge

Figures A3-1 to A3-4 show time-series plots of calculated hourly average stream discharges at gauging stations PFM005764, -2667, -2668 and -2669 for the hydrological year October 1, 2019–September 30, 2020. Hourly averages are calculated without the data periods excluded as a result of the regular quality control and the quality control of the 2019/2020 water-level dataset (Appendix 2).

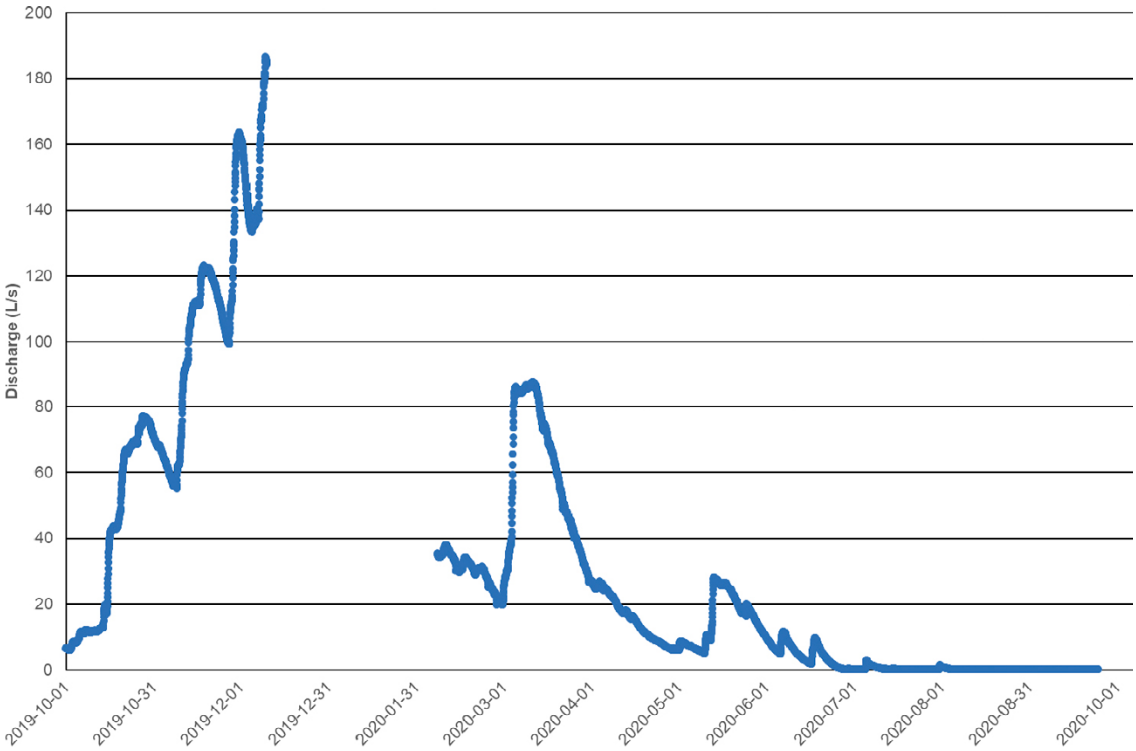

Figure A3-1. *Hourly average stream discharge at gauging station PFM005764 for the period Oct. 1, 2019–Sep. 30, 2020.*

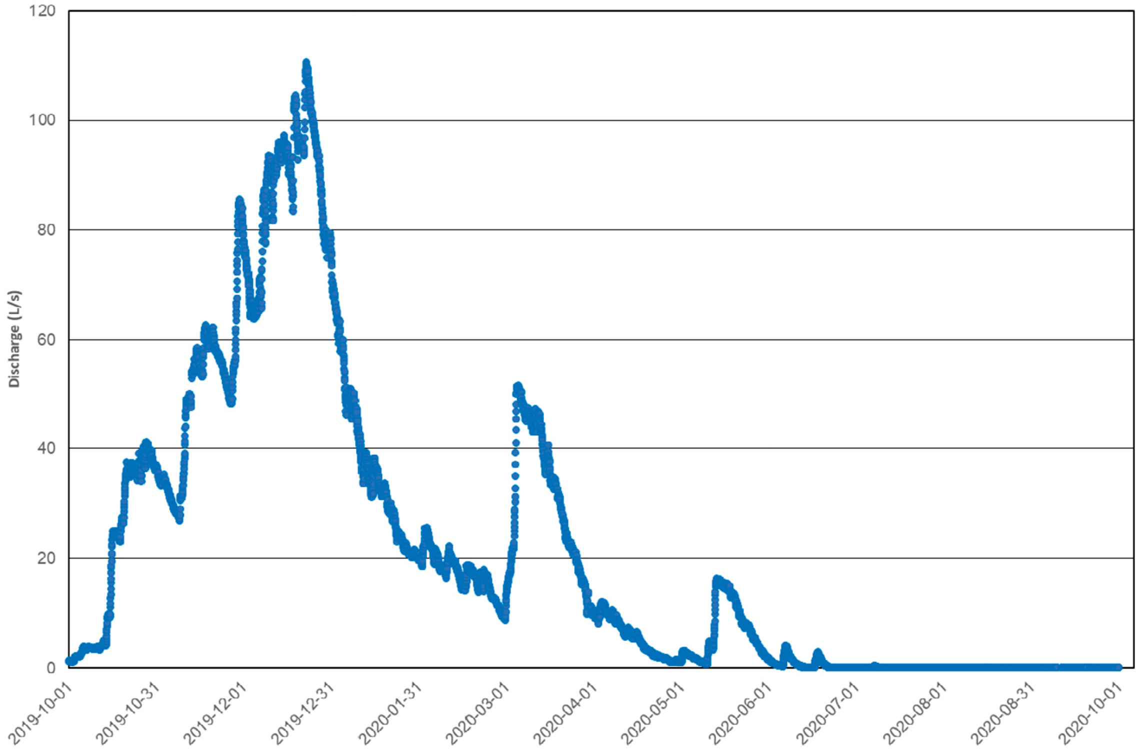

Figure A3-2. *Hourly average stream discharge at gauging station PFM002667 for the period Oct. 1, 2019–Sep. 30, 2020.*

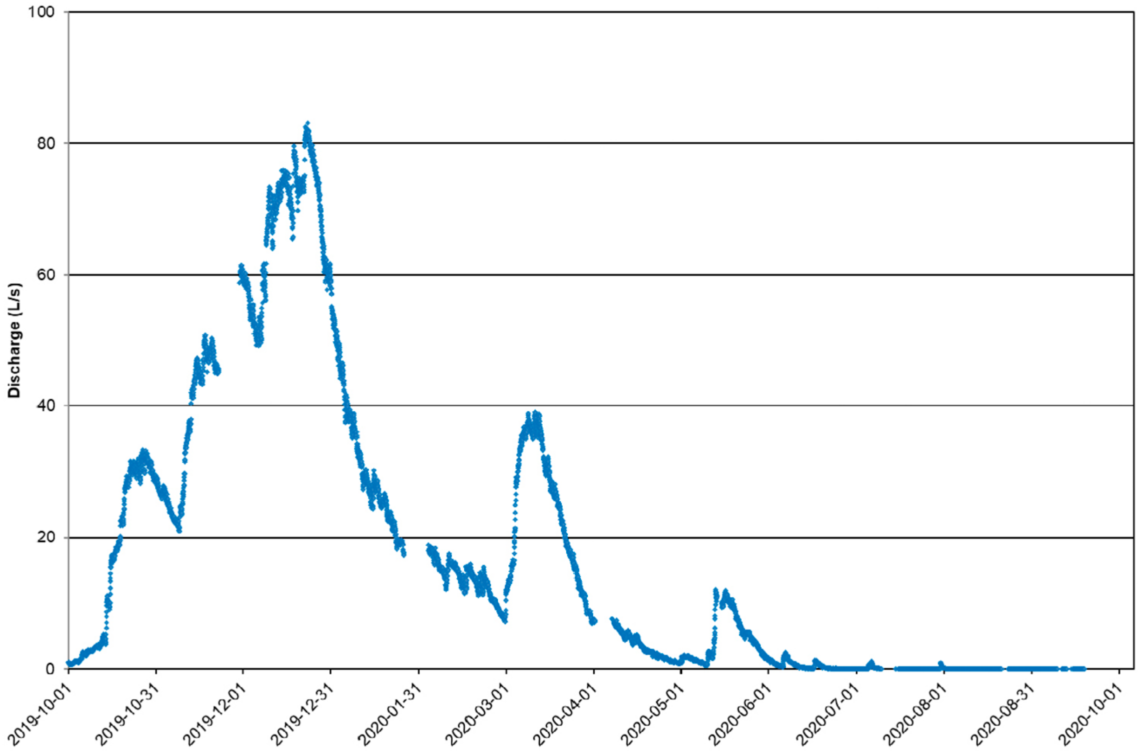

Figure A3-3. *Hourly average stream discharge at gauging station PFM002668 for the period Oct. 1, 2019–Sep. 30, 2020.*

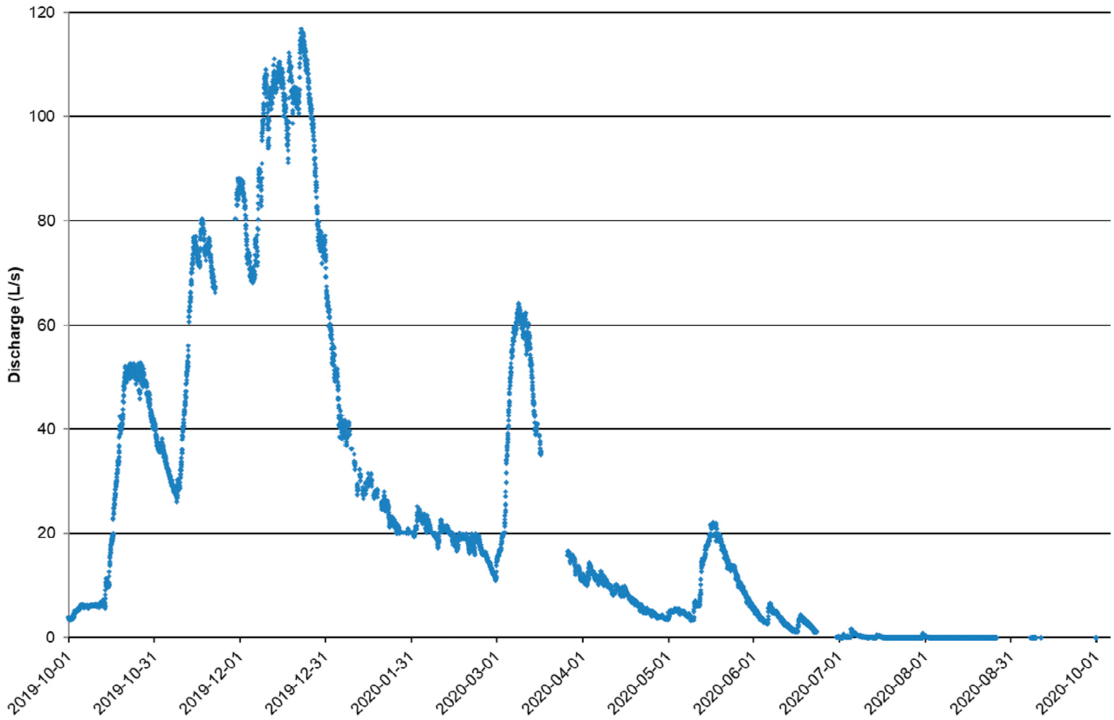

***Figure A3-4.** Hourly average stream discharge at gauging station PFM002669 for the period Oct. 1, 2019–Sep. 30, 2020.*

Appendix 4

Electrical conductivity

Figures A4-1 to A4-8 show EC time-series plots for gauging stations PFM005764, -2667, -2668 and -2669 for the period October 1, 2019–September 30, 2020. The plots also show manually measured EC values and data periods excluded (SCREEN) from the data transfer to the Sicada database as a result of the quality control of the 2019/2020 EC dataset.

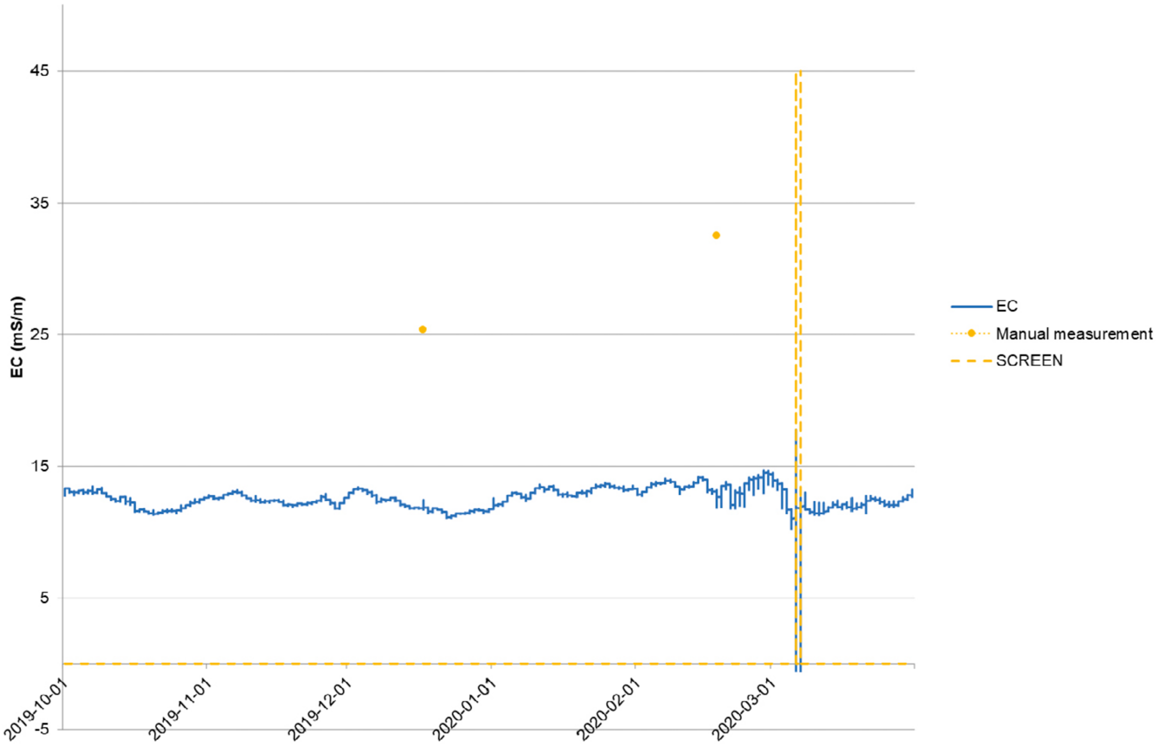

Figure A4-1. *EC time series for gauging station PFM005764 for the period Oct. 1, 2019–Mar. 31, 2020.*

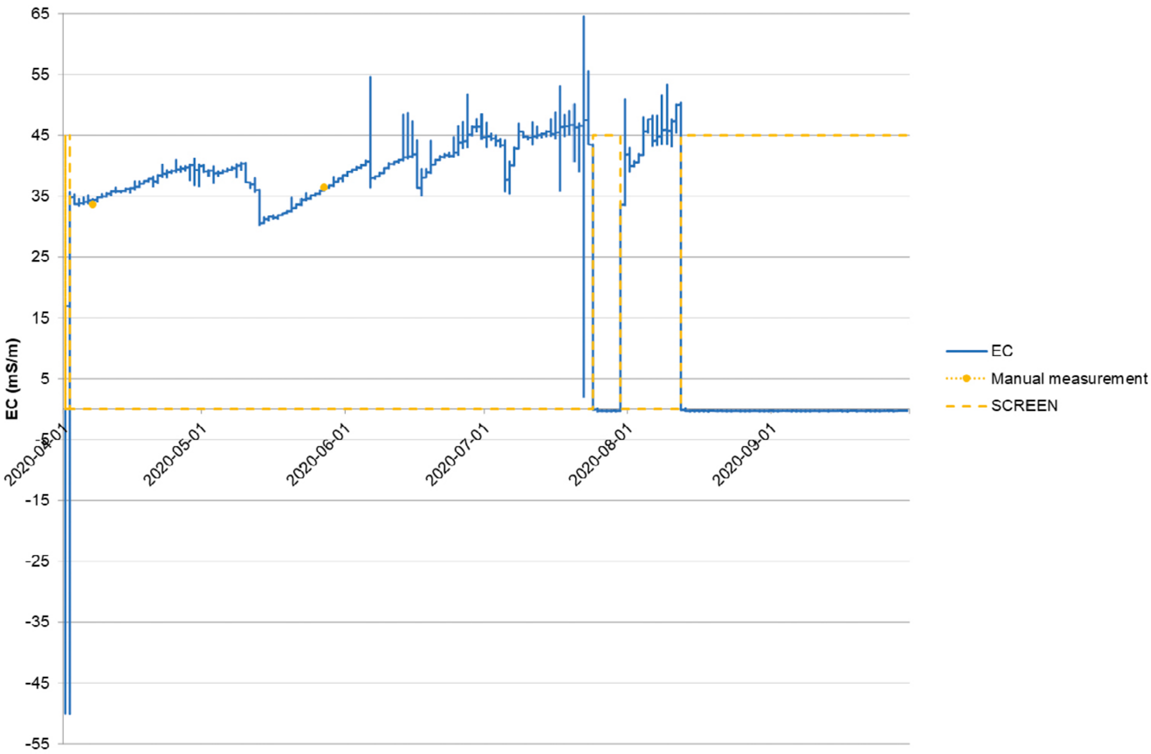

Figure A4-2. *EC time series for gauging station PFM005764 for the period Apr. 1–Sep. 30, 2020.*

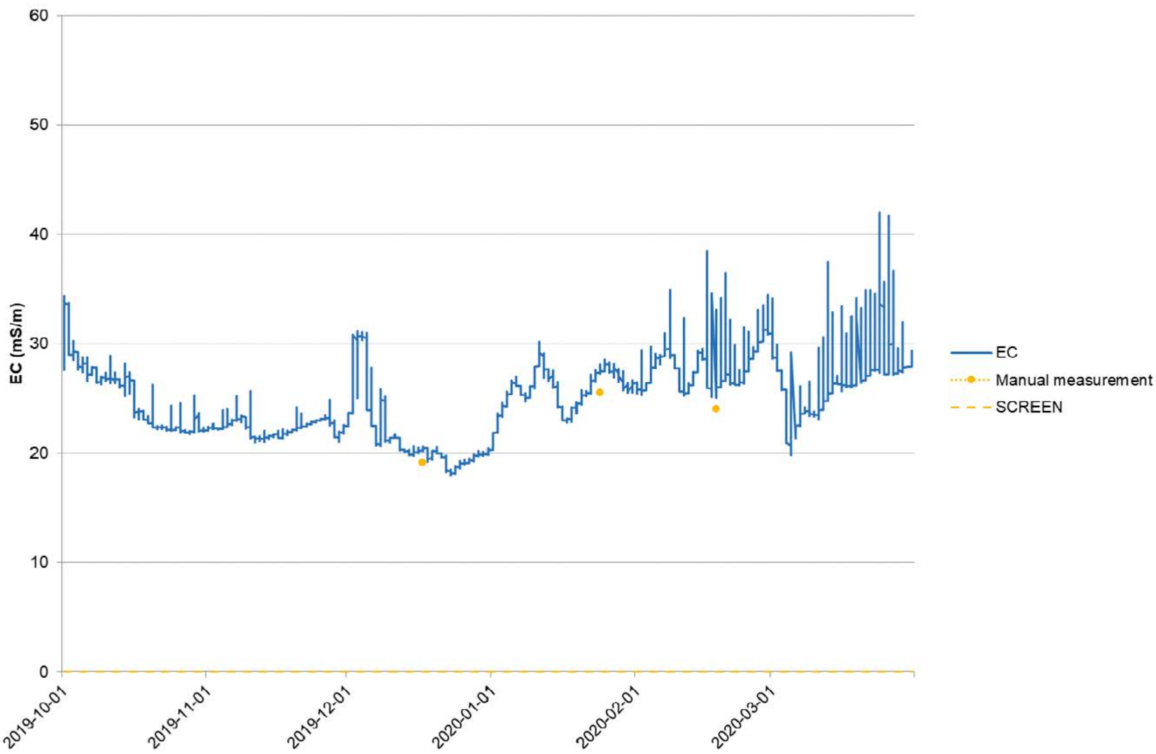

Figure A4-3. *EC time series for gauging station PFM002667 for the period Oct. 1, 2019–Mar. 31, 2020.*

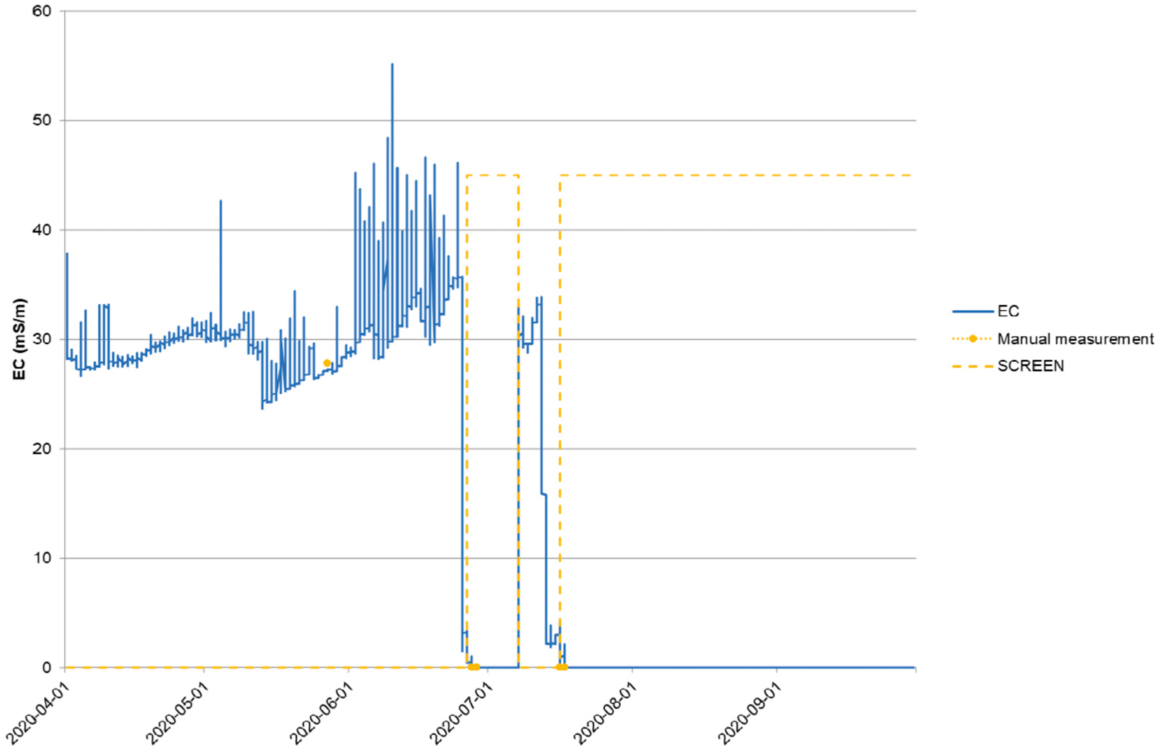

Figure A4-4. *EC time series for gauging station PFM002667 for the period Apr. 1–Sep. 30, 2020.*

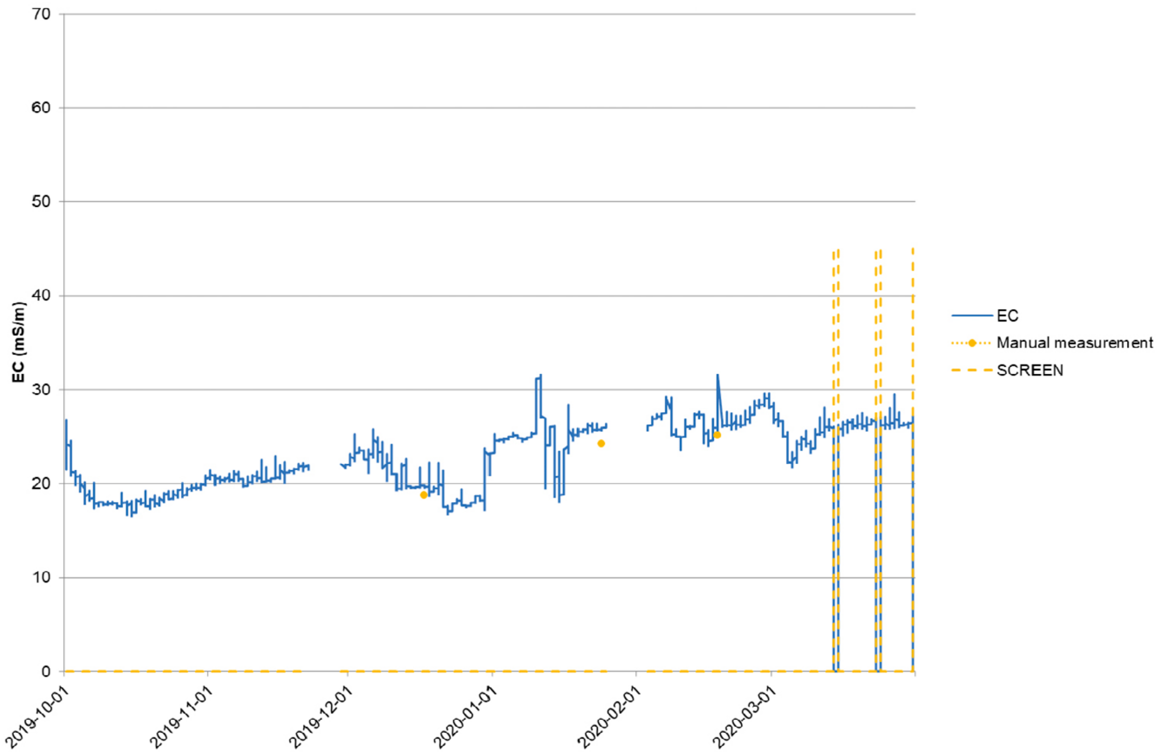

Figure A4-5. *EC time series for gauging station PFM002668 for the period Oct. 1, 2019–Mar. 31, 2020.*

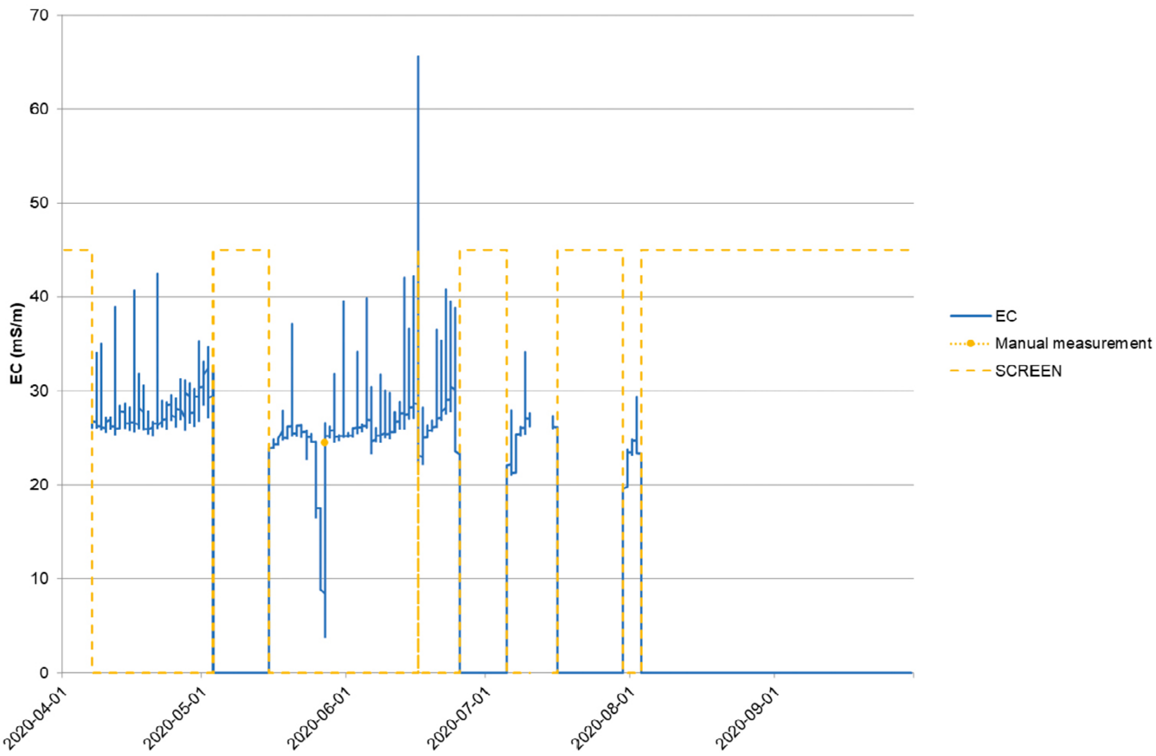

Figure A4-6. *EC time series for gauging station PFM002668 for the period Apr. 1–Sep. 30, 2020.*

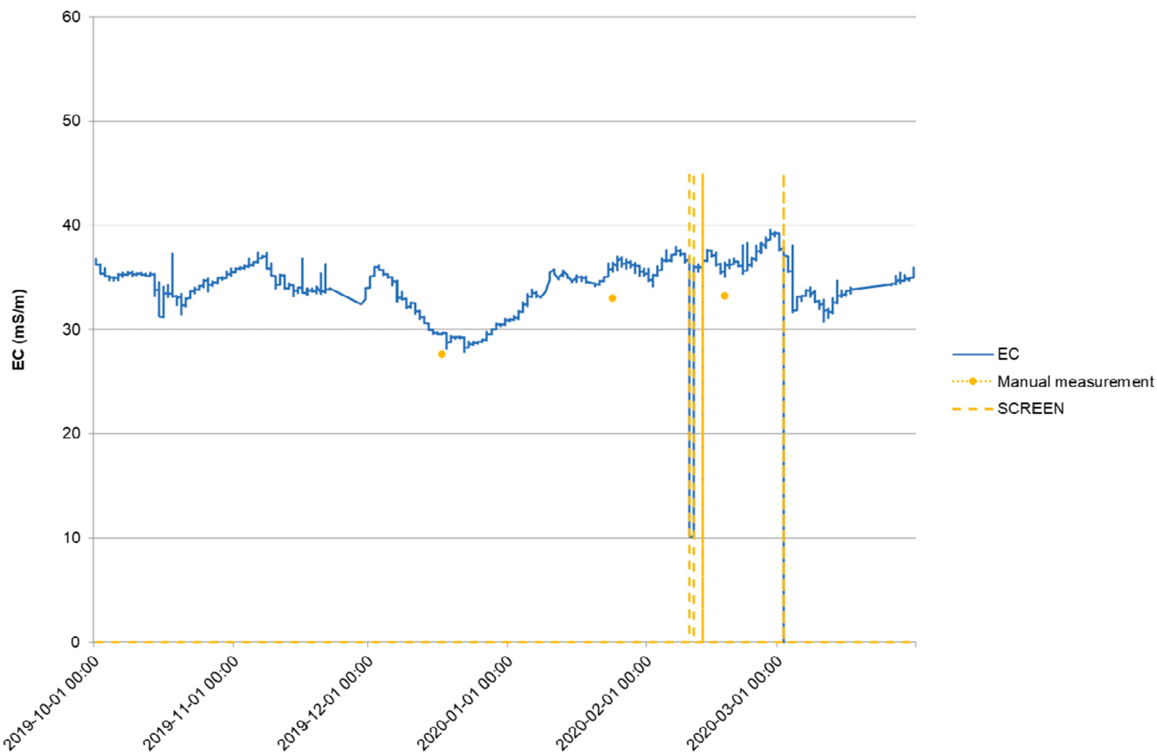

Figure A4-7. *EC time series for gauging station PFM002669 for the period Oct. 1, 2019–Mar. 31, 2020.*

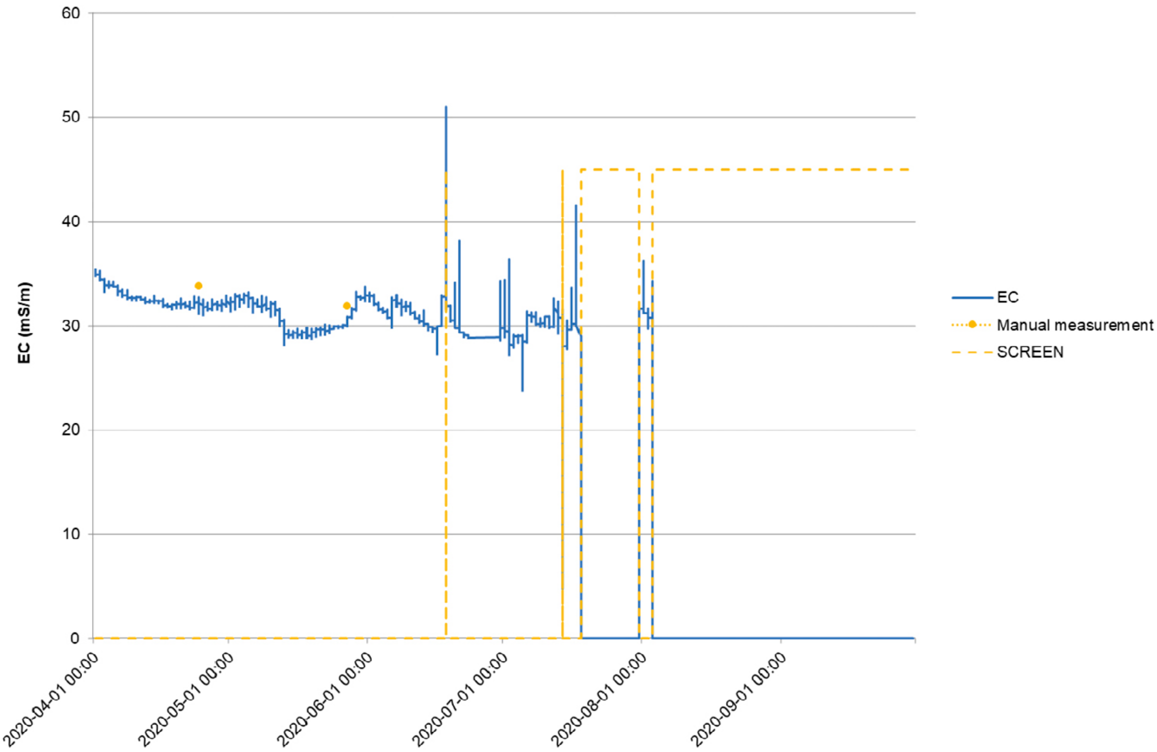

Figure A4-8. *EC time series for gauging station PFM002669 for the period Apr. 1–Sep. 30, 2020.*

Appendix 5

Temperature

Figures A5-1 to A5-8 show temperature time-series plots for gauging stations PFM005764, -2667, -2668 and -2669 for the period October 1, 2019–September 30, 2020. The plots also show manually measured temperature values and data periods excluded (SCREEN) from the data transfer to the Sicada database as a result of the quality control of the 2019/2020 temperature dataset.

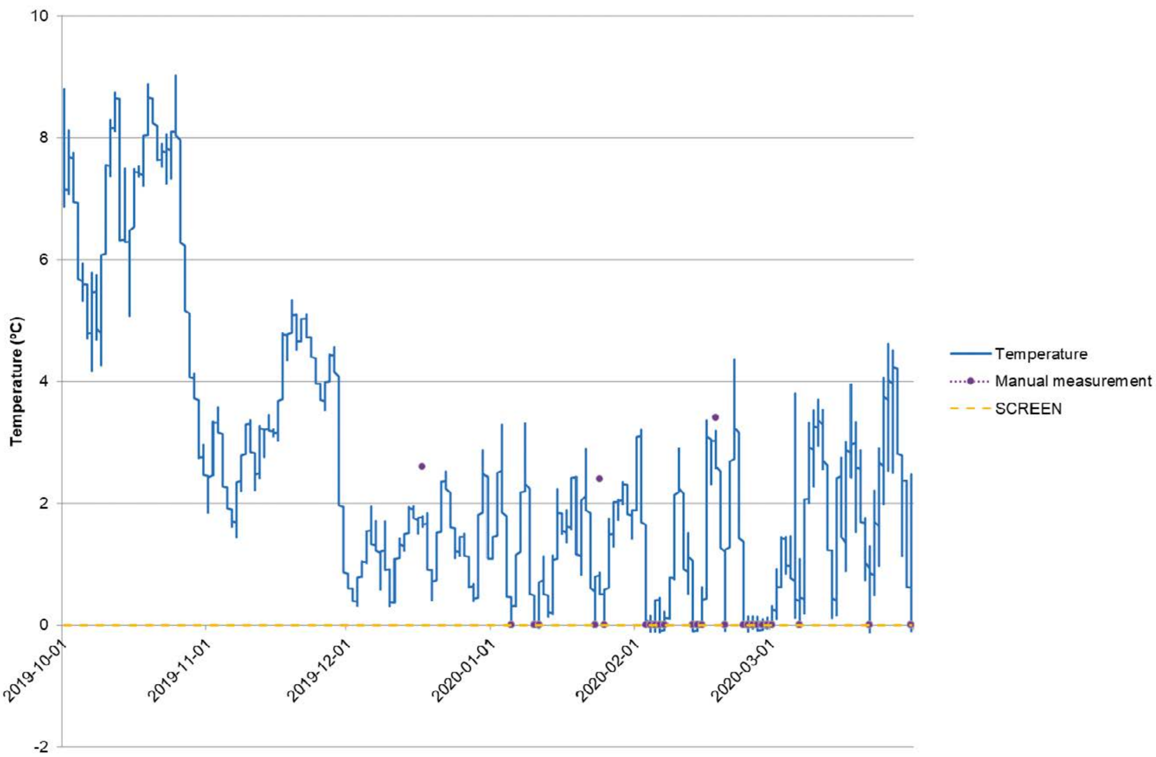

Figure A5-1. *Temperature time series for gauging station PFM005764 for the period Oct. 1, 2019–Mar. 31, 2020.*

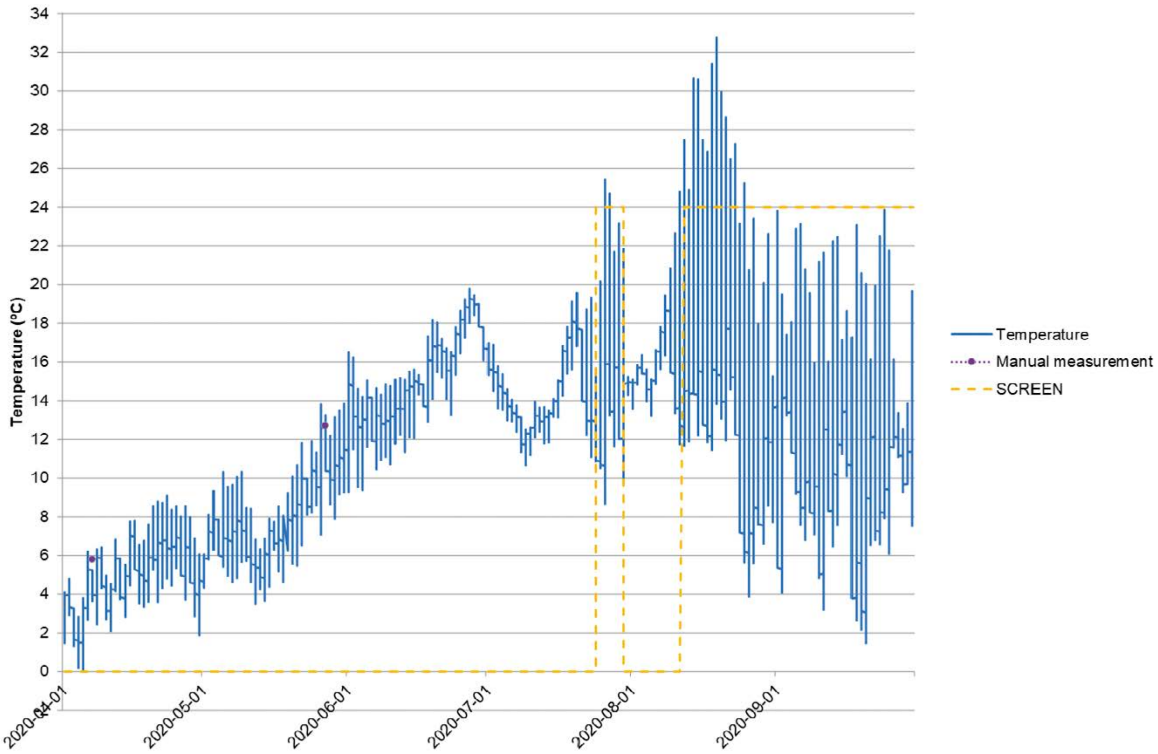

Figure A5-2. *Temperature time series for gauging station PFM005764 for the period Apr. 1–Sep. 30, 2020.*

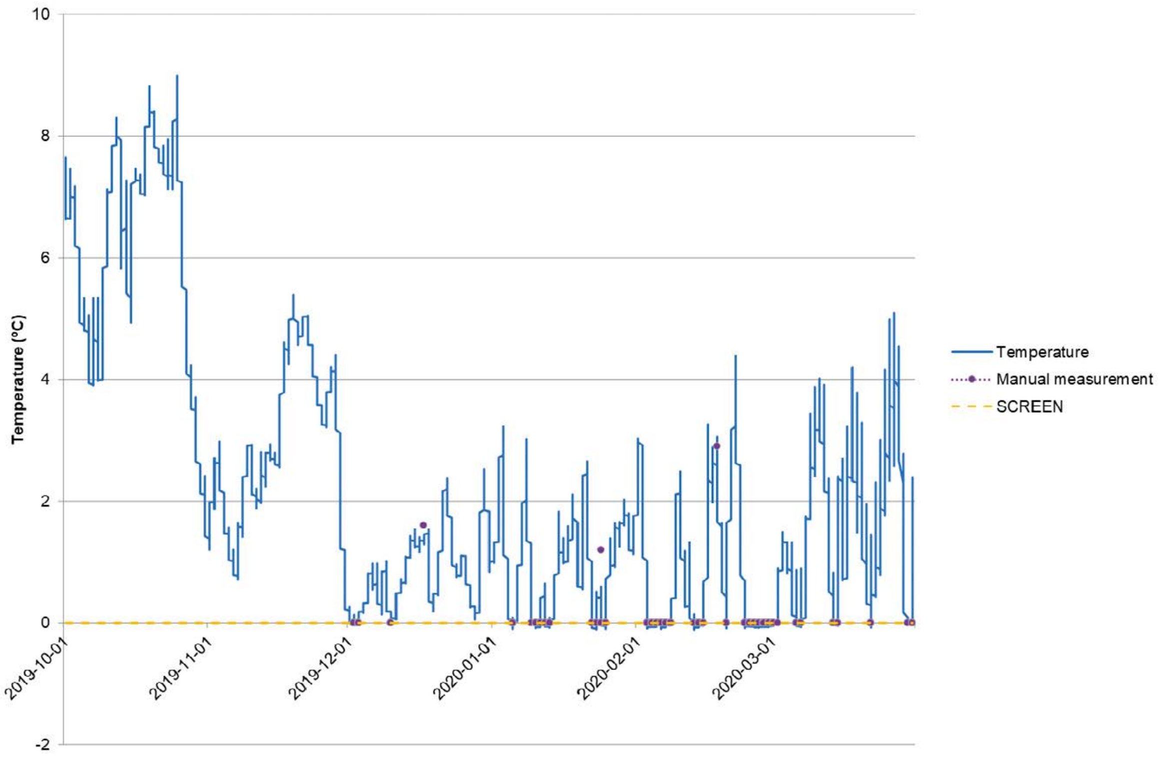

Figure A5-3. *Temperature time series for gauging station PFM002667 for the period Oct. 1, 2019–Mar. 31, 2020.*

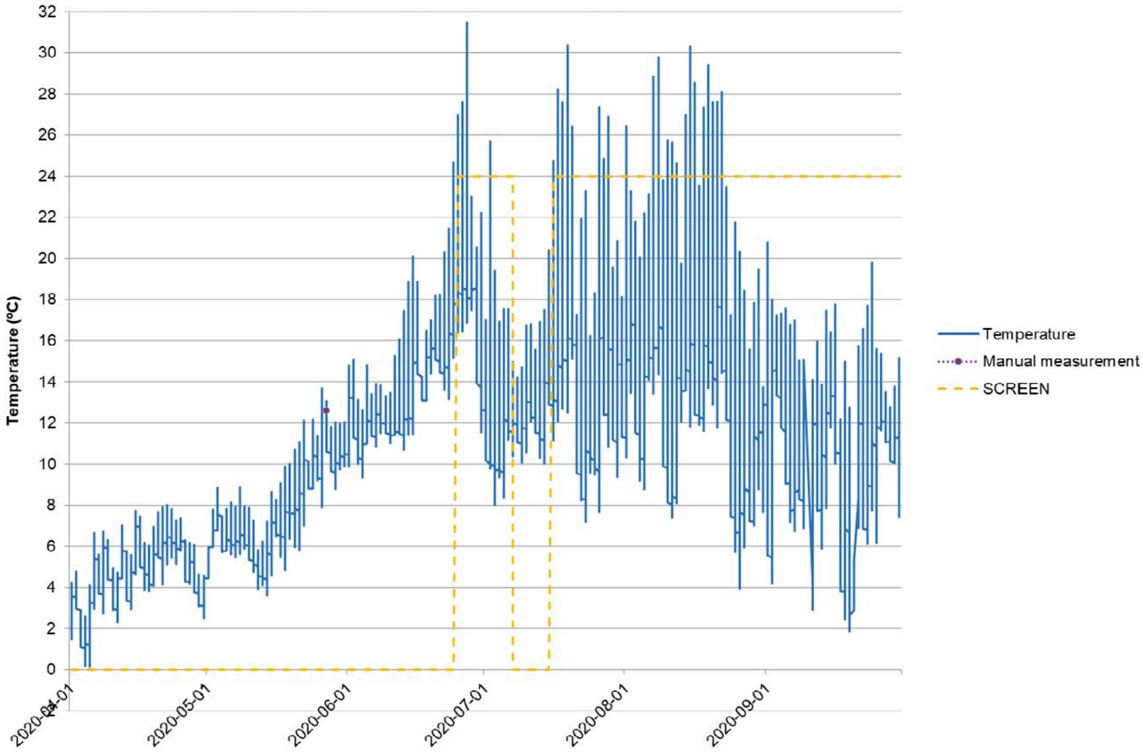

Figure A5-4. *Temperature time series for gauging station PFM002667 for the period Apr. 1–Sep. 30, 2020.*

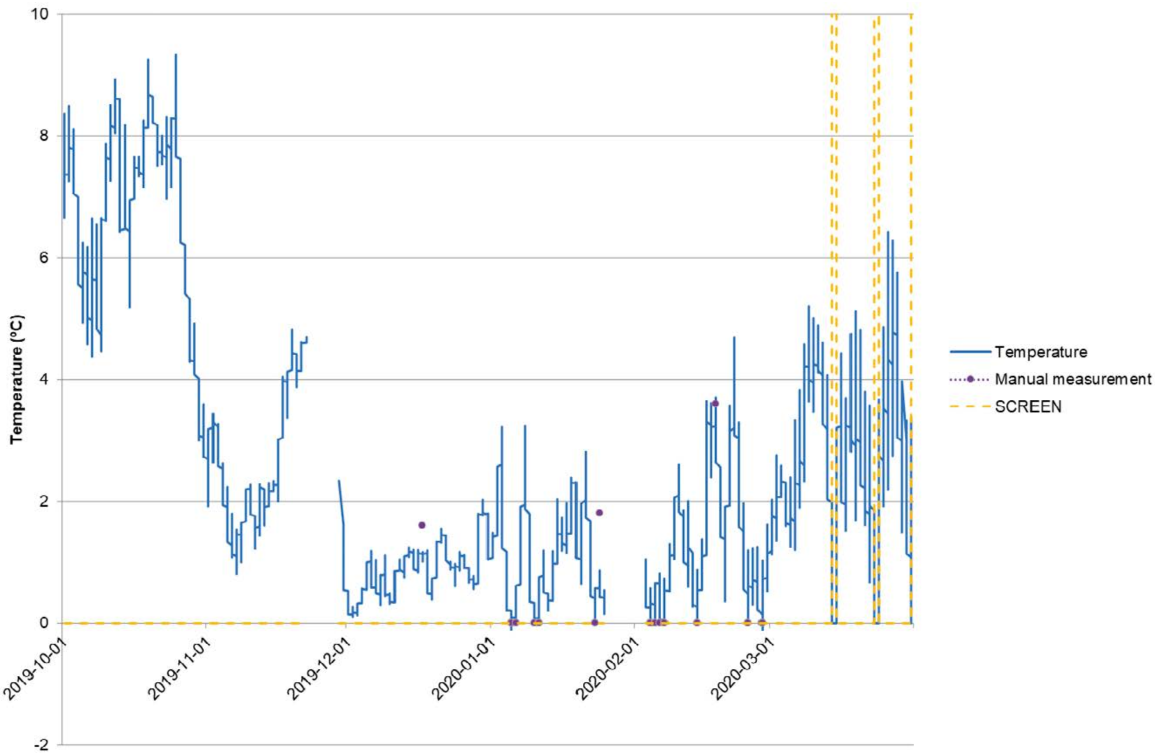

Figure A5-5. *Temperature time series for gauging station PFM002668 for the period Oct. 1, 2019–Mar. 31, 2020.*

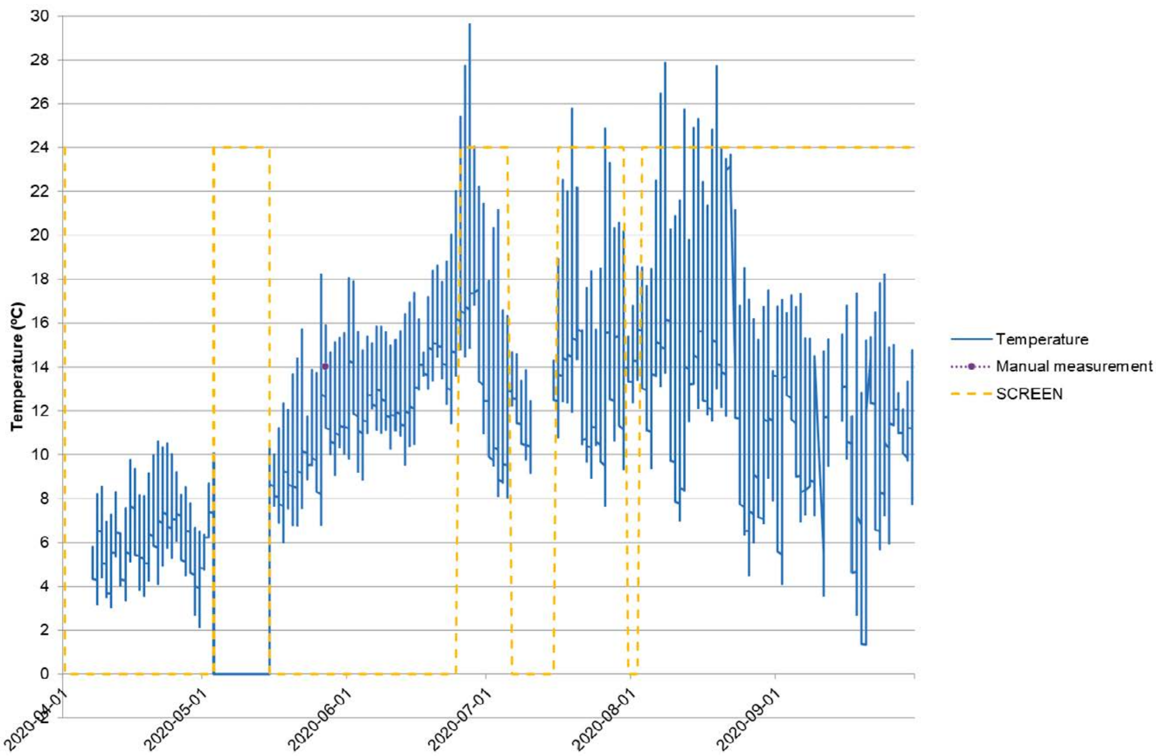

Figure A5-6. *Temperature time series for gauging station PFM002668 for the period Apr. 1–Sep. 30, 2020.*

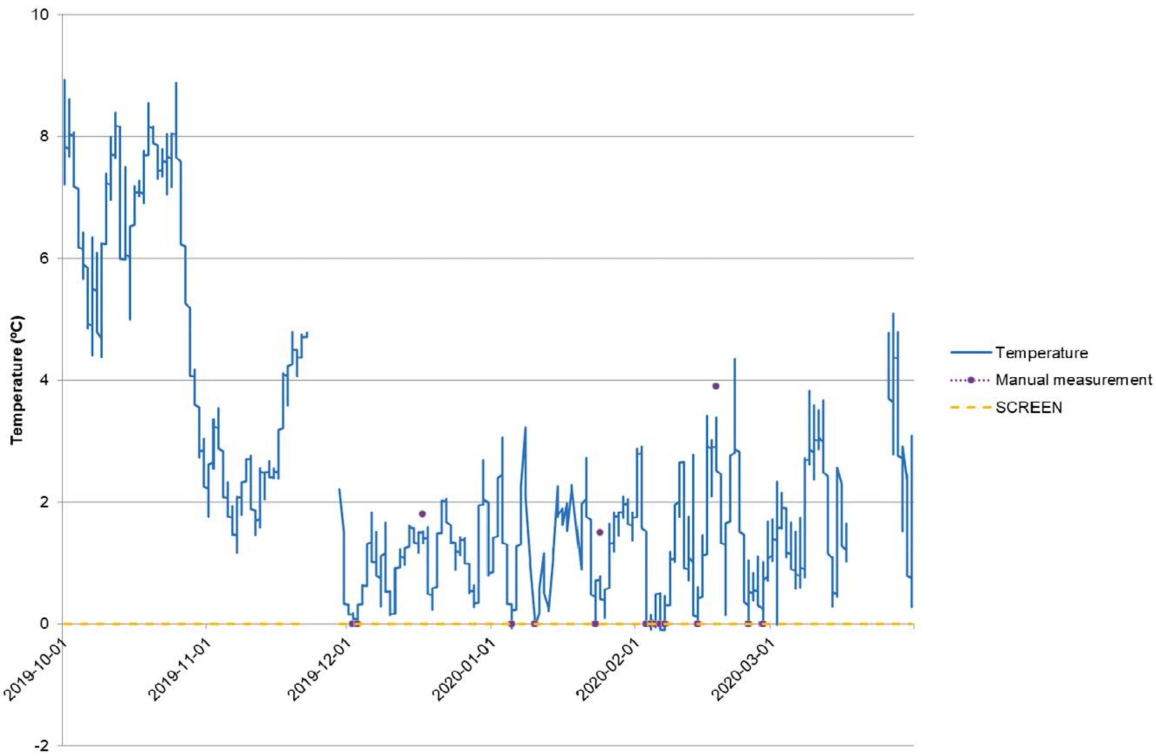

Figure A5-7. *Temperature time series for gauging station PFM002669 for the period Oct. 1, 2019–Mar. 31, 2020.*

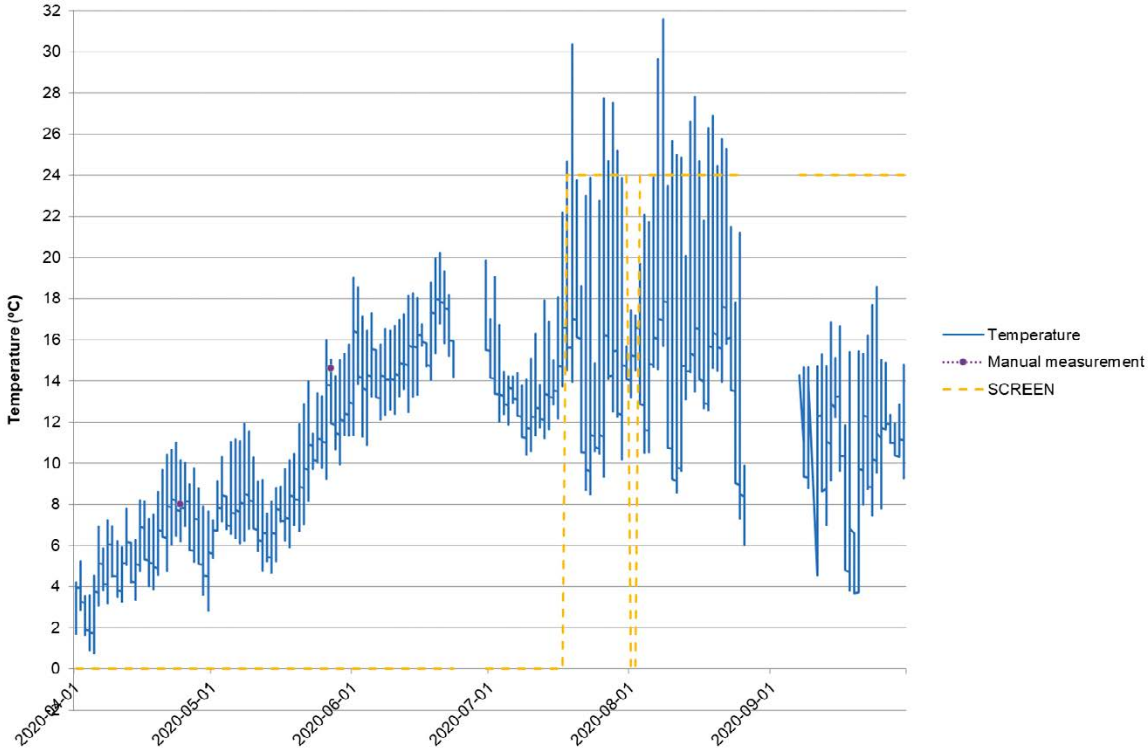

Figure A5-8. *Temperature time series for gauging station PFM002669 for the period Apr. 1–Sep. 30, 2020.*

Appendix 6

Soil temperature and soil moisture

Figures A6-1 to A6-6 show soil-temperature time-series plots and data interpretations for the temperature sensor-stations PFM007822 and PFM007823 (0 °C marked with dashed lines). Figures A6-7 to A6-14 show soil-temperature and soil-moisture time-series plots and data interpretations for the TDR stations PFM007874–7881. 0 °C marked with dashed lines. Data are obtained from the Sicada database.

Figure A6-1. Soil temperature at different depths below ground surface at PFM007822. Upper plot: High-resolution data (measurement interval 3 hours). Lower plot: Daily averages.

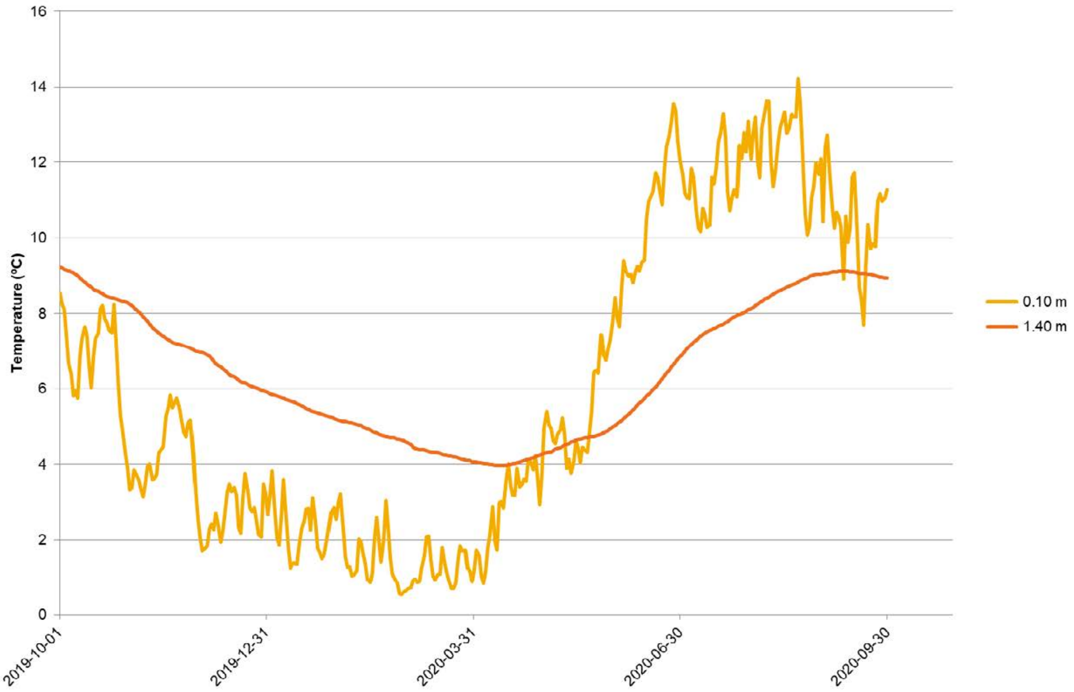

Figure A6-2. *Daily average soil temperatures at the depths 0.10 and 1.40 m below ground surface at PFM007822.*

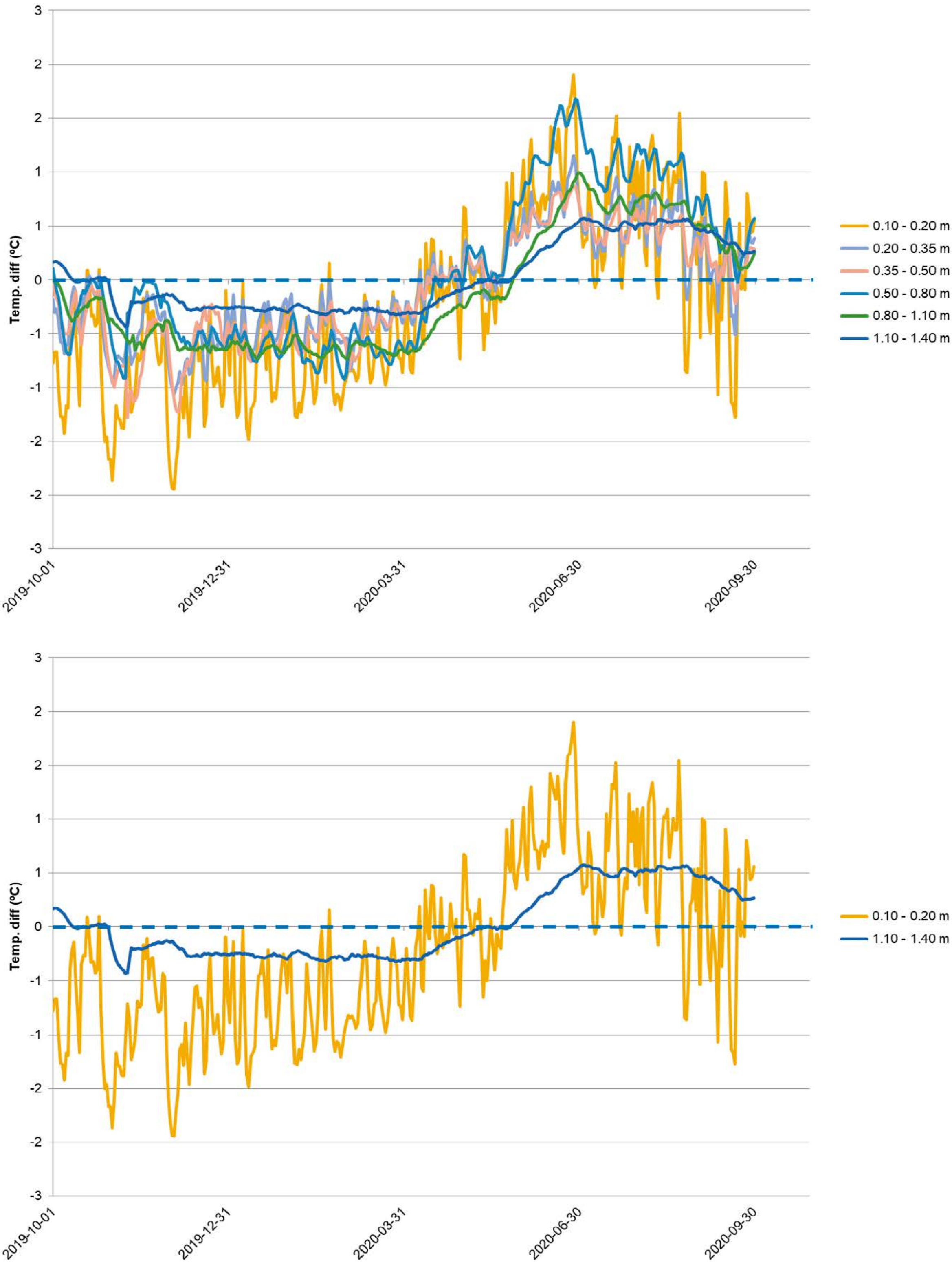

Figure A6-3. *Daily average soil-temperature differences between adjacent measurement depths below ground surface at PFM007822. Upper plot: All depths. Lower plot: Top and bottom measurement depths.*

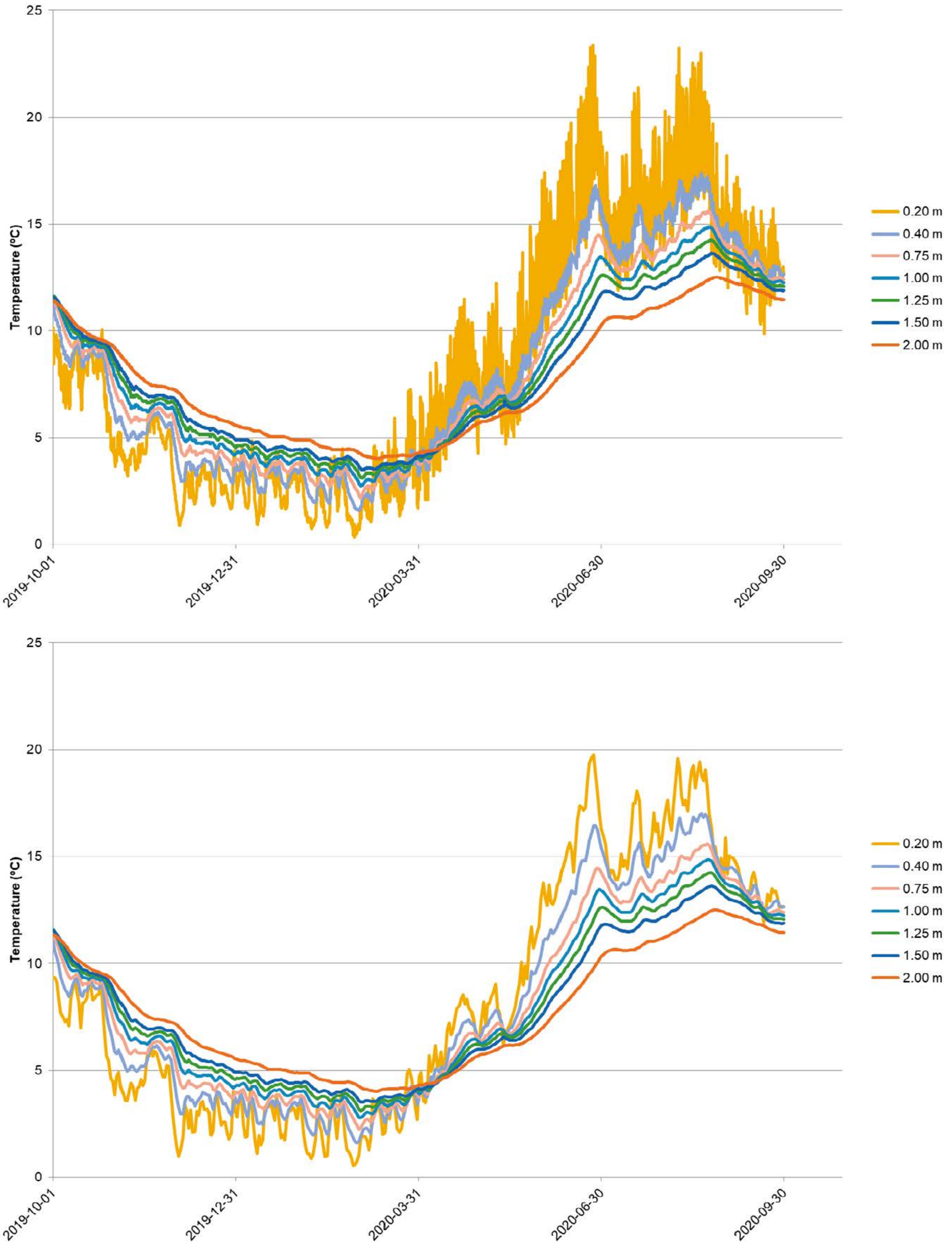

Figure A6-4. *Soil temperature at different depths below ground surface at PFM007823. Upper plot: High-resolution data (measurement interval 3 hours). Lower plot: Daily averages.*

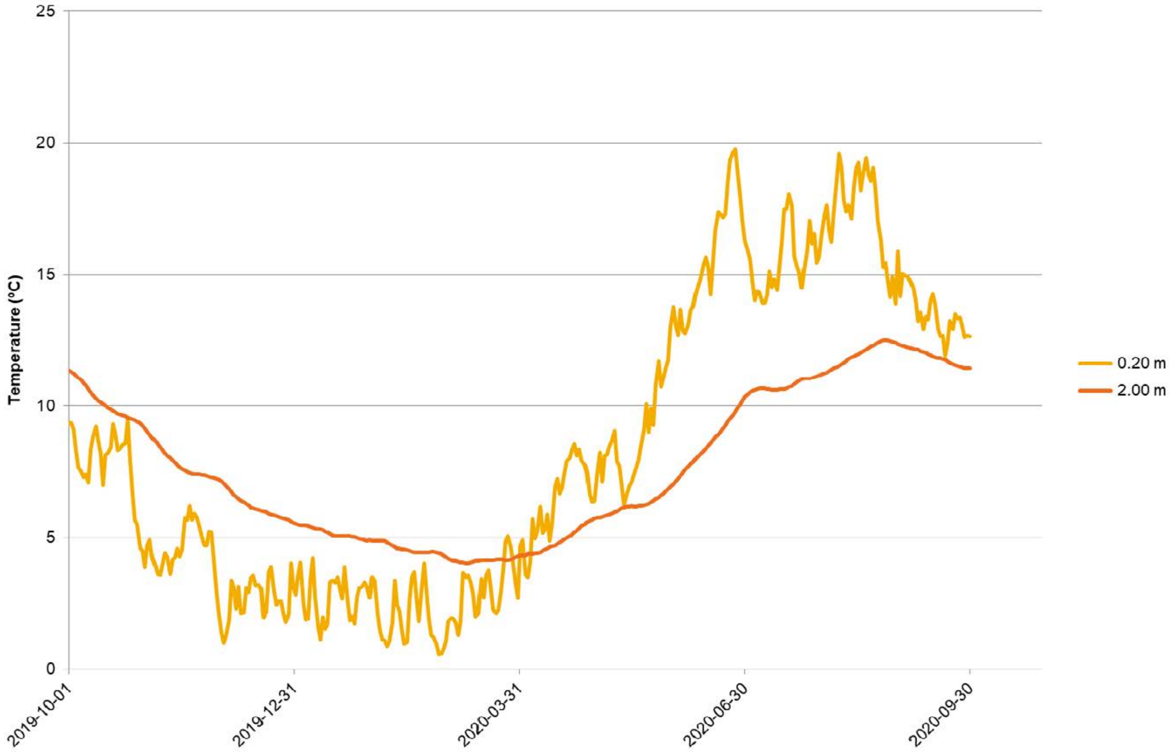

Figure A6-5. *Daily average soil temperatures at the depths 0.20 and 2.00 m below ground surface at PFM007823.*

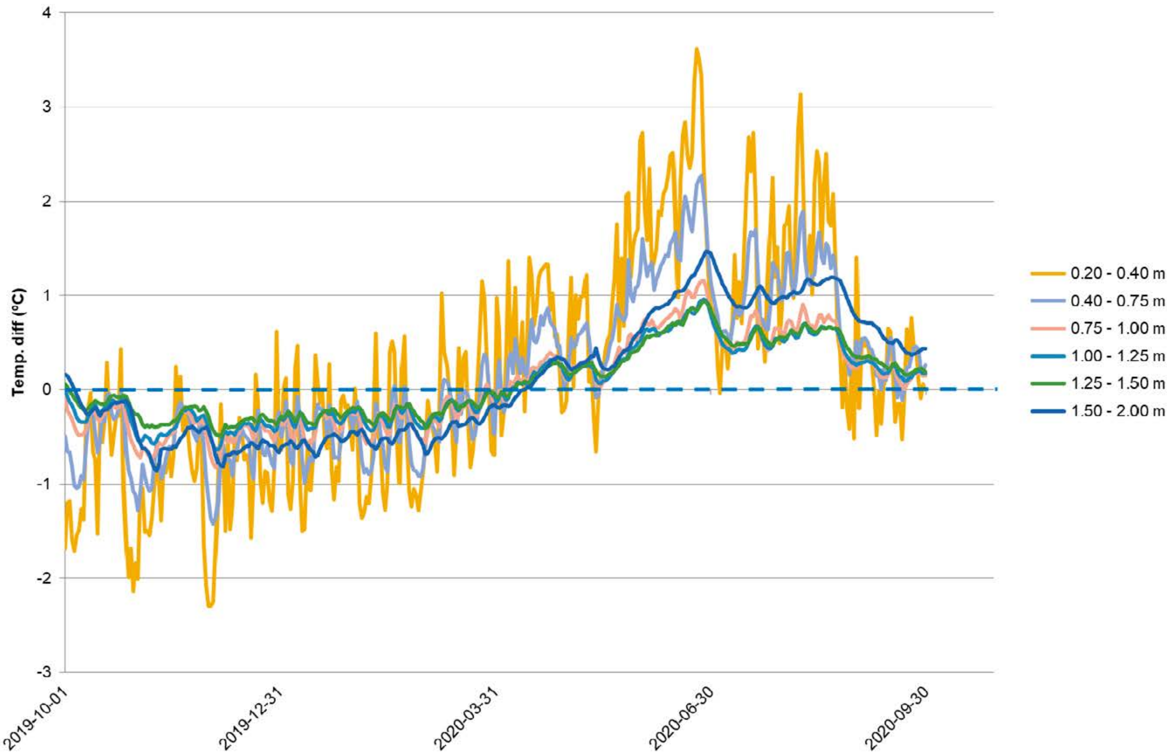

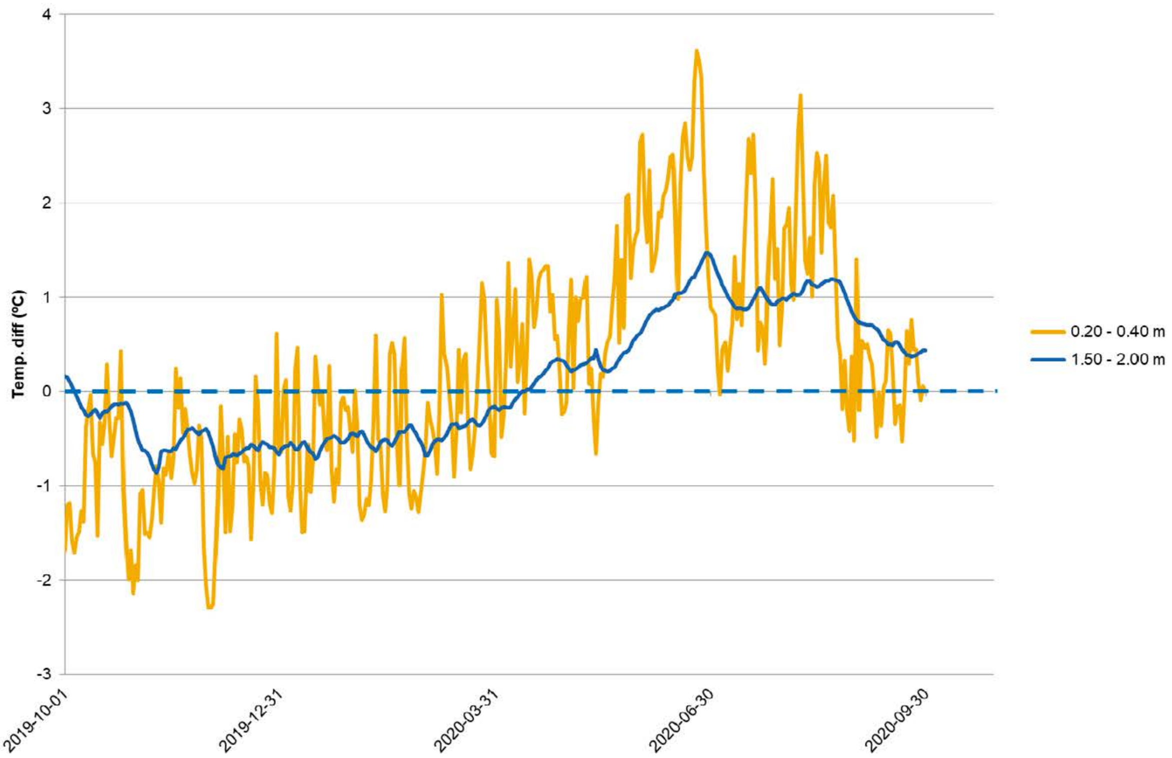

Figure A6-6. *Daily average soil-temperature differences between adjacent measurement depths below ground surface at PFM007823. Upper plot: All depths. Lower plot: Top and bottom measurement depths. 0 °C marked with dashed lines.*

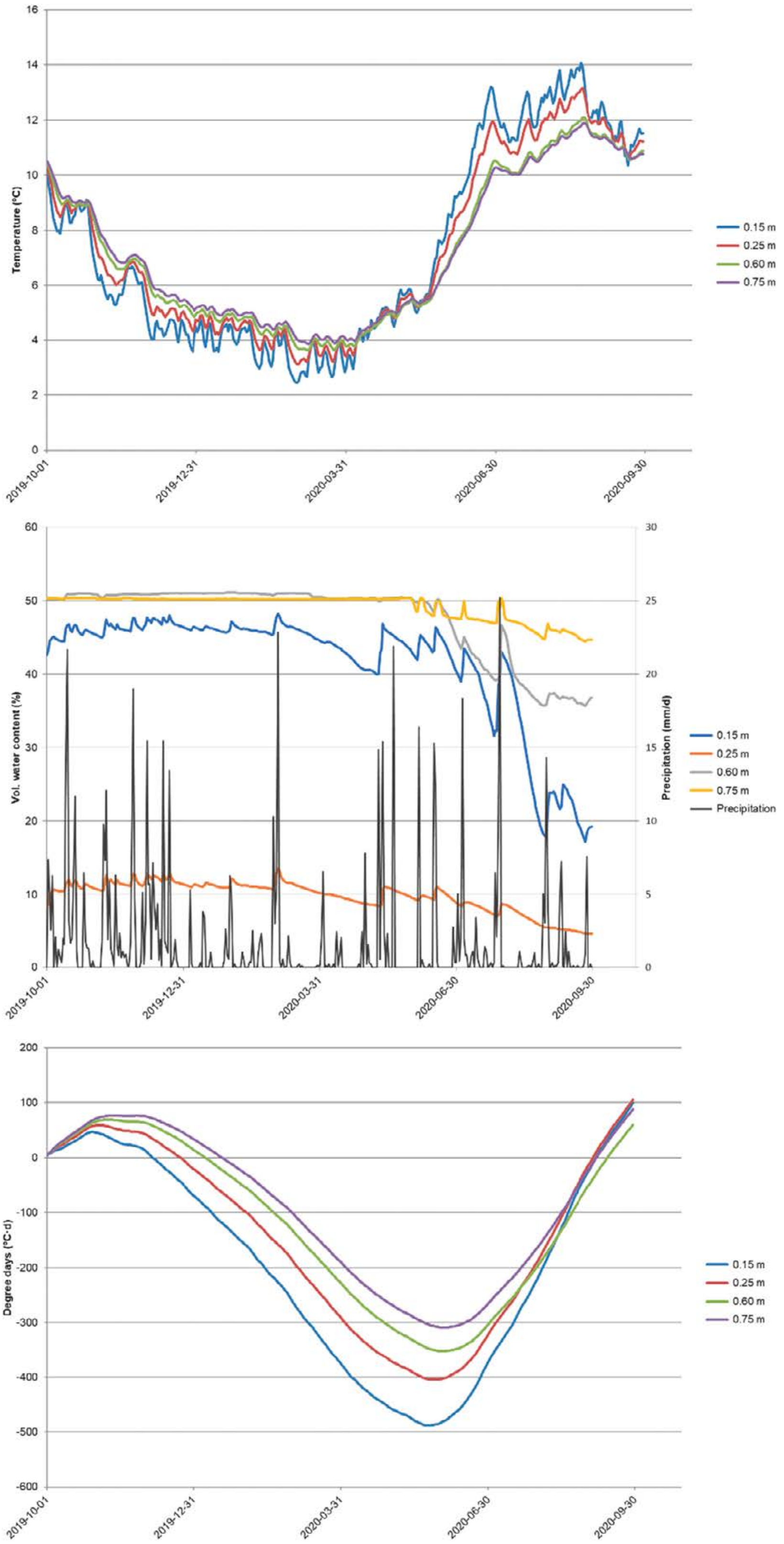

Figure A6-7. *Soil temperature (upper plot) and soil-water content (middle plot) at different depths below ground surface at PFM007874. The middle plot also shows daily sums of corrected precipitation at the Labbomasten station during the 2019/2020 hydrological year. The bottom plot shows cumulative degree days for degrees above 7 °C. The plots show daily averages of high-resolution data.*

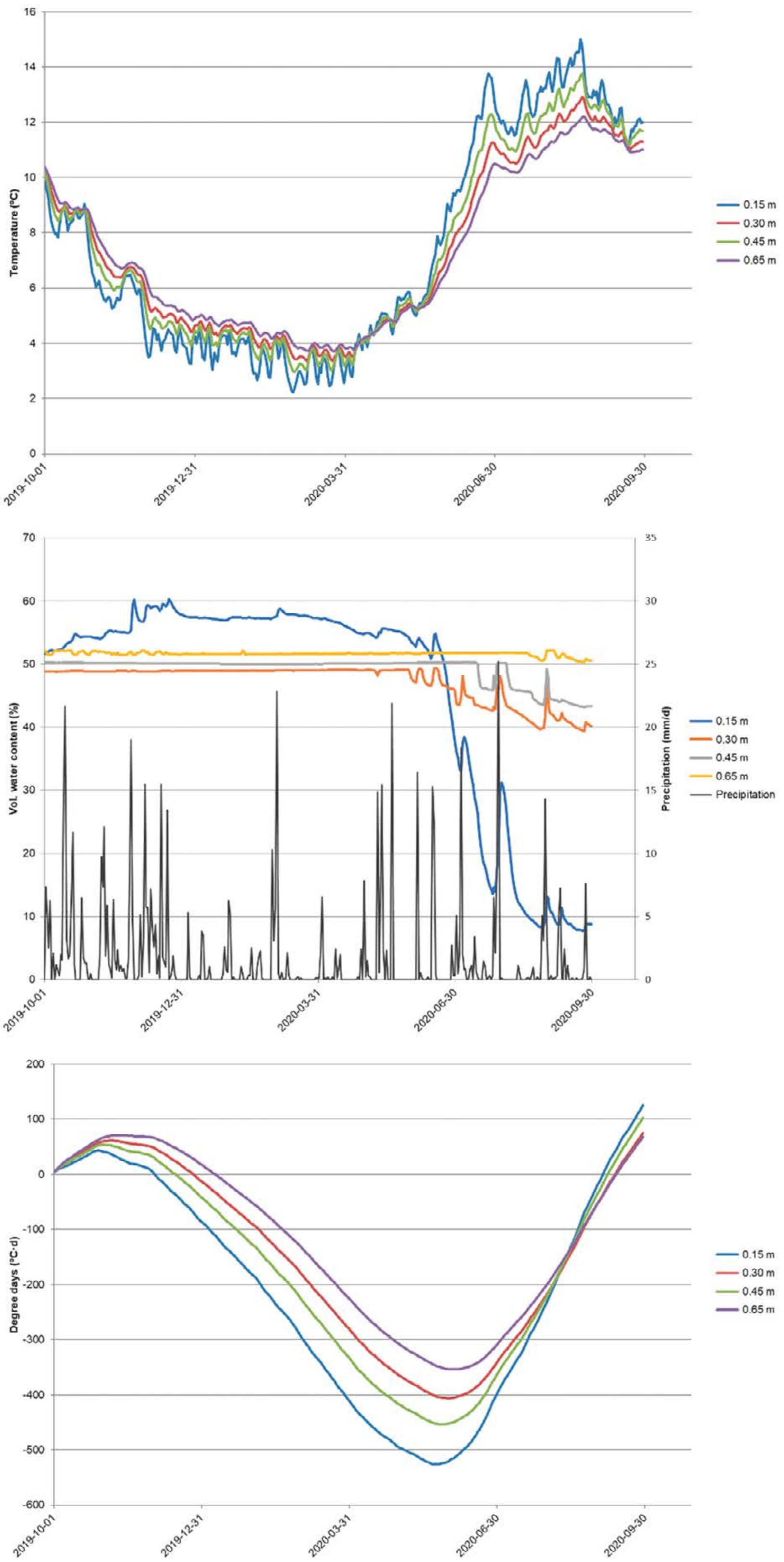

Figure A6-8. *Soil temperature (upper plot) and soil-water content (middle plot) at different depths below ground surface at PFM007875. The middle plot also shows daily sums of corrected precipitation at the Labbomasten station during the 2019/2020 hydrological year. The bottom plot shows cumulative degree days for degrees above 7 °C. The plots show daily averages of high-resolution data.*

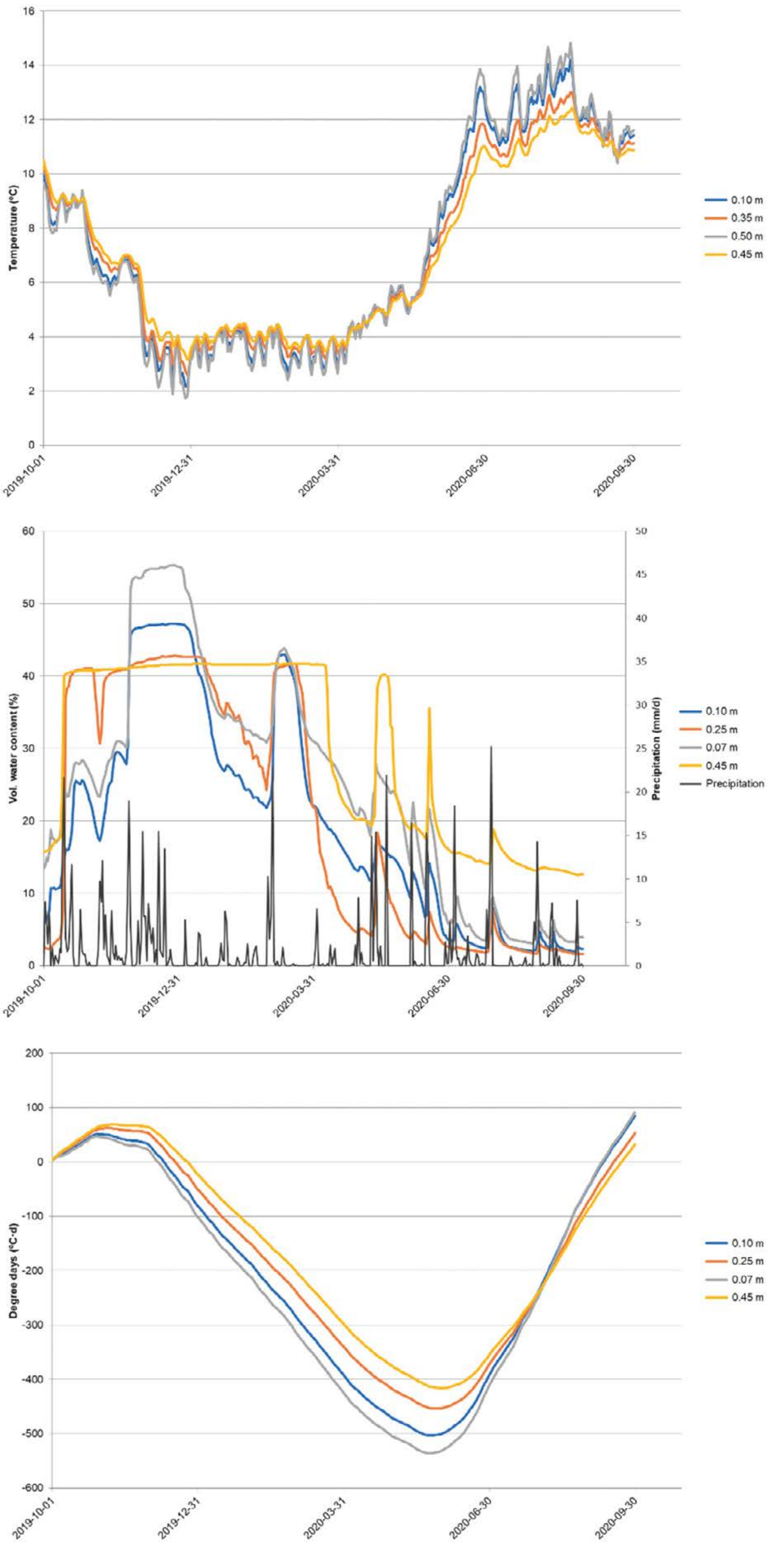

Figure A6-9. *Soil temperature (upper plot) and soil-water content (middle plot) at different depths below ground surface at PFM007876. The middle plot also shows daily sums of corrected precipitation at the Labbomasten station during the 2019/2020 hydrological year. The bottom plot shows cumulative degree days for degrees above 7 °C. The plots show daily averages of high-resolution data.*

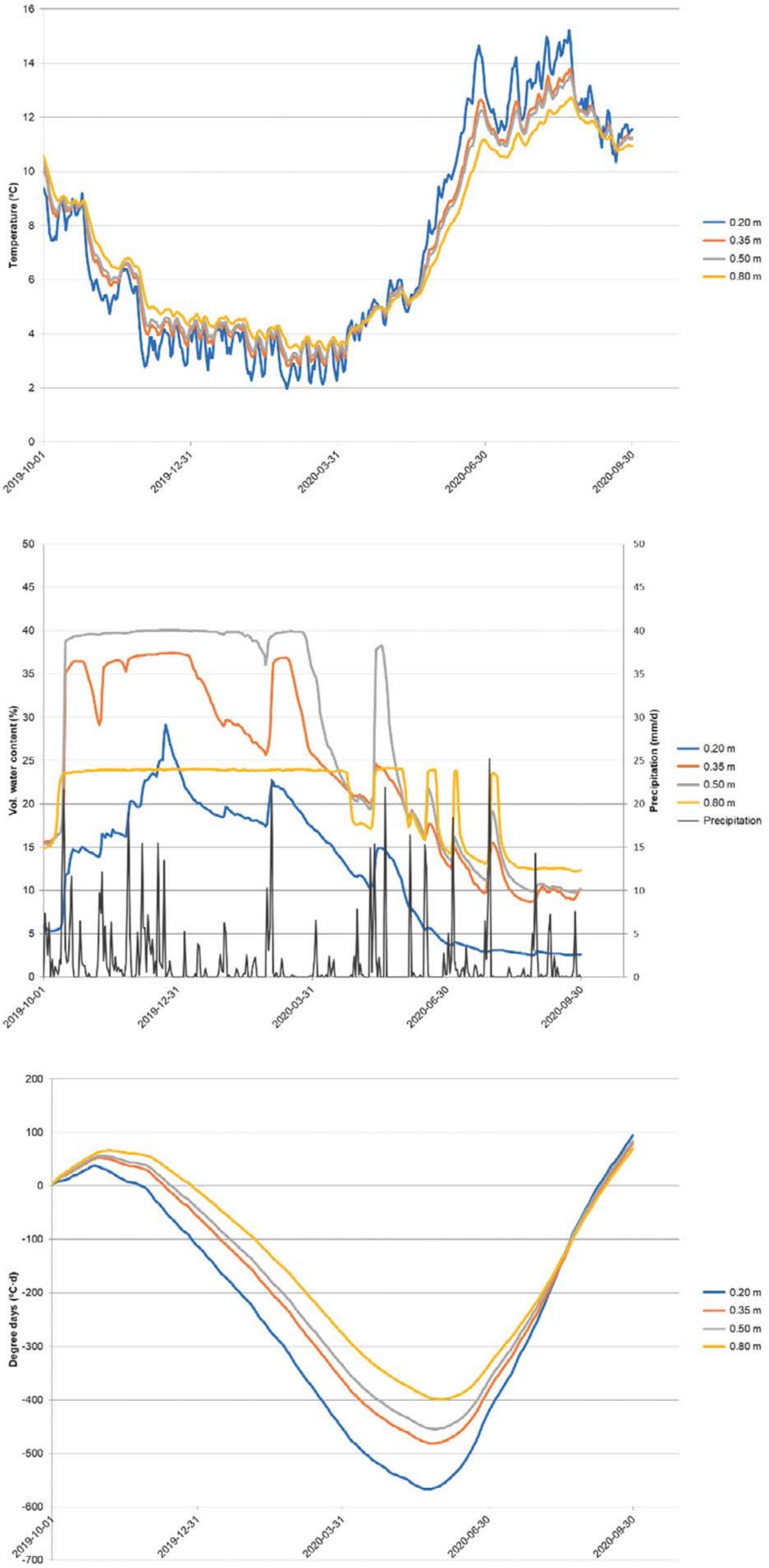

***Figure A6-10.** Soil temperature (upper plot) and soil-water content (middle plot) at different depths below ground surface at PFM007877. The middle plot also shows daily sums of corrected precipitation at the Labbomasten station during the 2019/2020 hydrological year. The bottom plot shows cumulative degree days for degrees above 7 °C. The plots show daily averages of high-resolution data.*

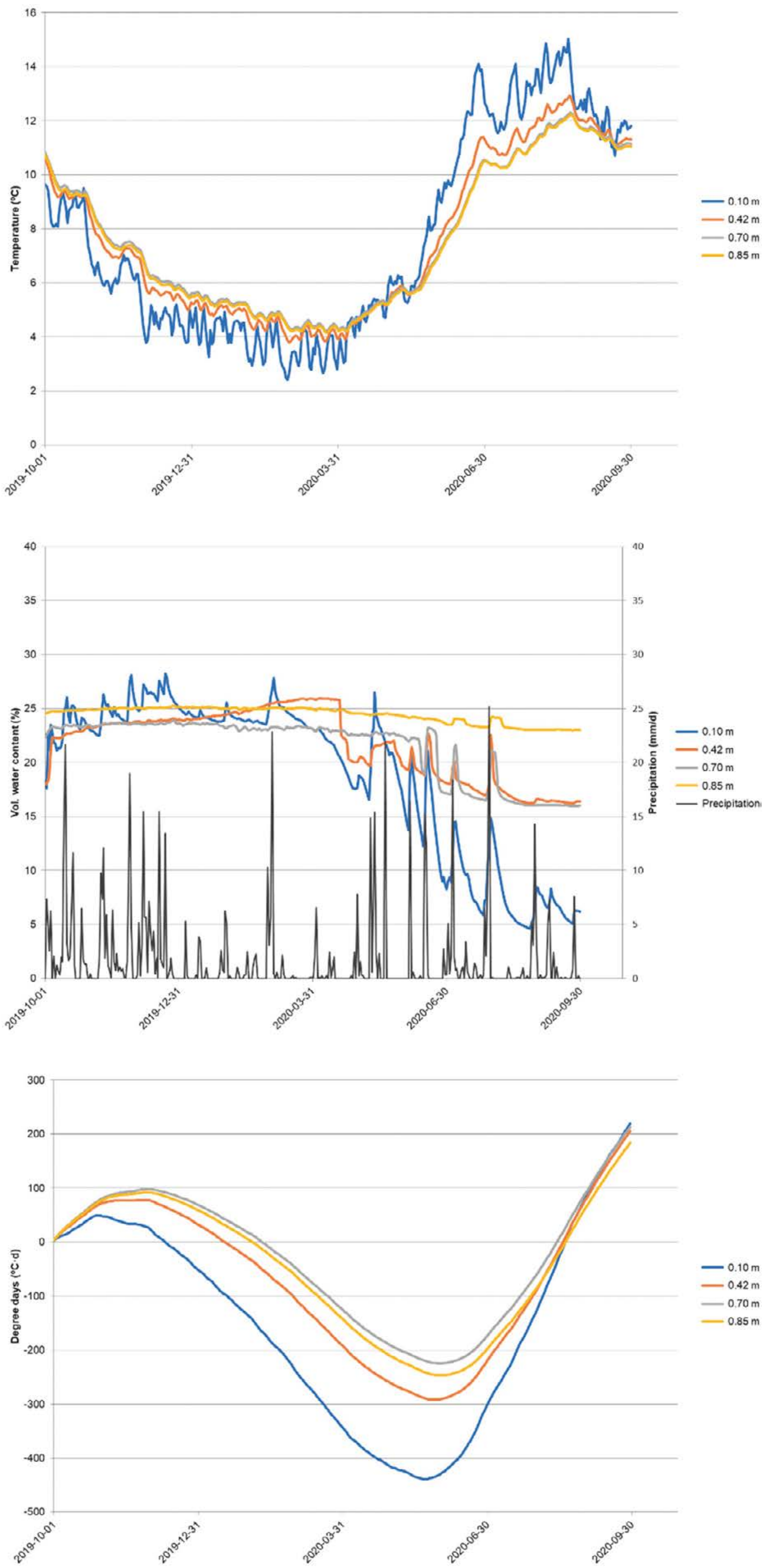

***Figure A6-11.** Soil temperature (upper plot) and soil-water content (middle plot) at different depths below ground surface at PFM007878. The middle plot also shows daily sums of corrected precipitation at the Labbomasten station during the 2019/2020 hydrological year. The bottom plot shows cumulative degree days for degrees above 7 °C. The plots show daily averages of high-resolution data.*

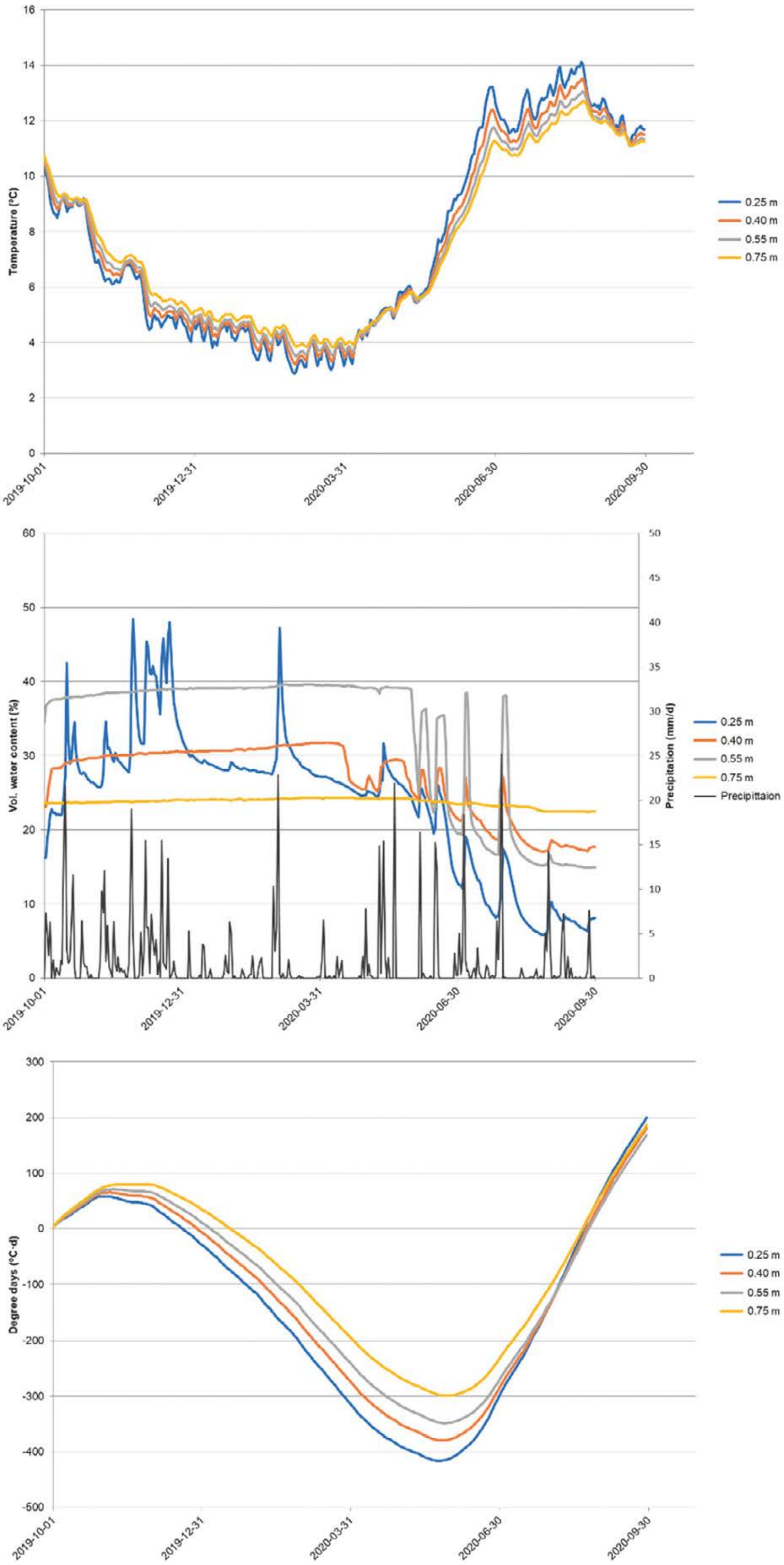

Figure A6-12. *Soil temperature (upper plot) and soil-water (middle plot) at different depths below ground surface at PFM007879. The middle plot also shows daily sums of corrected precipitation at the Labbomasten station during the 2019/2020 hydrological year. The bottom plot shows cumulative degree days for degrees above 7 °C. The plots show daily averages of high-resolution data.*

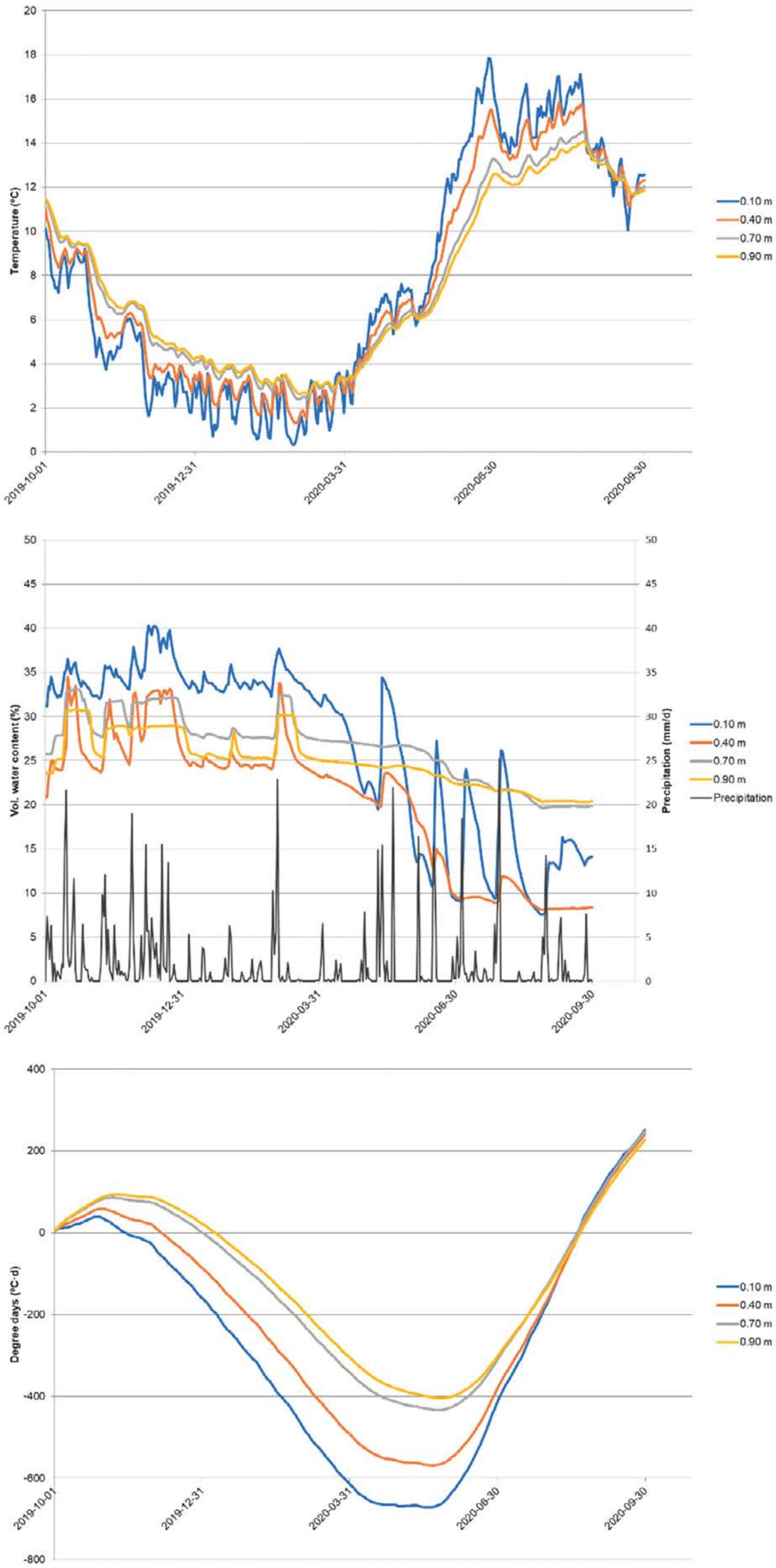

Figure A6-13. *Soil temperature (upper plot) and soil-water content (middle plot) at different depths below ground surface at PFM007880. The middle plot also shows daily sums of corrected precipitation at the Labbomasten station during the 2019/2020 hydrological year. The bottom plot shows cumulative degree days for degrees above 7 °C. The plots show daily averages of high-resolution data.*

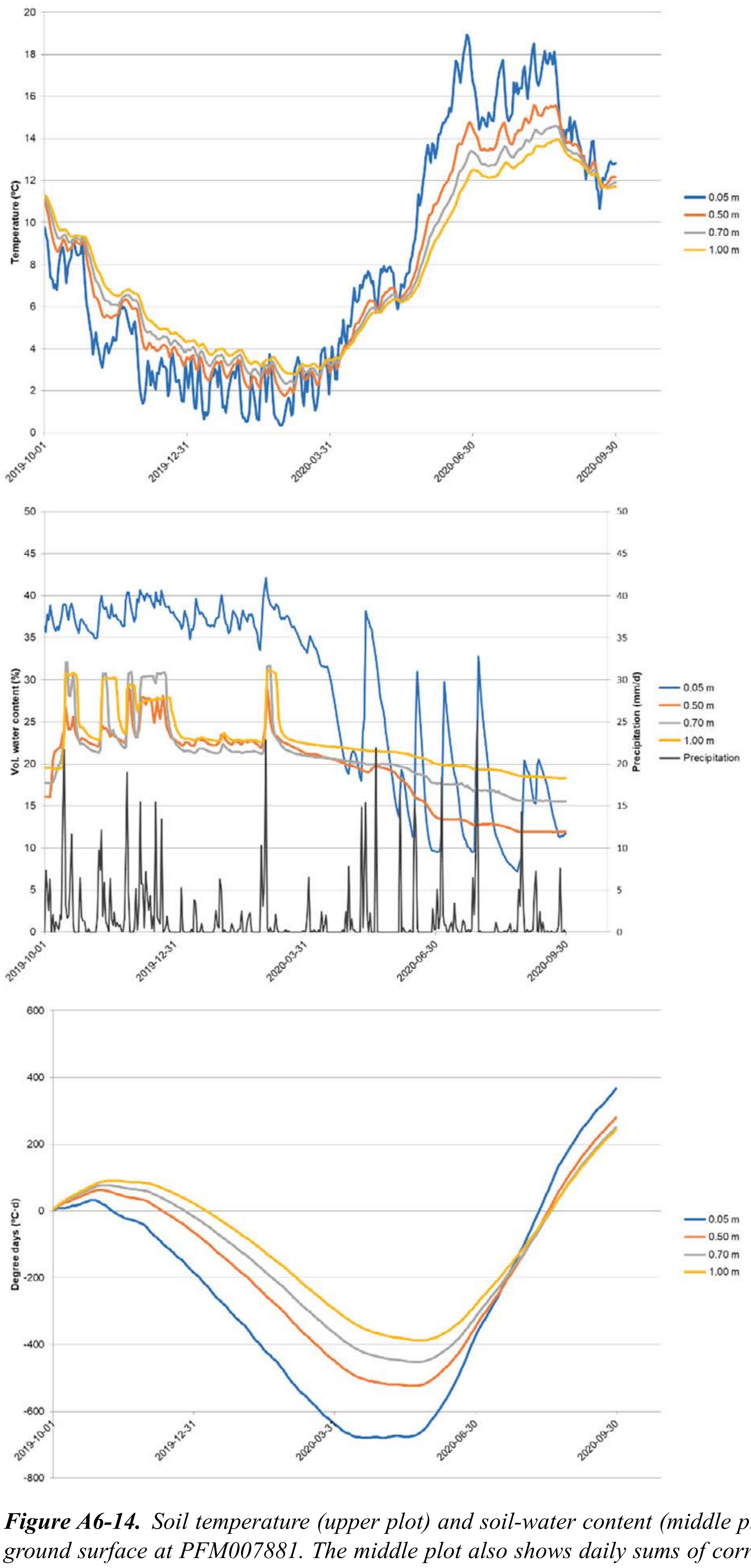

Figure A6-14. *Soil temperature (upper plot) and soil-water content (middle plot) at different depths below ground surface at PFM007881. The middle plot also shows daily sums of corrected precipitation at the Labbomasten station during the 2019/2020 hydrological year. The bottom plot shows cumulative degree days for degrees above 7 °C. The plots show daily averages of high-resolution data.*

Arkitektkopia AB, Bromma, 2022

SKB is responsible for managing spent nuclear fuel and radioactive waste produced by the Swedish nuclear power plants such that man and the environment are protected in the near and distant future.

skb.se